Synthesis and characterisation of sulphonated polyethersulphone membrane materials

by

Aishah El Boukili

A thesis submitted in compliance of the requirements for the degree of Magister Scientia in the Department of Chemistry, University of the Western Cape

Supervisor: Prof. B.J. Bladergroen

18 September 2020

Declaration

I, Aishah El Boukili, declare that the content of this thesis represents my own unaided work, and that the thesis has not previously been submitted for academic examination towards any qualification, and that all sources I have used or quoted have been indicated and acknowledged.

18 September 2020

Signed

Date

Aishah El Boukili

Acknowledgements

Above all, I am immensely grateful to Allah {سُبْحَانَهُ وَتَعَالَىٰ} for giving me the strength to push through in times of adversity. Having my computer and hard drive stolen in Cape Town and losing my MSc. research, and so much more, has been one of the most trying experiences of my life.

During this research, I have been in contact with numerous people whom have contributed one way or another. First and foremost, I would like to show my gratitude to professor Ben Bladergroen, for giving me the opportunity to conduct this research under his supervision. Thank you for sharing your expertise with me and guiding me throughout the process, and giving valuable insights. Thank you for being patient with me when things did not go as envisioned, and for giving me confidence when I needed it in challenging times. I would also like to thank my colleagues and supporting staff of SAIAMC for their help whenever I needed it.

I would like to thank professor Kitty Nijmeijer for giving me the opportunity to conduct part of my research in her group ''Membrane Materials and Processes'' at Eindhoven University of Technology. Thank you for making equipment and material available for me, for sharing your knowledge and experience, and for steering me in the right direction. I would also like to thank Pelin Oymaci for her guidance, patience, and advice throughout my time at TU/e. I am also thankful to the rest of the MMP team for their help.

I am profoundly grateful for the Water Research Commission for their financial support and for enabling me to conduct this research. Without them this study would not have been possible.

I am forever grateful for my family: my mother, sisters, and brothers. Thank you for believing in me and making it possible for me to achieve my goals, for motivating me to complete the study in times of adversity, and for supporting me in numerous ways throughout my studies.

Lastly, I want to thank my friends that have supported me throughout this MSc. study.

Summary

With current climate change, growing population, and rapid industrialization of developing countries, water is increasingly becoming a scare resource. Within a power plant, processes that consume most water are demineralized water production (boiler make-up), heat rejection (cooling) and emission control (wet flue gas desulfurization). Eskom's fleet of existing coal-fired power plants are not equipped with SO_2 abatement technologies and therefore retrofitting of the plants will be required to meet the compliance levels for SO_2 emissions.

Wet Flue Gas Desulphurization (WFGD) is the most commonly used flue gas desulphurization (FGD) system worldwide because of its high operational reliability and removal efficiency (up to 99%). However, it uses significant amounts of water. If water vapour could be removed from the flue gas stream before it is emitted to the atmosphere, large amounts of valuable water would be saved.

A proposed solution to recover this water vapour is a polymer-membrane assisted process. Recovery of water vapour from flue gas using polymer-based composite hollow fibre membranes post WFGD is potentially a viable method as up to 40% of the water in the flue gas can be recovered in highly purified form. However, these membranes are not commercially available. The purpose of this work was to explore the fabrication of a membrane that would be suitable for application in water recovery from flue gas.

The polymer used for the support material was polyethersulphone (PES), hollow fibre (HF) PES membranes were fabricated in a spin line set-up. This technique allows for the fabrication of uniform hollow fibre membranes. Parameters were adjusted until the ideal dimensions were achieved. The defect free PES HF were obtained with an average outer and inner diameter of 1,200 μm and 850 μm respectively. The average wall thickness was 170 μm.

The polymer, sulphonated polyethersulphone (SPES) for the selective layer was synthesized by a sulphonation reaction. The PES pellets were dissolved in N-4-methyl-2-pyrrolidone (NMP) in a 20/80 w/v concentration, followed by dropwise addition of chlorosulphonic acid into the solution. The sulphonation reaction parameters were varied by temperature (5, 10, and 20˚C), by reaction time (5, 7, 9, and 25 hours), and by stirring rate (250, 400 and 500 rpm), resulting in sulphonation degrees of SPES of approximately 2, 5, 15, 20, 25, 40, and 45 mol%.

PES and SPES (including commercial SPES from Konishi) samples were characterised by FTIR, and ^{1}H NMR spectroscopy. TGA confirmed that an increasing degree of sulphonation resulted in an increased glass transition temperature and decreased decomposition temperature of the polymers.

To prepare for dip-coating of the PES hollow fibres with SPES, solubility experiments of both polymers were performed. The solubilities of PES hollow fibres and SPES polymer were tested in ethanol and methanol to ensure that SPES was dissolving while the PES HF was not. It was established that SPES samples with a degree of sulphonation >30 % were soluble in methanol. Therefore, dip-coating was performed using these samples with methanol as the solvent. The dip-coated membranes were analysed by Scanning Electron Microscopy (SEM) and the presence of a thin selective layer with a thickness of approximately 10µm was confirmed after dip-coating the same hollow fibre twice.

''The most all penetrating spirit before which will open the possibility of tilting not tables but planets, is the spirit of free human inquiry. Believe only in that.''

Dimitri Mendeleev

Table of contents

List of figures

List of tables

List of symbols

Symbols

J	Flux	$l/hr/m^2$
P	Permeability coefficient	Barrer
f	Fugacity	cmHg
p	Permeate volume	cm^3_{STP}
d	(Membrane) thickness	cm
A	Area	m^3
t	Time	sec
ΔP	Pressure difference	Torr
D	Diffusion coefficient	cm^2/s
S	Solubility coefficient	cm^3_{STP}/cm^3 cmHg
Tg	Glass transition temperature	˚C
V	Volume	m^3 STP
M	Concentration	mol dm^{-3}
MW	Molecular weight	g/mol
d	Diameter	mm, µm or cm

Greek symbols

α	Selectivity
Σ	Sum

Subscripts

i	Individual component present in the stream
STP	Standard Temperature and Pressure

Abbreviations

DS	Degree of Sulphonation
ESP	Electrostatic precipitator
FGD	Flue Gas Desulphurization
FTIR	Fourier Transform Infrared (spectroscopy)
GS	Gas separation
IEC	Ion Exchange Capacity
NG	Nucleation and growth
NMP	N-4-methyl-2-pyrrolidone
NMR	Nuclear Magnetic Resonance
PEO-PBT	Poly(butylene terephthalate) block polymer
PES	Polyethersulphone
SAIAMC	South African Institute for Advanced Materials Chemistry
SI	Système International (d'unités), International System of Units
SD	Spinodal composition
SEM	Scanning Electron Microscopy
SPEEK	Sulphonated polyetheretherketone
SPES	Sulphonated polyethersulphone
TGA	Thermal Gravimetric Analysis
TU/e	Eindhoven University of Technology
WFGD	Wet Flue Gas Desulphurization
WRC	Water Research Commission

Chapter 1 Introduction

1.1 Background to water scarcity and power production

With current climate change, growing global population, and rapid industrialization of developing countries, water is increasingly becoming a scare resource. Besides our daily need for water, it is in great demand in agriculture and industry. The agriculture sector accounts for 67% of total water consumption in South Africa. In some countries the energy sector is the second largest consumer of fresh water (up to 45% in the USA). In South Africa, the energy sector accounts for 2-3% of the total water consumption. The water use per sector is depicted in Figure 1. In the process of electricity production, large volumes of water are utilized for efficient operation, mainly for cooling purposes (Srivastava and Jozewicz, 2001).

Water scarcity is a grave concern for an industry that largely depends on water for its production facilities. This has led to the need to use water more efficiently, and exploring possibilities provided by water reuse, recycling and resource recovery. In addition to decreasing water usage, alternative sources for water are being explored, such as local water harvesting systems (for rainwater, greywater and stormwater), groundwater development (finding new resources and artificial aquifer recharge), desalination, and atmospheric water generation (Bronkhorst *et al.*, 2017).

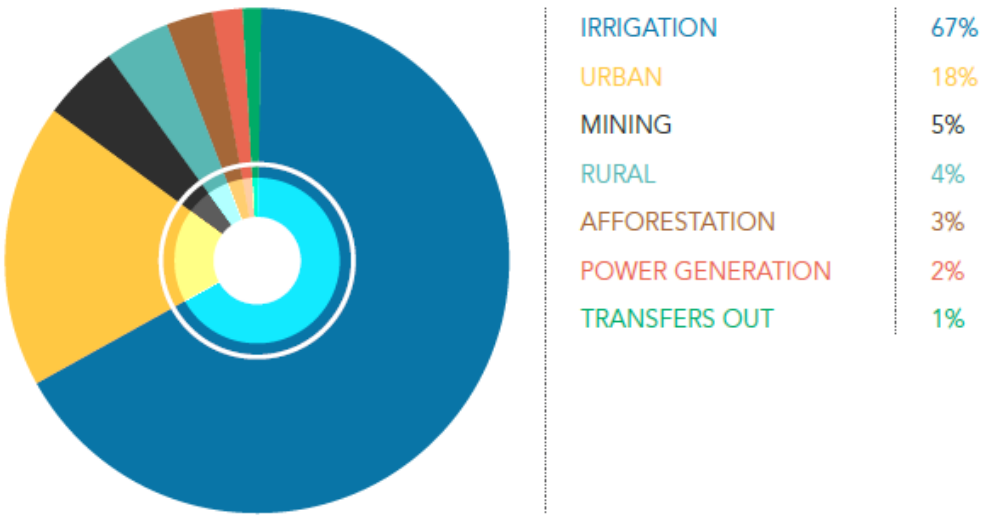

Figure 1 Water use per sector (Bronkhorst *et al.*, 2017)

To avert the looming water crisis, certain measures should be adopted. These include but are not limited to:

i) Water conservation
ii) Reducing pollutants entering the water system
iii) Upgrading current infrastructure
iv) Improving fresh water generation technologies (Bagheri, 2018).

Eskom Holdings SOC Ltd is the largest producer and distributor of electricity in Africa with a total generating capacity of approximately 42 GW. Eskom depends largely on coal as a primary fuel source for its electricity production, and it is expected to continue to do so due to South Africa's large coal reserves. Eskom is recognized as being a large consumer of fresh water, therefore one of Eskom´s environmental management strategic objectives is to reduce fresh water usage and eliminate liquid effluent discharge to avoid impacting water resources through effective water management processes (Eskom, 2018). There are several ways to decrease water consumption of pulverized coal (PC) power plants; e.g. implementing alternative cooling systems (such as hybrid or dry cooling systems) that require virtually no water, drying the coal prior to combustion, and the use of dry flue gas desulphurization systems as opposed to wet flue gas desulphurization units.

There are different types of coal-fired powerplants. Eskom's fleet of power plants consist of pulverised coal-fired boilers that generate thermal energy by burning pulverized coal. The pulverized coal is burned to heat water, the water is converted into steam in the boiler and fed to turbines where the thermal energy is converted into mechanical energy (Delgado Martin, 2012). After the turbine, the steam is condensed and directed to the boiler to be heated again (this is a Rankine cycle) (Delgado Martin, 2012).

The efficiency of these power plants ranges between 20-45% depending on the steam parameters achieved (Babcock&Wilcox, 2015). There are different power plant types: subcritical, supercritical and ultra-supercritical, based on different temperatures and pressures the steam generator is operated on (Delgado Martin, 2012). Supercritical and

ultra-supercritical power plants use higher temperature and pressure to lower the heat rate, making them more efficient and decreasing their water consumption (Delgado Martin, 2012).

In thermoelectric power plants, such as PC power plants, most of the water is used for cooling purposes. Figure 2 shows the water consumption and discharge of a subcritical 500MW power plant with a cooling tower and wet flue gas desulphurisation. Eskom latest additions to their fleet are two PC super-critical power plants Medupi in Limpopo and Kusile in Mpumalanga. Their constructing started in 2007 and 2008 respectively, and each one is equipped with 6 units of 800 MW. They are built to be dry cooled power plants to reduce water consumption. Dry cooling reduces the water consumption from approximately 2 L/kWh to 0.14 L/kWh (African Development Bank Group, 2018).

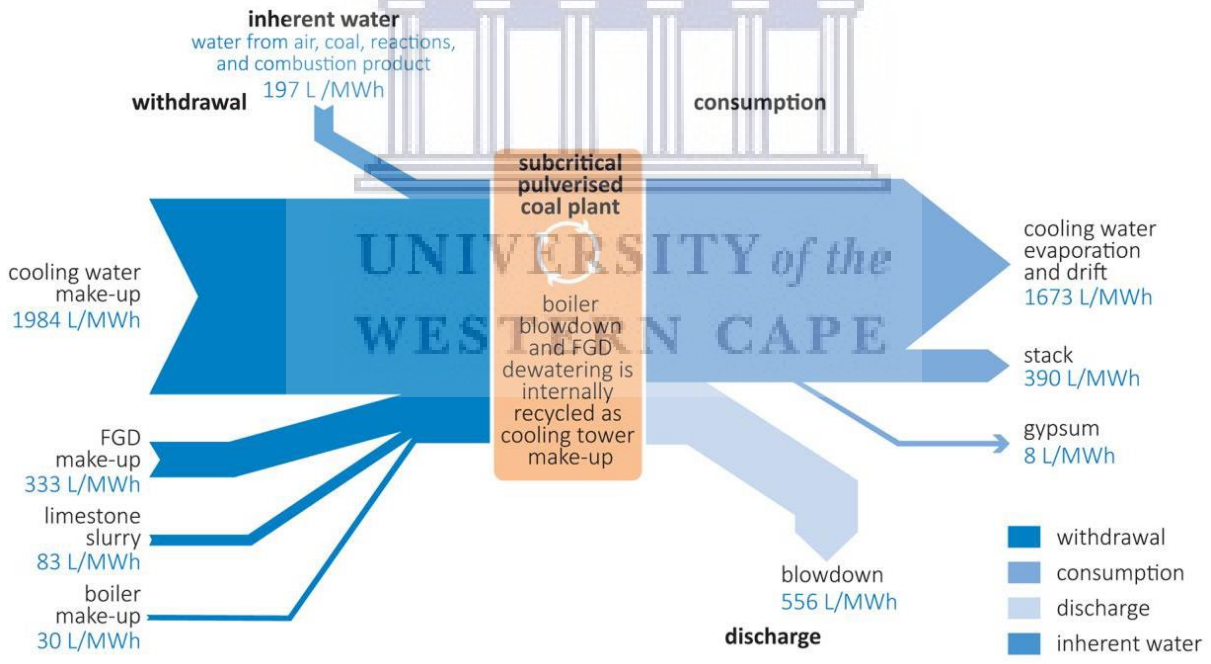

Figure 2 Water balance subcritical power plant (Carpenter, 2017)

In a dry cooling power plant, air is the cooling media and not water. The condensate is cooled inside a heat exchanger as ambient air is forced via large fans to flow around finned tubes (this is called the air cooled condenser) (Carney, Barbera;Shuster, 2014).

However, the choice of dry cooling as opposed to wet cooling operation affects the energy efficiency of a powerplant. According to the 0U.S. Environmental Protection Agency, the annual performance penalty is 6.9 % when switching from wet cooling to dry cooling (USA national average). This is the result of back pressure of the power plant turbine (Macknick *et al.*, 2012).

The majority of all sulphur oxides emission is produced when sulphur containing fuels undergo combustion. During the combustion of coal in power plants large volumes of flue gas are produced. Flue gas contains N_2, CO_2, O_2, H_2O, but also pollutants such as NO_x, SO_x and fly ash. Sulphur oxides (SO_x), consisting mainly of SO_2 and small amounts of SO_3, have detrimental effects on human health and the natural environment when present in elevated concentrations. Exposure to high ambient concentrations causes breathing difficulties, respiratory illness, and aggravation of existing cardiovascular diseases. Additionally high SO_2 levels cause acid deposition in the environment, causing acidification in lakes and streams and damage to tree foliage and agricultural crops (Srivastava and Jozewicz, 2001).

SO_2 emissions have been regulated in Europe for many years (UNECE, 2012). Power plants in Europe burn coal with a higher calorific value and lower ash content but higher sulphur contents compared to South Africa (Stephen, 2017). Even though South African coals are considered to be low sulphur coals, their low calorific value and high ash contents (which makes it a low grade coal), result in a relative high coal consumptions. Due to the lack of desulphurisation installations this consequently results in high SO_2 emissions (Stephen, 2017). South Africa has therefore implemented regulations to limit the exhaust as well as the ambient concentration levels of SO_2 (Stephen, 2017).

In 2004, the Department of Environmental Affairs (DEA) put in place various measures to prevent pollution and set national norms and standards for the regulation of air quality with the South African Air Quality Act. Under this Act, the Ambient Air Quality Standards [Act 39/2004] and the Minimum Emission Standards (Notice 248; 31 March 2010) came into existence. The implementation of these new regulations limit the amount of air

pollutants that are allowed to be emitted from coal-fired powerplants and other industrial facilities. The emission standards for SO_2 are shown in Table 1. Power stations, both existing as well as newly built power plants, need to adhere to these emission standards.

Table 1 Emission standards for SO_2 (Stephen, 2017)

SO_2 Emissions Limit	**Applicable to**	**Compliance date**
500 mg/Nm^3 at 10% O_2	New plants	2010
3500 mg/Nm^3 at 10% O_2	Existing plants	2015
500 mg/Nm^3 at 10% O_2	New and existing plants	2020

By 2020 the minimum allowable emission for SO_2 will be limited to 500 mg/Nm^3 at 10% O_2 for both new and existing power plants. As a result, Eskom is interested in determining ways to comply with these new emission standards. Eskom's fleet of existing coal-fired power plants are not equipped with SO_2 abatement technologies and therefore retrofitting of the plants will be necessary to meet the compliance levels for SO_2 emissions (Stephen, 2017).

1.2 SO_2 emission abatement technologies

There is a wide range of technologies available to reduce SO_2 emissions from coal combustion. Flue Gas Desulphurization is an effective measure that is widely applied in coal-fired power plants. The market for FGD equipment is expected to grow as power plants install FGD systems in order to comply with the more stringent SO_2 emission levels. FGD can be categorized in FGD pre-combustion, during combustion, and post-combustion. The technologies with high SO_2 removal efficiencies fall within the post combustion types, which are shown in Figure 3. The technologies are further classified by their water usage, namely wet processes, which consumes the largest amount of water, followed by semi-dry processes, where the water consumption is decreased by 60% compared to WFGD, and eventually the dry process, which virtually consumes no process water (Carpenter, 2012).

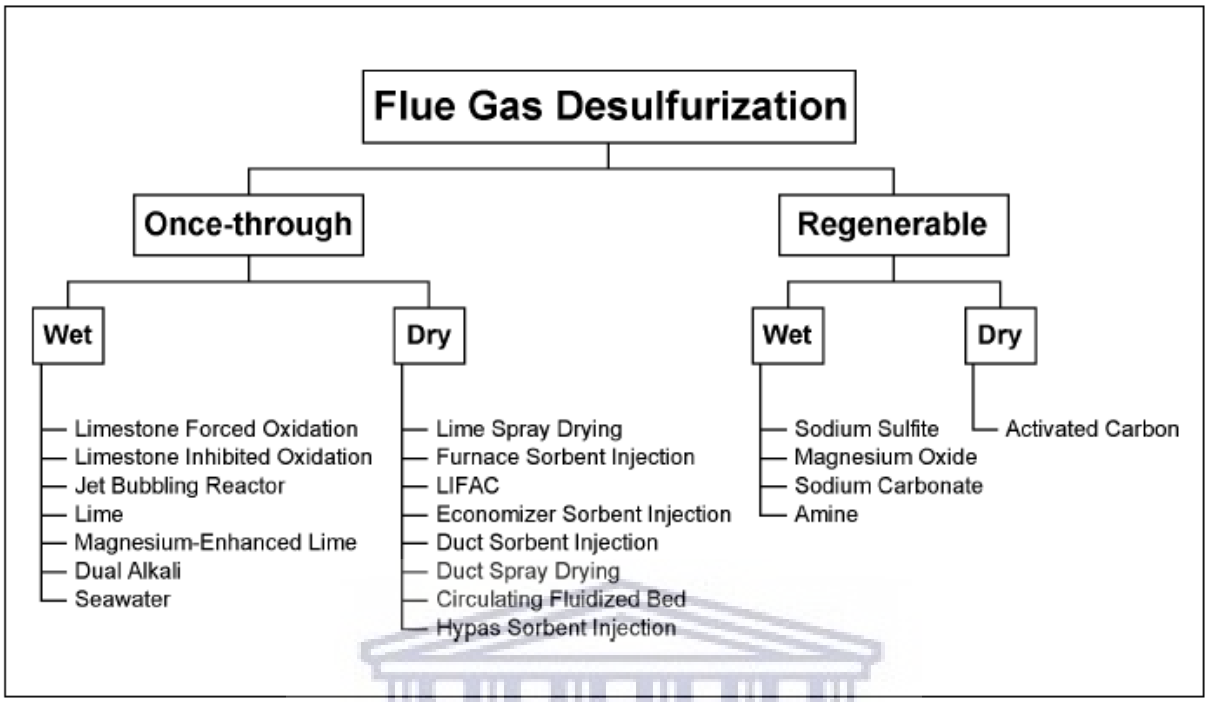

Figure 3 Classification of FGD processes (Srivastava and Jozewicz, 2001)

FGD processes are based on SO_x being acidic and their removal happens by reaction with a suitable alkaline sorbent. The most commonly used materials for this purpose are limestone (calcium carbonate, $CaCO_3$) and lime (CaCO), because of their availability and price. There are once-through and regenerable processes, based on the handling of the solids that are generated. Once-through systems either dispose the spent sorbent as a waste or utilise it as a by-product, whereas regenerable systems recycle the sorbent back into the system (Carpenter, 2012).

In WFGD units, all reactions take place in a single integrated absorber, and per boiler only a single absorber vessel is required, this results in reduced capital costs and energy consumption (Poullikkas, 2015; African Development Bank Group, 2018). With a WFGD system, hydrogen chloride, hydrogen fluoride, and oxidized mercury could also be removed. They have been installed on units burning low and high sulphur coals. However, as a result of the reaction of limestone with SO_2, CO_2 is produced and is emitted with the scrubbed flue gas (Carpenter, 2017). A potential solution for this would be to capture the CO_2 using membranes.

The water loss in the flue gas through evaporation is substantial: a 500MW supercritical plant loses approximately 3096 L/min (359 L/MWh), and the additional water that is added to make up for the evaporative water losses accounts for 1899 L/min (220 L/MWh) (Carpenter, 2017).

Wet Flue Gas Desulphurization is the most commonly used FGD system worldwide because of its high SO_2 removal efficiency (95-99 %) (Poullikkas, 2015). It has a global installed capacity of 80 %, whereas semi-dry processes account for less than 10 %, and dry processes account for approximately 2% of global installed capacity (Carpenter, 2017).

In WFGD processes, coarse particles (fly ash) are removed first by an electrostatic precipitator (ESP). The flue gas is then brought into contact with the sorbent (in the form of a solution or slurry) in a separate absorber unit (wet scrubber/spray tower). This is done by passing the flue gas into the spray tower and inject the aqueous sorbent into the flue gas. SO_2 in the flue gas dissolves in the water to form a dilute acid solution that then reacts with and is neutralised by the dissolved alkaline sorbent. Some of the water in the spray droplets evaporates, reduces the temperature of the flue gas and saturates it with water (Carpenter, 2012). The WFGD process is depicted in Figure 4.

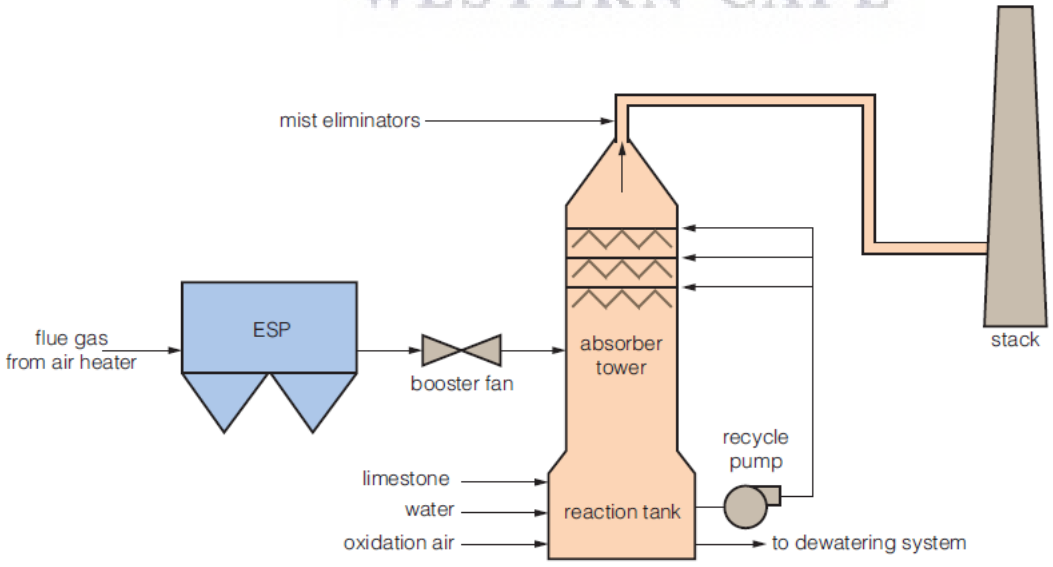

Figure 4 Schematic view of a limestone wet scrubber system (Carpenter, 2012)

After reacting, the sorbent slurry falls to the bottom of the absorber where it is collected and further processed. The flue gas leaves the WFGD unit in a saturated or supersaturated state, carrying a significant amount of moisture, some in the form of water droplets. Some of these droplets were created by supercooling of the flue gas while others are a result of the scrubbing liquid sprays. The treated flue gas is passed through a mist eliminator to remove any remaining droplets (Sarunac, 2020).

The saturated flue gas stream together with any further reduction of the flue gas temperature downstream the absorber will allow for condensation of the water vapour to be formed in the stack, which in combination with trace amounts of acidic impurities causes corrosion of the duct and stack (Black & Veatch, 1996). To prevent condensation, reheating of the flue gas is required, which results in a higher energy consumption and reduces the overall energy efficiency of the power plant. Reheating of the flue gas is usually done by a furnace or by reusing the heat of the exhaust gas leaving the boiler. Alternatively, this water vapour could be removed from the flue gas stream before it enters the stack, to make heating redundant, resulting in significant energy savings, improving the overall efficiency, and saving large amounts of valuable water from being emitted into the atmosphere (Sijbesma *et al.*, 2008).

The H_2O concentration in flue gas is 7-17 vol%, depending on the type of coal (different types of coal have different total coal moisture), SO_3 concentration and other factors. For bituminous coal, the mostly used coal in South Africa, the H_2O content in flue gas is 7.31 vol%. After the flue gas has passed the WFGD unit the H_2O vol% becomes ~14.3 %. When there is no reheater, the moisture content of the flue gas increases up to ~15.9 % (Sarunac, 2020).

By using WFGD to reduce SO_2 exhaust, large volumes of water are being used to absorb the SO_2. In power plants with dry cooling, the WFGD unit is the largest water consumer with a water requirement of 0.35 L/kWh (Carpenter, 2012; Chang, Daniel; van Wijk, Leon; Bagus, 2018). Capturing the water vapour in flue gas would significantly lower the power plant's water consumption. Since Medupi and Kusile are dry cooled powerplants that are

required to be retrofitted with WFGD, water vapour recovery technology is strongly advisable.

The water evaporated in the flue gas could be utilized in multiple ways. The captured water could be used as WFGD make-up water, as boiler feed water, blowdown water or it could be transported elsewhere in the process as additional water to compensate for the steam losses (Carpenter, 2012).

There are three main methods of recovering water from flue gas:

I. Mechanical heat rejection by condensing the water by cooling (using condensing heat exchangers)
II. Using a desiccant
III. Extract the water using a membrane

Condensing heat exchangers could be placed between the ESP and the FGD unit to capture the sensible heat, and any additional heat exchanger could be placed between the FGD unit and stack in order to cool both the flue gas (sensible heat transfer) and condense water vapour from the flue gas (latent heat transfer) (Carpenter, 2012). Condensing heat exchangers require a large cooling capacity, are limited by high ambient temperatures, and discharge non-buoyant stack gas. The process has a decreased gas turbine performance as a result of high back pressure due to closed heat exchangers in the flow path (exhaust pressure drop), which can be compensated with an internal draught fan (Copen, Sullivan and Folkedahl, 2005; Carpenter, 2012). In addition, because of acid formation during condensation, the use of expensive alloys is required to minimize corrosion of the heat exchangers (Singh and Berchtold, 2017).

(Liquid) desiccant dehumidification systems can also be used to recover useful amounts of water during power plant operation. In this system, the flue gas is cooled before passing it through an absorption tower in which the liquid desiccant (such as calcium chloride, lithium bromide or triethyleneglycol) is injected (Carpenter, 2012). The flue gas, lean in water, exits the absorber and is passed through a mist eliminator to remove remnant desiccant droplets before discharging it through the stack. The water loaded desiccant is

heated via a heat exchanger before entering the regenerator, because separation of the water gets easier at elevated desiccant temperature. The water vapour is separated from the desiccant solution in a flash drum by differential pressure, after which it is recovered in a downstream condenser. To remove insoluble contaminants, the regenerated hot desiccant is filtered and then cooled via a heat exchanger before injecting it back into the absorber (Carpenter, 2012).

Overall, the desiccant system requires minimal heat rejection equipment, can function across the entire ambient range, and results in only a small increase in exhaust pressure. The drawbacks of these systems is that it is very energy intensive, because of its parasitic energy loss in desiccant regeneration, and it produces low quality water (Copen, Sullivan and Folkedahl, 2005).

The use of membranes for capturing water vapour from flue gas is a more energy efficient and attractive alternative. Besides being reliable, it is easy to implement, operate and scale up. Additionally, CO_2 emission can also be reduced using membranes, and high purity water is produced (Potreck, 2009). This makes membrane technology a promising alternative for this purpose.

1.3 Motivation for research

Reducing water loss is especially important in arid regions of the world, which South Africa is considered to be. Therefore, low water consuming FGD processes would be preferred, such as the semi-dry FGD system which consumes around 60% less water than the conventional wet scrubbers, and dry FGD processes, which consume practically no water (Carpenter, 2012). While WFGD systems have a global preference to bring SO_2 to acceptable limits, it proves a challenge when water is not readily available.

Since Medupi and Kusile were commissioned after the Air Quality Act was passed, they qualify as a new-built power generation facility and are therefore required by law to limit the SO_2 limit in flue gas emission to 500 mg/Nm^3. Moreover, a legal requirement of the loan agreement between Eskom and the World Bank was that Eskom would retrofit their

power plants with a ''well-established flue gas desulphurization technology'' after 6-8 years from commissioning date. This meant that Wet Flue Gas Desulphurization was the technology that would be implemented (*Eskom Investment Support Project*, 2010).

It is expected that Eskom's water consumption will increase over the next 10 years, not only because of the expected annual increase in electricity demand, but also because of a need to make their coal fired power stations compliant with the Air Quality Act. A gradually increasing number of WFGD units will require an increase of the total water demand. Fortunately, Eskom already recognised that the organisation would have to find ways of limiting increases in water consumption and contribute to sustainable water use in South Africa. Eskom stated its commitment to support the drive to improve the management of South Africa's scarce water resources, and to investigate viable options that reduce water consumption in their power plants, such as dry cooling and in the WFGD system (Eskom Holdings, 2020).

The areas in which Eskom's power stations were built are relatively water scarce. Particularly for air cooled power stations equipped with WFGD units, it may be economically viable to remove the water vapour from the flue gas stream before it is emitted into the atmosphere as a way to decrease water consumption of the WFGD unit.

This study is part of a collaboration between the South African Institute for Advanced Material Science (SAIAMC) and the Water Research Commission (WRC). The Water Research Commission plays an important role in the development of South Africa's water management industry. The WRC has also been, to a large extent, the driver of water related membrane research in South Africa. Through funding, the WRC is stimulating research and materialising opportunities for local companies to produce membranes for water related challenges in South Africa. Up to date, it has commissioned extensive research into the broad field of membrane technology.

Some of the experiments were performed at the research group ''Membrane Materials and Processes'' of the Eindhoven University of Technology (TU/e) in the Netherlands in

pursuit of knowledge transfer, as they have extensive expertise on membrane development. The ''Membrane Materials and Processes'' research group carries out fundamental academic research, valorisation, as well as application-oriented research in collaboration with the process and manufacturing industry.

1.4 Problem statement

Eskom's newly built power plants Medupi in Limpopo and Kusile in Mpumalanga were the first power plants in Eskom's fleet to be fitted with WFGD technology. These power plants were designed with air cooled condensers in a closed loop cycle to minimize water consumption. The addition of WFGD to Medupi and Kusile power stations, increased water consumption with 7.5 million m^3/annum (Black & Veatch, no date). This increase in water consumption was challenging as the additional water after operation of the WFGD units, had to be pumped from Makolo Dam and Crocodile-West water system.

In the search for water consumption reducing technologies for WFGD, membrane technology could play an important role. Membranes allow the selective removal of water vapour from the flue gas streams up to 40 %. The amount of water recovered could potentially be sufficient to meet all the make-up water requirements in dry cooled power plants with WFGD (Carpenter, 2017).

Membrana GmbH stopped supplying their water vapour selective hollow fibre membranes to the South African Institute for Advanced Materials Chemistry, after their acquisition by the company 3M, so interest grew to see if water vapour selective membranes could be fabricated locally to ensure a steady supply of membranes for the membrane modules needed in South Africa.

1.5 Aims and objectives

A collaboration between the South African Institute of Advanced Materials Chemistry and the Water Research Commission has led to a project to assess the use of polymer membranes for water vapour recovery from humid gases. The project encompasses three different research tasks, with one focused on membrane development, another one on membrane module development, and a third one on the economic viability of water vapour recovery from flue gas using these membrane modules specifically on the Medupi power station.

The aim of this study is to synthesize and characterize a polymer membrane material that could potentially be used in water vapor recovery membranes modules.

The objectives that emerge of this are as follows:

- Selection of polymer material and fabrication of a suitable hollow fibre support membrane
- Identification and synthesis of a suitable polymer compatible with the support layer and that has a promising permeability towards water vapour and a significantly high H_2O/N_2 selectivity
- Application of a continuous selective thin film of the synthesized polymer onto the hollow fibre support structure. Selection of suitable solvent for this process that would not dissolve the support structure
- Obtain control over the sulphonation reaction under variable reaction conditions
- Determination of the ideal sulphonation degree of selected polymer
- Characterisation of synthesized polymer materials.

1.6 Scope of the research

The aim of this research is to develop membrane materials for water vapour recovery. To this extent, the optimal material and process conditions for the fabrication of hollow fibre support based on polyethersulphone (PES) should be determined. Furthermore, determining the optimal material and synthesis conditions of the water selective polymer. This is achieved through a meticulous experimental study.

The scope of the research consists of two parts to explore the potential of this separation process for the purpose of water vapor recovery. The first part is a literature survey, aiming to give context in terms of using membranes in the power generating industry. It gives the theory on gas transport through membranes, membrane materials, membrane module configurations, and the application of membranes for water vapour recovery.

The second part documents the fabrication of the PES hollow fibre support, and the synthesis of SPES material for the selective layer, whereby the synthesis parameters are varied to obtain different degrees of sulphonation (DS), after which the optimum degree of sulphonation is determined. Additionally, PES hollow fibre support is coated with a selective layer of SPES by dip-coating, and the compatibility between these two layers is investigated. Both PES and SPES are extensively characterized. The morphology of PES and SPES is analysed using Scanning Electron Microscopy (SEM). Thermogravimetric Analysis (TGA) is conducted to investigate the thermostability of the polymer, and using Fourier Transfer InfraRed Spectroscopy (FTIR), the introduction of the sulphonate groups into PES is investigated. The sulphonation degree is determined using two methods: ^{1}H Nuclear Magnetic Resonance (NMR) analysis, and titration using the ion-exchange capacity (IEC). The synthesis of the support, the selective material and the characterisation thereof is a major output of this study.

1.4 Thesis outline

Chapter 1

This chapter sets up the background and motivation for this study, combined with the technological concepts, and a brief description of the research structure.

Chapter 2

A detailed literature review is provided where membrane technology as a means of water vapour recovery is elaborated on. Polymeric materials used for water selective membranes are presented while building a framework that addresses the study aims.

Chapter 3

The methodology used to conduct the research and experiments is formulated. The rationale for selecting polymeric materials of choice is discussed, as well as the methods of data collection and analysis.

Chapter 4

The execution of the experiments is discussed. The findings with regard to the synthesis of support material as well as the composite material are discussed to bridge the gap between theory and practice. The findings with regards to characterisation of obtained polymer materials is described extensively. Furthermore, this chapter portrays an assessment of the compatibility of the supportive and selective polymer layers.

Chapter 5

The interpretation of the results is discussed in relation to the significance of the findings and their potential contributions including their limitations and anomalies. Furthermore, the scope for further research is proposed.

Chapter 2 Literature Review

2.1 General Description of Membrane Technology

2.1.1 Membrane technology versus conventional separation technologies

The main advantage of membrane technology compared to conventional separation technologies (e.g. distillation, extraction, and crystallization) is the low energy requirement. The reason for this low energy requirement is that no phase transition is taking place (except with pervaporation). Other advantages of membrane technology are ease of operation, high reliability, adaptability, low operating and capital cost, ease of scale-up, compact size, modular configuration, and environmentally friendliness (Bitter, 1991; Mannan *et al.*, 2013).

2.1.2 Membrane classification

A membrane is generally defined as a barrier or thin interface that selectively passes certain molecules while retaining other molecules (Mulder, 1992). This interface can be either molecular homogeneous (uniform in composition and structure) or chemically or physically heterogeneous (containing pores of different dimensions). The molecules to be separated can be either in liquid or gas form (Baker, 2012). Membranes can be categorized in different ways. Figure 5 depicts a classification based on morphology: symmetric and asymmetric membranes are further broken down into different types of membranes. Symmetric membranes have uniform pore size or structural morphology throughout the cross section of the membrane. In asymmetric or anisotropic membranes there is a gradient in pore morphology. This is usually a dense skin layer on a porous support layer (Gohil, JM;Choudhury, 2019). If the dense layer is produced from the same material as the underlying support layer, it is known as an integrally asymmetric membrane. If the top dense layer is made from another material it is called a composite membrane. Thin film composite membranes consist of an extremely thin nonporous gas selective surface layer supported on a much thicker highly porous carrier material (Baker, 2012).

The porous carrier material provides the required mechanical strength but does not contribute to transport resistance. Because material transport is inversely proportional to the membrane thickness this configuration gives sufficiently high flux. Only integrated asymmetrical and composite membranes are currently used industrially for the separation of gases (Maier, 1998).

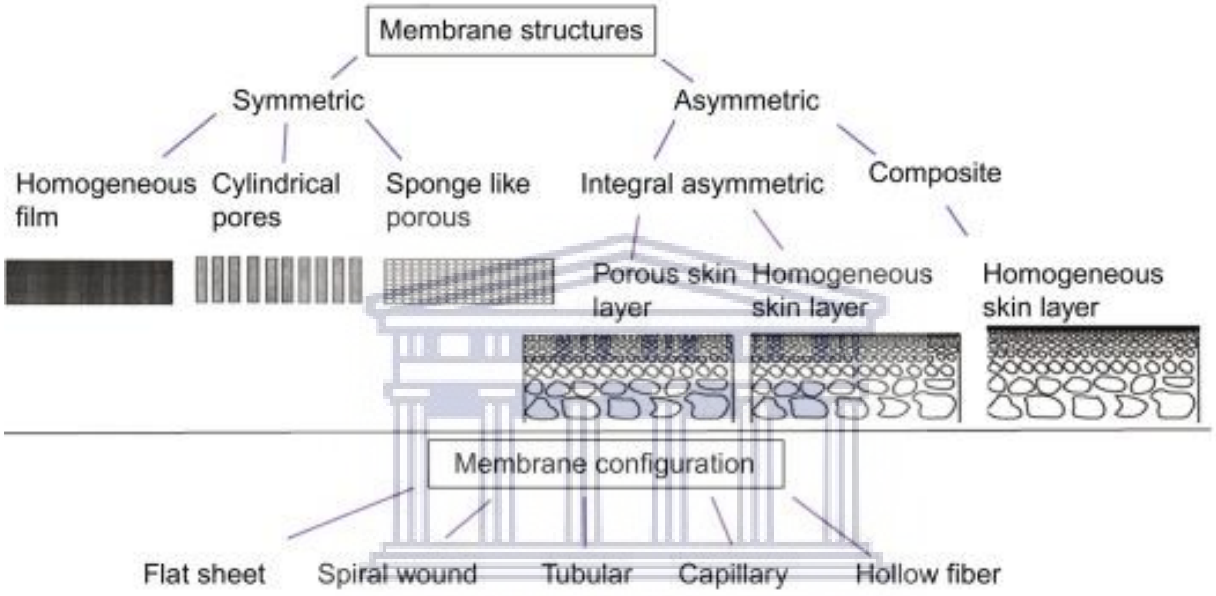

Figure 5 Membrane classification according to morphology (Gohil, JM;Choudhury, 2019)

Porous membranes are mainly used for microfiltration and ultrafiltration, whereas dense membranes are used for gas separation and pervaporation (Mulder, 1992). The membranes that this research focusses on are anisotropic thin film composite membranes, with two layers of different polymers. The support layer is a porous polyethersulphone (PES) layer, and the composite substrate is a dense sulphonated polyethersulphone (SPES).

2.1.3 Gas transport through membranes

The fundamental parameters characterizing membrane separation performance are permeability and selectivity (Freeman, 1999). In gas separation, a gas stream is separated into a retentate and permeate. Separation of a mixture of gases is based on their transport rate within the membrane, which depends on their solubility and diffusivity in the

membrane material. This method of describing the transport is known as the solution-diffusion model. Permeants dissolve in the membrane material and then diffuse through the membrane under the driving force of pressure, concentration or an electrical potential gradient. In gas separation and vapour permeation, mostly dense membranes with an anisotropic structure are used to improve the rate of transfer (flux) (Baker, 2012).

In 1866, Graham postulated the mechanisms of gas permeation; the rate at which gases passed through a membrane did not correlate to the gas diffusion constant. This meant that transport does not occur through pores, but through the membrane material itself (through the voids of two polymer chains). Graham's model describes the transport of a gas through a nonporous polymer film occurring in three stages; first, the gas is dissolved in the membrane material (sorption), then the gas particles diffuse through the polymer (permeation), and finally the gas is released (desorption) (Freeman and Pinnau, 2004).

The permeability coefficient is an intrinsic material property, it gives the amount of gas permeating per second through a material with a surface area of 1 cm^2 and a thickness of 1 cm normalized for the driving force in cmHg. The gas permeating is expressed as a flux of gas at standard temperature and pressure ($cm^3_{STP}/(cm^2\ s)$) (Metz, 2003).

$$J = \frac{P}{d}\,(f\,i, feed - f\,i, permeate) \qquad 1$$

Where J is the flux, P is the permeability coefficient expressed in the unconventional but widely accepted unit of Barrer (1 Barrer= $1*10^{-10}$ cm^3_{STP} cm/-cm^2 s cmHg), d the membrane thickness (cm), and $f_{i,\,feed}$ and $f_{i,\,permeate}$ the fugacity's of component i on the high pressure side (feed) and low pressure side (permeate) (cmHg). For low pressure applications the fugacity's are equal to the partial pressure (Metz, 2003).

According to this relationship, the quantity of a gas that passes through the membrane per unit time and area is proportional to the difference in pressure between the feed ($f_{i,\,feed}$) and permeate side $f_{i,\,permeate}$, and inversely proportional to the membrane thickness (d) (Maier, 1998).

Permeability is the proportionality constant, it is substance-specific and characteristic for each membrane material. It is the ability of a membrane to permeate molecules and is defined as:

$$P[Barrer] = 10^{-10} \frac{V[cm3\ (STP)]\ d\ [cm]}{A\ [cm2]\ t[s]\ \Delta p[Torr]} \quad 2$$

Where V is the permeate volume at standard pressure and temperature (STP), d is the membrane thickness, A is the membrane area, t is the time, and Δp is the pressure difference between the feed and the permeate sides (Maier, 1998).

$$P = D * S \quad 3$$

Where D is the diffusion coefficient (cm^2/s), and S is the solubility coefficient ($cm^3_{STP}/(cm^3\ cmHg)$) (Metz, 2003). It can thus be viewed as the product of the solubility coefficient and the diffusion coefficient (Maier, 1998).

Besides the permeability, another key characteristic of gas separating membranes is their selectivity. This ability of a membrane to separate two molecules is the ratio of their permeabilities, and is defined as:

$$\alpha_{AB} = P_A / P_B \quad 4$$

where P_A and P_B are the permeability coefficients of gases A and B, whereby the more permeable gas is taken as A in order for α_{AB} to be >1 (Yampolskii, 2012). Combining the ideal selectivity can be describes as:

$$\alpha_{AB} = (D_A/D_B) * (S_A/S_B)$$

$$\alpha AB = \frac{DA}{DB}\ \frac{SA}{SB} \quad 5$$

Where D_A/D_B is the diffusivity selectivity and S_A/S_B is the solubility selectivity (Yampolskii, 2012).

There is a relation between the permeability and selectivity of gases in polymer membranes; a highly selective polymer will show low permeabilities whereas a highly permeable polymer will be less selective. This is visualized in the Robeson plot, where the selectivity versus the permeability show this trade-off. In this plot, a linear upper bound in the double logarithmic of the permeability and selectivity is observed as is depicted in Figure 6. This correlation was analysed for thirteen gas pairs. The H_2O/N_2 gas pair is not among these gas pairs. Reason for this is that the relation does not hold for the permeance of water vapour in a mixture with a permanent gas. Most of the highly selective polymers also have a very high water permeability (Metz, 2003; Pereira Nunes and Peinemann, 2006).

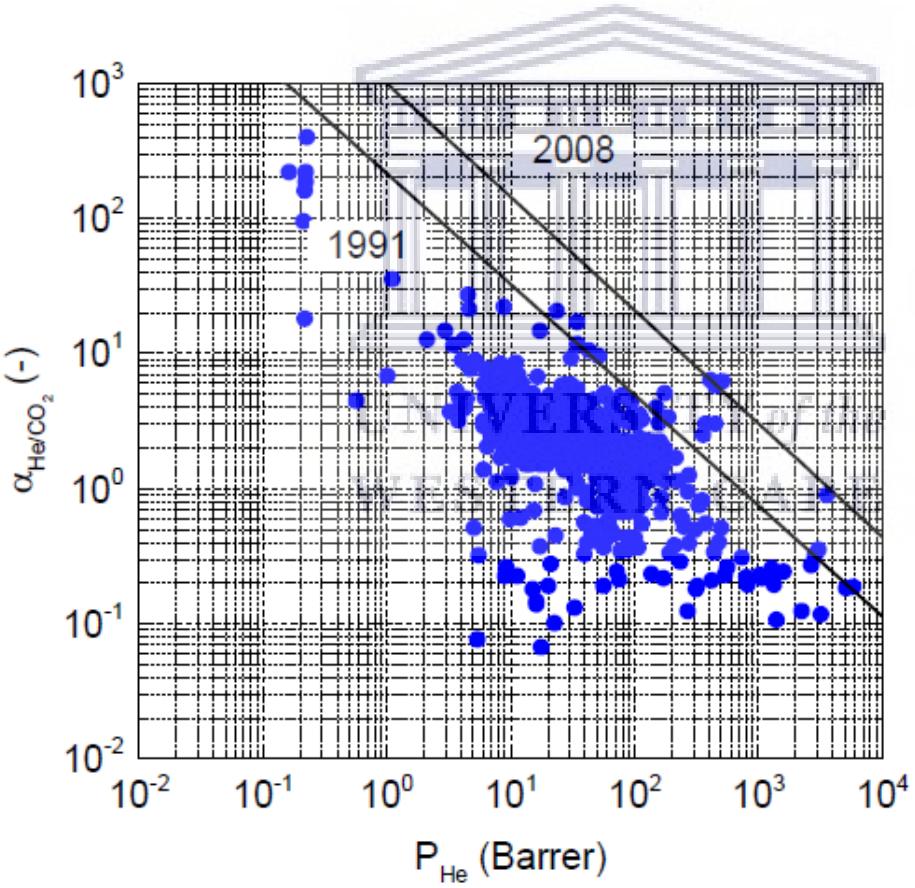

Figure 6 Robeson plot for He/CO_2 gas pair. The two upper bounds visualize the improvement in polymer materials for this separation from 1991 to 2008. All data points are measured at P=2 bar and T =35°C (B.G. van Campenhout, 2017)

Because one component is more readily transported than other components, the retained molecules will accumulate near the membrane surface, this results in a highly

concentrated layer near the membrane surface which applies a resistance towards mass transfer. This phenomenon is known as concentration polarization. Concentration polarization reduces the permeation through the membrane and consequently the selectivity. This phenomenon is inherent to membrane separation processes (Mulder, 1992; Baker, 2012).

The efficiency of membranes depends upon the chosen material (permeability, selectivity), the membrane structure and thickness (permeance), the membrane configuration (e.g. flat sheet or hollow fibres), and the module and system design. In the next sections the relevant topics are discussed in regards to membranes for water vapour recovery. In addition, the fabrication process of membranes are discussed, as well as polymer modification methods.

Despite the widely accepted reference to the Barrer as a unit for permeability, this unit is converted into the SI unit in present study (1 Barrer = 10^{-10} mol/(m^2 s Pa)).

2.1.4 Polymer classification

Polymers can be classified based on their molecular rigidity; rubbery with an elastic molecular structure, and glassy polymers with a rigid molecular structure. An amorphous polymer kept above its glass transition temperature (Tg) is in a rubbery state, it has a relatively large amount of free-volume because of transient voids between the highly mobile polymer chains. When the temperature is lowered below its Tg, the polymer behaves as a rigid glass; the fractional free-volume decreases, which results in insufficient space for large-scale collective movements of the polymer backbone (Bernardo, Drioli and Golemme, 2009).

In general, glassy polymers tend to be more selective, and less permeable, whereas rubbery polymers tend to be more permeable and less selective. This behaviour can be understood on the basis of the structural properties of glassy and rubbery polymers. The rigidity of glassy polymers restricts the passage of gas molecules, resulting in a high selectivity, the polymers prefer the permeation of small molecules over larger ones.

Whereas in rubbery polymers with their flexible polymer chains that can rotate along their axis, gas passes at a high rate, permeation of large molecules is preferred over small ones resulting in increased permeability, but at the expense of selectivity (Baker, 2006). The reason selectivity of gas pairs is different in glassy and rubbery polymers is the competing effect of the mobility selectivity term and the solubility selectivity term. The diffusion coefficient decreases with increasing molecular size, because large molecules interact with more segments of the polymer chain than small molecules, therefore the mobility selectivity always favours the permeation of small molecules over large ones. The solubility coefficient of gases and vapours is a measure of the energy required for the gas to be sorbed by the polymer, and increases with increasing condensability of the permeant. The dependence on condensability means that the solubility coefficient usually increases with molecular size, because large molecules are more condensable than smaller ones. Therefore, the solubility selectivity favours the permeation of larger more condensable molecules, such as hydrocarbon vapours over permanent gases such as oxygen and nitrogen. It can be concluded that the effects of permeant molecule size on the mobility and sorption selectivities are opposed (Baker, 2006).

The selection of a polymer material for a gas separation (GS) application is based on a good combination between permeability and separation selectivity, excellent film-forming properties, durability, mechanical strength, thermal and chemical stability under required operating conditions, absence of micro-defects, and lack of aging (because it leads to reduced permeability over time). Almost all industrial membrane GS processes utilize glassy polymers because of their high gas selectivity and good mechanical properties (Mannan *et al.*, 2013).

2.1.5 Membrane configurations

The configuration of membranes refers to the geometry of the membranes and their position in space in relation to the flow fluid and of the permeate. It includes the manner in which the membrane is packed inside the modules, as most industrial installations are of modular design. Different configurations are possible for the membranes; plate-and-frame, spiral-wound, tubular, capillary and hollow fibres are the most commonly used

configurations for polymeric membranes. The geometry is planar/flat in the first two and cylindrical in the latter three. The diameter size differences between the cylindrical membranes is shown in Table 2. The membrane surface area per volume is a function of the dimensions of the tubes. The choice for a certain membrane configuration is based on economic consideration, ease of cleaning, maintenance and operation, compactness, scale, and potential membrane replacement (Harmison, no date).

Table 2 Membranes with cylindrical configuration (Harmison, no date)

Configuration	Diameter (mm)
Tubular	10.0
Capillary	0.5-10.0
Hollow fibre	<0.5

In the plate and frame module a set of two membranes are placed in a sandwich-like fashion with their feed sides facing each other. A suitable spacer is placed between the two membranes. This spacer improves mass transfer and reduces concentration polarization. Stacking several membrane sets builds up to a plate-and-frame module. Figure 7 shows the schematic flow in a plate-and-frame module.

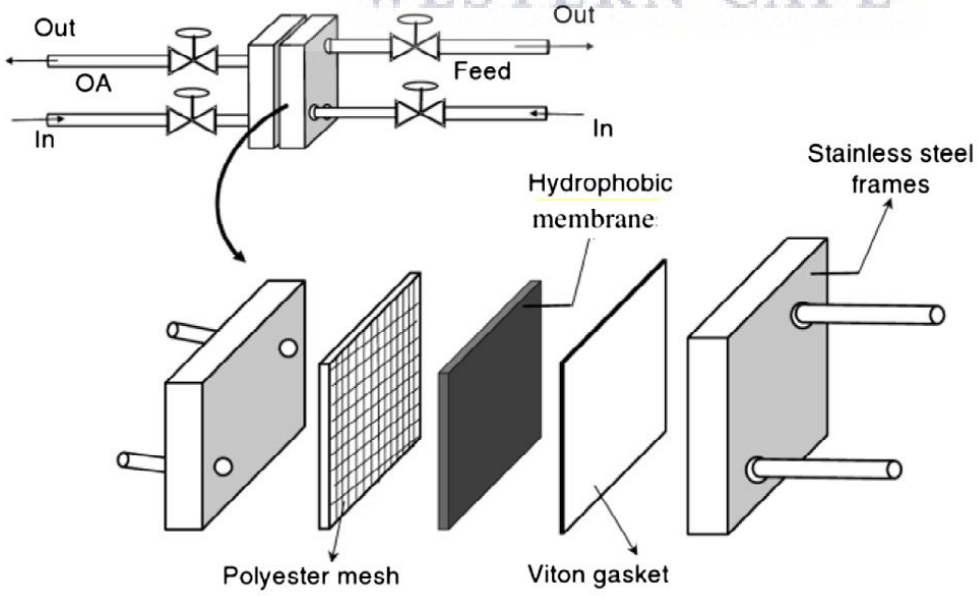

Figure 7 Schematic view of plate and frame module (Pabby, A.K; Rizvi, S.S.H; Sastre Requena, 2015)

The spiral-wound module is in fact a plate-and-frame system wrapped around a central collection pipe. The packing density of this module is between 300-1,000 m^2/m^3. Membrane and permeate-side spacer material are glued along three edges to build a membrane envelope. The feed flows axially through the cylindrical module parallel along the central pipe whereas the permeate flows radically towards the central pipe. Figure 8 shows a schematic view of a spiral-wound module. Spiral wound modules are encased in a separate pressure vessel that is independent of the module itself (*Minnesota Water Works Operational Manual*, 2009).

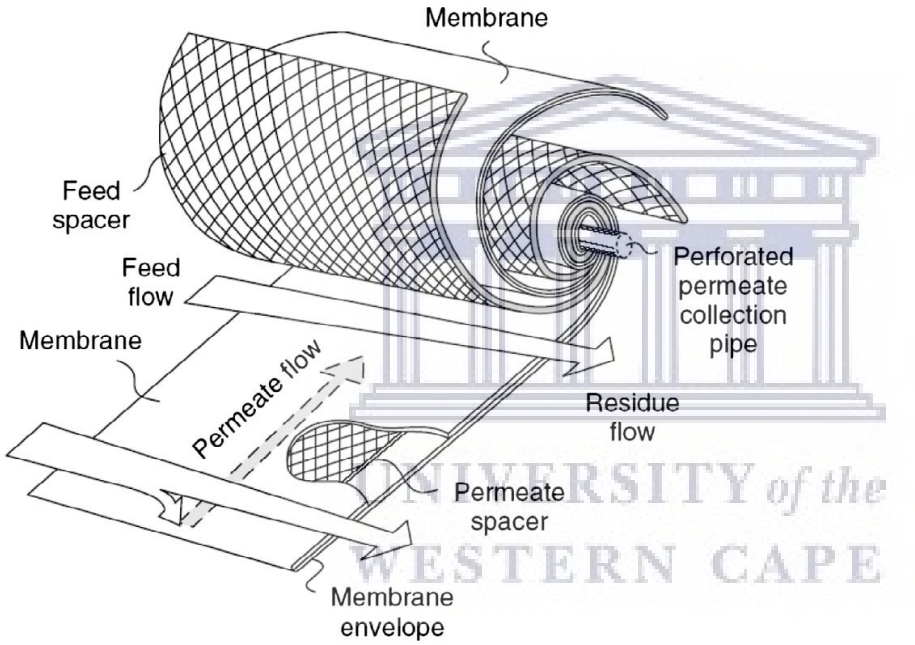

Figure 8 Schematic view of spiral-wound module (Zhani, K; Zarzoum, K;BenBacha, H; Koschikowski, J; Pfeifle, 2015)

When designing a membrane module system, a high permeance is desirable. A high permeance means a high flux using a relative small amount of membrane area to produce a given volume flow of permeate gas, which results in the need of fewer membrane modules and lower capital costs (Baker, 2006).

For water vapour selective membrane applications, the desired production rate is in the order of several cubic meters per day, meaning that several thousands square meters of membrane area are required. Configurations showing high packing densities are

therefore attractive. Flat membrane module configurations may be more reliable, but a higher packing density is achieved with a cylindrical configuration which is often also more economical (Bergmair, 2015).

In contrast to capillaries and hollow fibres, tubular modules are not self-supporting. Tubular modules are placed inside porous stainless steel, ceramic, or plastic tubes, with the tube diameter generally being more than 10 mm. The feed solution always flows through the centre of the tubes into the module housing as is shown in Figure 9.

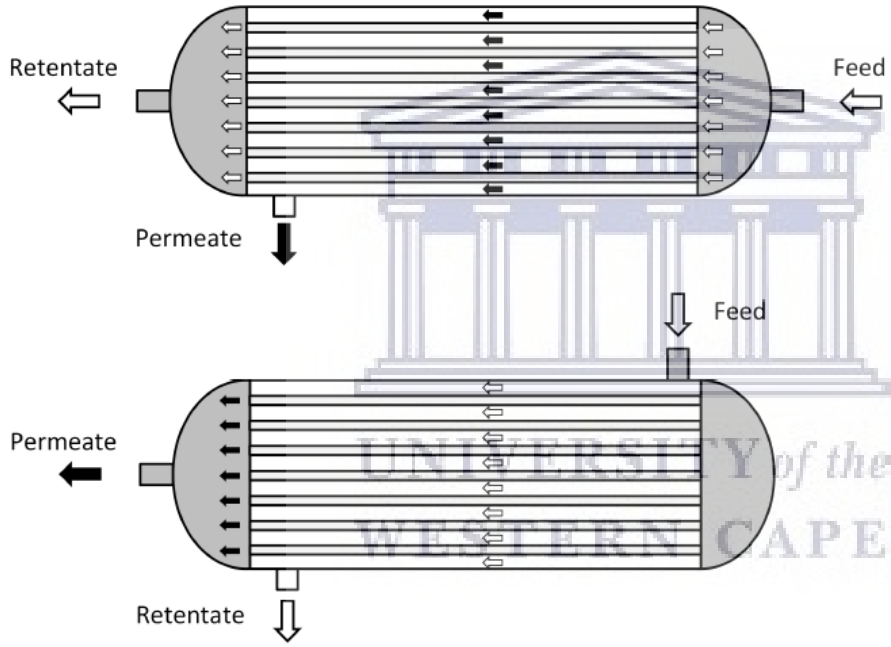

Figure 9 Tubular membrane module; bore feed and shell feed type, white arrows indicate retentate flow, black arrows indicate permeate flow (Chourou *et al.*, 2017)

Capillary modules consist of a large number of capillaries assembled together. The ends of the fibres are sealed with agents such as epoxy resin, polyurethanes or silicone rubber. A packing density of 600-1,200 m^2/m^3 is obtained with modules containing capillaries.

The concept of hollow fibre modules is similar to the capillary modules, the difference is in the dimensions. The hollow fibres are arranged in a loop and are sealed on the permeate side. The hollow fibre membrane module is the configuration with the highest packing

density; 30,000 m^2/m^3. They have the advantage of a high surface area, can easily be developed into modules, have a high membrane area to module volume ratio which results in high productivity per volume unit and cost efficient production. In addition, polymers are easily processed into hollow fibres (Bernardo, Drioli and Golemme, 2009). The hollow fibre membrane in microscale, and multiple membranes built into a module (macroscale) is depicted in Figure 10.

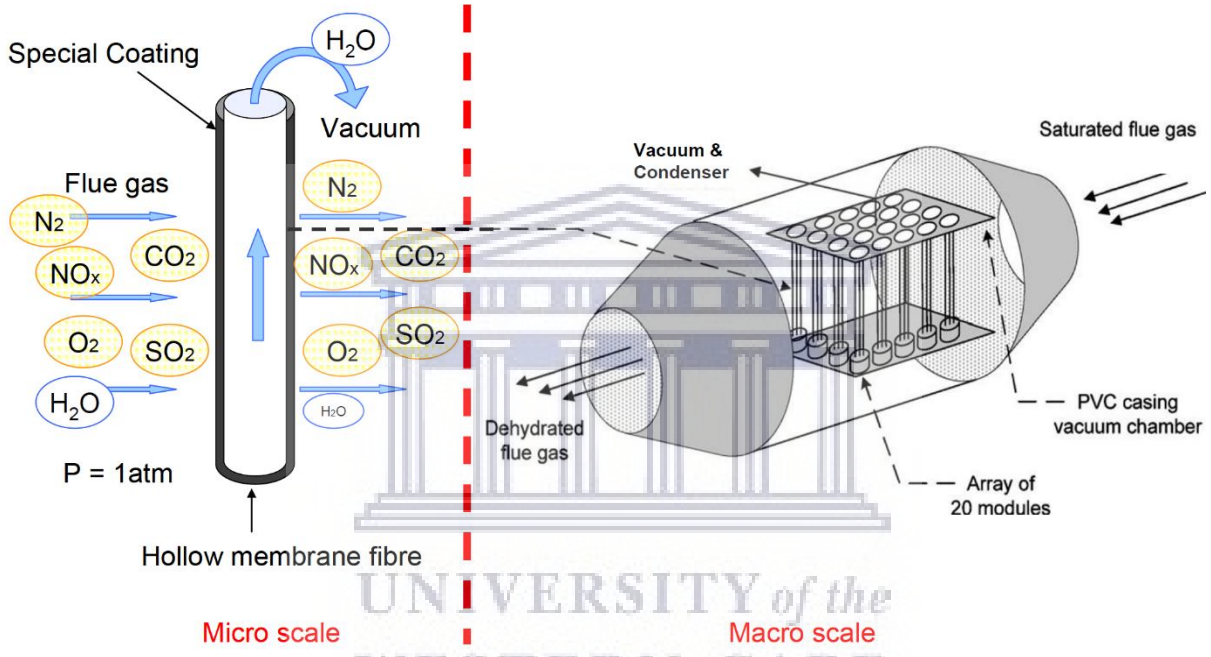

Figure 10 Schematic view of a HF membrane and HF membrane module

An overview of certain characteristics of these different configurations is provided in Table 3.

Table 3 Overview of properties of module configurations (Rackley, 2007)

	Tubular	Plate and frame	Spiral-wound	Capillary	Hollow fibre
Packing density (m^2/m^3)	Low 300-1,000	200	300-1,000	600-1,200	Very high 1,500-10,000
Module cost (ZAR/m^2)	High	→	→	→	Low
Fouling tendency	Low	→	→	→	Very high
Cleaning	Good	→	→	→	Poor
Membrane replacement	Yes/No	Yes	No	No	No

The operational modes for the capillary and hollow fibre membrane modules can be divided in two flow patterns: a) flowing the feed through the bore (lumen) of the capillaries/fibre, and collecting the permeate on the outside of the capillaries/fibres; this is the inside-out mode, or b) the other way around, outside-in, whereby the feed solution enters the module on the shell side (external) of the capillaries/fibres and then the permeate passes into the fibre bore.

The flow of the feed through the membrane module determines the pressure loss and thus the work requirement. Additionally the flow pattern influences the local vapour distribution and therefore the permeation efficiency. Boundary layer effects such as concentration polarization can play an important role in the resistance to vapour permeation. Comparing the two operational modes, the inside-out configuration provides a more controllable environment where boundary layer effects can be accounted for (Bergmair, 2015). Concentration polarization is discussed in the following paragraph.

There are different flow operations possible: co-current, cross-flow, counter current, and perfect mixing. Figure 11 shows a schematic overview of the various flow operation modes. To reduce concentration polarization and fouling as much as possible, the membrane process is generally operated in a cross-flow mode. Fouling is the partial

blocking of the membrane due to the deposition of fly ash or condensed water, which results in a decreased permeation flux of membranes. The adsorption of solutes onto solid surfaces could be attributed to different types of interactions, such as hydrophobic interactions, H-bonding and van der Waals interactions, and electrostatic effects (Kim, Choi and Tak, 1999). As far as these flow operation modes matter, counter current flow is the best possible flow operation mode.

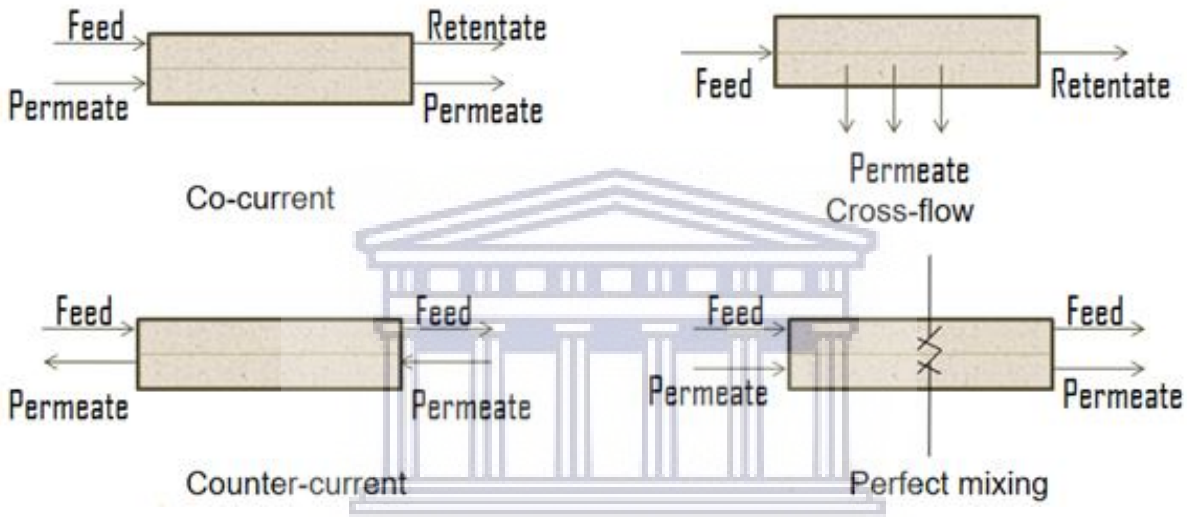

Figure 11 Various flow operation modes (Harmison, no date)

Furthermore, there are several modes of operation; single-pass, batch, fed-batch, continuous and multi-stage. In the single pass system, the retentate is not recirculated through the membrane module as is the case with the other modes. Because the permeate flux in membrane filtration is usually very low compared to the flow rate across the membrane surface, single pass processes achieve only small values of the volume concentration ratio. Therefore, the application of single pass operations is limited to situations in which the rate throughput is low and a large membrane surface is available. The modes of operation won't be discussed here as it falls outside the scope of this study (Doran, 2013).

2.1.6 Membrane applications for gas separation

Polymeric membranes for gas separation and purification can be used for separation of many imaginable gas mixtures. However, economically viable gas separations are currently limited to the following industrial processes:

- Hydrogen removal from ammonia purge gas (first application of GS membranes)
- Separation of air into its constituent gases to obtain nitrogen or oxygen enriched air (for the food and medical industry, and industrial combustion)
- Hydrogen recovery from the effluent streams of natural gas (separation of H_2/N_2 H_2/CH_4 and H_2/CO in refineries and the petrochemical industry at large)
- Removal of water, H_2S and CO_2 for natural gas upgrading (natural gas sweetening) which minimizes pipeline corrosion and improves the calorific value
- CO_2 removal for enhanced oil recovery
- Separation of CO_2/N_2 mixtures (for the treatment of flue gas)
- Separation of CO/H_2 during production of a variety of organic and inorganic compounds such as alcohols, aldehydes, acrylic acids and ammonia
- Recovery/recycling of helium from natural gas
- (Organic) solvent dehydration such as the production of anhydrous ethanol for the pharmaceutical industry (Bolto, Hoang and Xie, 2012; Yampolskii, 2012).

The rapid growth of membrane technology in gas separation is due to the implementation of new preparation methods (such as hollow fibre spinning) that allowed for a reduction of the effective thickness of the selective layer with increased permeation rate and membrane surface area as a result. In addition, the progress achieved in material science (improved and tailored properties of the materials) and in the design of membrane units (patterns closer to ideal counter current flow mode) allowed for this advancement in membrane technology (Bernardo and Clarizia, 2013).

Not yet industrialized but promising future applications include:

- Removal of SO_2 (desulphurization) and NO_x from exhaust fumes
- Separation of paraffin/olefin (de Miranda *et al.*, 2019)

Membrane technology for gas separations is gaining attention from the industry because of their advantages over conventional separation technologies, such as energy efficiency with low capital investment, simplicity and ease of installation, low operation and maintenance costs, low weight and space requirement with high process flexibility (Maier, 1998; Srivastava and Jozewicz, 2001; Yampolskii, 2012; Mannan *et al.*, 2013; Sridhar, Bee and Bhargava, 2014).

2.2 Water Vapour Recovery using membrane technology

2.2.1 Flue gas and dehumidification

The energy content of flue gas consists of both sensible heat and latent heat (Delgado and Herzog, 2012). The temperature of the flue gas leaving the boiler is typically in the range of 300-450˚C and it is common practice to recover the sensible heat in the air heater until the temperature of flue gas reached approximately 150˚C (Babcock&Wilcox, 2015). Regenerative type heat exchangers are commonly used for this purpose. Thereafter, the flue gas is heated again to prevent acid condensation on the heat transfer surfaces of heat exchanger and stack. The temperature of flue gas at the air heater/reheater exit is typically 10˚C above the acid dew point temperature (Sarunac, 2010). The remaining sensible heat cannot be recovered because of the risk of acid condensation. It is eventually lost with discharge of flue gas through the WFGD unit or, in plants without a WFGD unit, it is lost through the stack (Sarunac, 2010). The voluminous gas stream is transported to the stack using ventilators or induced draught fans, after which it is emitted into the atmosphere (Copen, Sullivan and Folkedahl, 2005). Figure 12 shows a simplified schematic view of a pulverized coal power plant.

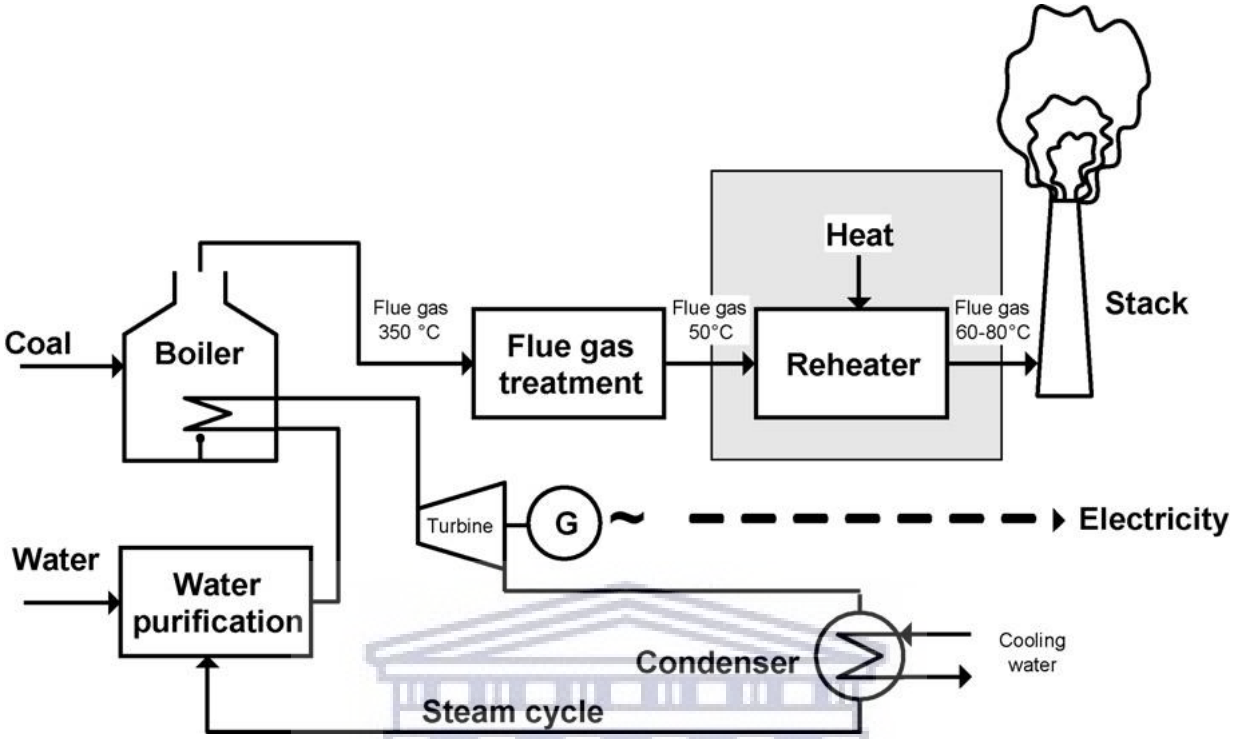

Figure 12 Simplified diagram of power generation in a coal fired power plant (Sijbesma *et al.*, 2008)

As discussed in the introduction, the removal of water vapour from flue gas would make reheating of flue gas redundant. Membrane technology is an attractive alternative for molecular separations including water vapour removal because of its high energy efficiency and its reliability (due to the lack of moving parts). The process is continuous, has a small footprint, and no regeneration is needed. It allows the selective removal of water vapour from flue gas streams and produces water with high purities without additional heating. The polymers used for water vapour recovery are chemically robust under corrosive conditions (Sijbesma *et al.*, 2008; Singh and Berchtold, 2017).

A driving force for permeation in the membrane is required: this can either be a sweep gas or a vacuum at the permeate side. Using a vacuum is beneficial because water vapour condenses easily, and by condensing the permeate, the vacuum can be retained because the permeate pressure stays constant. It is economical because the overcapacity of the condenser that is already present in the power plant is providing the driving force for water vapour permeation. Additionally, removal of non-condensable gasses such as N_2, O_2, CO_2 and acidic gases takes place (Sijbesma *et al.*, 2008).

After applying a vacuum, a natural diffusion mechanism begins in order to re-establish the equal distribution of the gas molecules inside and outside the tubes. Since the membrane is highly selective towards water molecules, only water molecules can pass through the membranes, collecting on the inside of the tubes (Sijbesma *et al.*, 2008). The recovered water is of high quality and mineral-free. It can be transported directly to the existing condenser system, where it is added to the water steam cycle as additional water to compensate for the steam/water losses (Carpenter, 2012). No waste water is produced, and the pressure drop that occurs over the membrane unit is compensated with an induced draught fan. The major energy input is electricity to run the vacuum pumps. Furthermore, the water selective membranes can be combined with CO_2 selective membranes to lower CO_2 emissions simultaneously (Carpenter, 2012). Ultimately, reheating the flue gas to avoid condensation in the stack would no longer be necessary if water is removed below the dew point of the exiting flue gas.

The flue gas stream is a chemically challenging stream due to the presence of SO_x and NO_x, which are corrosive. Table 4 shows the typical flue gas composition after the flue gas desulphurization unit and before reheating.

Table 4 Typical flue gas composition (Sijbesma *et al.*, 2008)

Typical flue gas composition	
N_2	70-72 %
CO_2	13-14 %
O_2	3-4 %
H_2O	6-20 %
SO_x	200 ppm
NO_x	200 ppm
HF/HCl	10 ppm
Temperature	50-180˚C

2.2.2 Positioning of water vapour recovery membrane unit

The membrane unit can be positioned directly into the flue gas stream, after the flue gas treatment unit, or before the stack as is shown in the diagram in Figure 13. The reheating

unit (needed to prevent condensation of the otherwise saturated flue gas stream) may still be required to assist with the dissipation of the plum. Ideally, the membrane dehydration unit would be placed directly downstream the flue gas desulphurization unit. The flue gas desulphurization unit uses aqueous lime/limestone slurry and fully saturates the flue gas stream. This, combined with high temperature before flue gas purification and high concentrations of aggressive gases and fly ash, makes the use of polymeric membranes earlier in the process unattractive (Sijbesma *et al.*, 2008). However, a drawback of placing the membranes directly into the flue gas stream is fouling. Fouling is caused by the deposition of fly ash or other particles onto the membrane. This decreases the water vapour permeation. It is reported that fly ash dust and gypsum crystals were deposited onto membranes that were operational in a real flue gas stream (Sijbesma *et al.*, 2008; Bram *et al.*, 2011). Since the membranes were partly covered with these particles, the effective membrane area available for permeation was reduced which resulted in a decrease in the water vapor permeability. Cleaning of the membranes restored the water flux to 65-70 % of its original value (Sijbesma *et al.*, 2008).

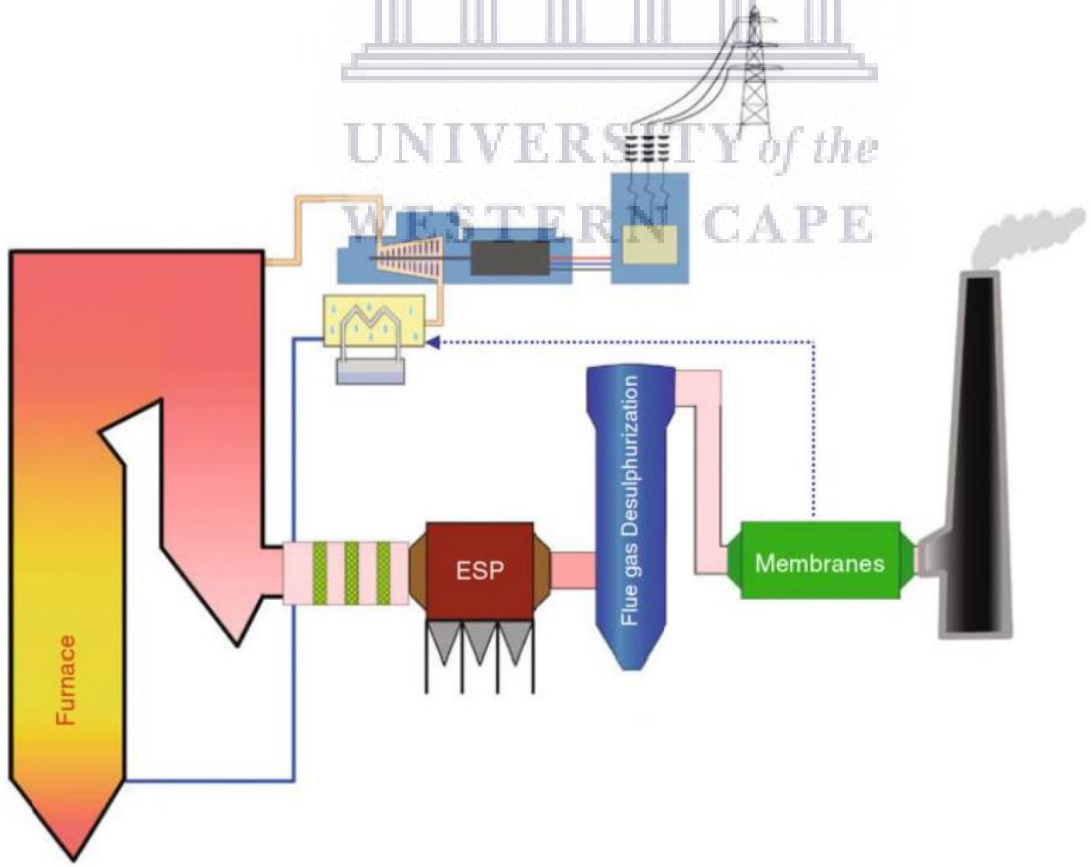

Figure 13 Position of a water vapour recovery membrane module in a power plant

The membranes to be used for water vapour recovery require high water vapour permeability because of the large volumetric flow rates of flue gas associated with the production of electricity combined with the limited driving force. Additionally, the membranes must have high water vapour selectivity over non-condensable gases. Essentially, applying energy should aim at the removal of water and not other gases to make the process more economically attractive (Metz, 2003).

There are four preliminary process configurations possible:

- Membrane contactor (Gas-Liquid), which is based on the water vapour pressure difference between hot flue gas and cold boiler water.
- Sweeping gas configuration, where a sweep gas is used to create a partial pressure driving force followed by condensation of water from the sweep gas to get clean water.
- Pervaporation configuration, whereby a partial pressure driving force is created by applying a vacuum on the permeate side. This is followed by the use of a condenser to recover clean water. A low gas permeability is required to minimize vacuum duty. Cooling water is used for water vapour condensation at the permeate side.
- Vapour compression configuration is a variation of the above mentioned pervaporation configuration. It uses vapour compression to condense water vapour. A very low gas permeability (N_2 and CO_2) is required to minimize compression duty (Singh and Berchtold, 2017).

2.3 Membrane types, materials and synthesis

For gas separation purposes, nonporous membranes are preferred. Symmetric dense films are capable of separating mixtures effectively. However, transport in dense membranes usually takes place by diffusion and has a low permeation rate (flux). Hence, the selectivity might be high, but permeability remains low. The usual membrane thicknesses (20-200 μm) have low permeation rates as the flux is inversely proportional to the membrane thickness. To increase the flux through these membranes, the effective membrane thickness must be reduced as much as possible. However, if they are made

thinner (0.1-1 μm) to improve permeation, mechanical strength might be compromised. Therefore, the development of anisotropic (asymmetric) membranes is of major importance. In these membranes a thin dense layer of membrane material (<0.5 μm) is deposited upon a more porous sublayer (50-200 μm). The selectivity and permeation rates are determined by the thin top layer whereas the porous layer provides the required mechanical support. This results in a higher permeation rate than symmetric membranes of comparable thickness (Mulder, 1992).

The advantage of anisotropic/thin film composite membranes is: (i) the independent selection of material from which the separating layer and porous support layer are formed (ii) the preparation of the separating (selective) layer and the porous (support) layer is done independently, which allows for optimization of each structural element with respect to selectivity, permeation rate, chemical and thermal stability, and (iii) expensive material can be used for the formation of the selective layer because only a small amount of material is required (~1 g polymer/m^2 of membrane for a 1 μm thin selective layer) (Pinnau, 2000). The porous support structure is typically an asymmetric ultrafiltration type of membrane prepared by the immersion precipitation process (phase inversion) as described in Appendix 2.

The following properties for the support structure are required: (i) the porous structure should be chemically resistant against the solvent/solvent mixture from which the thin selective layer is formed (ii) the porous support should have high surface porosity and small pore size. High porosity is essential because the support layer should not provide any significant resistance to mass transport in a composite membrane, and a small pore size is important for the deposition of ultrathin defect-free coatings (Pinnau, 2000).

For applying the selective thin film onto the support structure, several techniques are possible, such as lamination of a pre-formed film, plasma polymerization, interfacial polymerization, in-situ polymerization, grafting, dynamic membrane formation and solution coating (dip-coating). Besides dip-coating all these techniques involve polymerization reactions (Pereira Nunes and Peinemann, 2006).

In this work dip-coating is the method used to prepare the selective top layer, therefore it is discussed in detail. Dip-coating is a very simple and useful technique for preparing composite membranes with a very thin but dense top layer. A porous asymmetric membrane is immersed in the coating solution containing the polymer, prepolymer or monomer with a low concentration of the solute (<1 %). When the support membrane is removed from the bath containing the coating material and the solvent, a thin layer of solution adheres to it. By heating the prepared membrane in an oven the solvent evaporates and crosslinking occurs, which is the formation of chemical bonds between the polymer chains. Crosslinking leads to the thin dense layer becoming fixed to the porous sublayer and is needed because the coated layer has no mechanical or chemical stability itself, and its separation performance is not sufficiently high in the non-crosslinked state (Pereira Nunes and Peinemann, 2006).

In choosing the polymer for the support structure and the polymer for the selective layer, compatibility between the two layers is crucial. In choosing the solvent for the polymer of the selective layer (SPES), a requirement is that the solvent does not dissolve the support polymer (PES) as well.

2.3.1 Selection of polymer materials

Several polymers have been used to prepare membranes for the dehydration of gas streams. Requirements for polymers to be used in membranes for water vapour recovery are chemically robustness under corrosive conditions, good selectivity and permeability, and the ability to form very thin skin layers of composite membranes. (Bergmair, 2015; Singh and Berchtold, 2017) Furthermore, the materials should be almost impermeable to other gases like nitrogen or carbon dioxide. The commercial polymers Pebax®, Nafion®, as well as experimental sulphonated polyetheretherketone (SPEEK), polyethylene-oxide poly(butylene terephthalate) block polymer (PEO-PBT), and poly-dopamine are some of the polymers that are water vapour selective. Additionally, graphene based polymers have shown extremely high vapour permeance (Bergmair, 2015).

The chemical structure of a polymer determines the permeability for water vapour as well as the permeability for other gases. Table 5 shows the permeability values and corresponding values for the H_2O/N_2 selectivity of the most commonly used polymers for water vapour separation.

Table 5 Permeability and selectivity of main polymers (Sijbesma *et al.*, 2008)

Material	Water vapour permeability (Barrer)	Water vapour/N_2 selectivity (a.u.)
SPES	$1.5*10^4$	$2*10^5$
SPEEK	$7*10^4$	$1*10^7$
PEBAX1074	$1.6*10^5$	$2*10^5$

Water vapour permeability and H_2O/N_2 selectivity depend strongly on which material is used for the membrane. Materials that are interesting for flue gas dehydration are located in the shaded area in the upper right corner of Figure 14. It is seen that SPEEK, SPES and PEBAX1074 are the most promising materials (Metz, 2003). PEBAX combines a high water vapour permeability with a moderate selectivity and is commercially available. SPEEK combines an even higher water vapour permeability with an extremely high water vapour-N_2 selectivity.

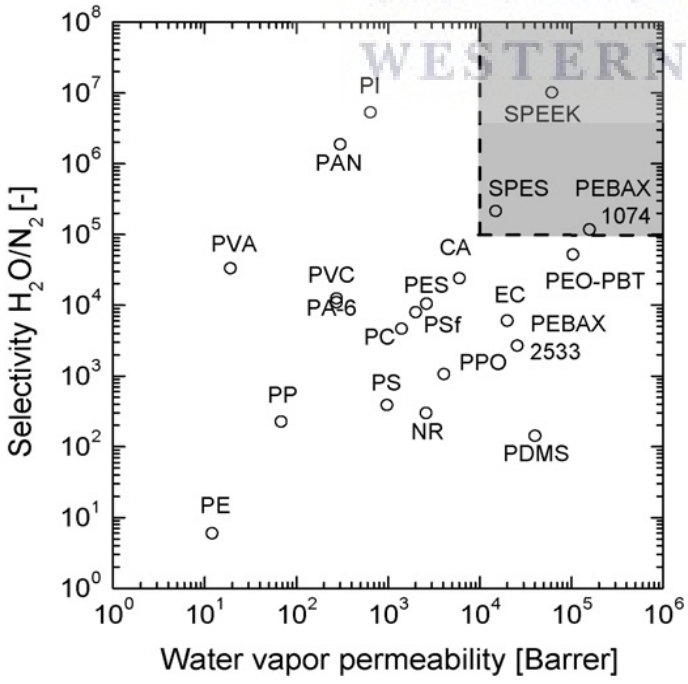

Figure 14 Water vapour permeability versus H_2O/N_2 selectivity for various polymeric membranes at 30°C (Sijbesma *et al.*, 2008)

SPES may not have the superior permeability and selectivity as SPEEK but this may be related to limited research efforts. The results available in literature do not disclose the sulphonation degree which is an important parameter. SPES is likely to be more compatible with PES support structure since it has the same polymer backbone. A better compatibility may allow for thinner membranes to be formed yielding a higher permeance despite the lower perceived permeability.

As described previously, a higher selectivity is accompanied by a lower permeability. However, this relation does not hold for the permeance of water vapour in a mixture with a permanent gas. Most of the highly selective polymers also possess a very high permeability (Metz, 2003). However, these permeability and selectivity values are obtained from pure gas permeabilities by calculating the ratio of the permeabilities for each species. In real gas mixtures, water may swell the membrane and may affect the transport rate of the other permeating species. The effect of the process conditions on the transport of water/gas mixtures is hardly researched (Metz *et al.*, 2005).

2.3.2 Sulphonated polyethersulphone

Polyethersulphone is a high performance engineering thermoplastic polymer which is fully devoid of aliphatic hydrocarbon groups. Its glass transition temperature is 230°C. The structure formula is shown in Figure 15. PES has good mechanical properties, and excellent thermal and chemical stability. However, the hydrophobic character of polyethersulphone, which prevents spontaneous wetting with aqueous media, is a drawback (Pereira Nunes and Peinemann, 2006). As a result, the fibres should be prevented from drying completely as this causes irreversible damage such as pore collapse/shrinkage due to capillary forces and fibre brittleness. To avoid damage to the membranes, the fibres should be treated with a hydrophobic agent such as glycerine before drying and storage. Another disadvantage of hydrophobic material is the fact that it often possesses a powerful nonspecific adsorption capacity which causes fouling and leads to rapid deterioration of the membrane permeability. To circumvent the disadvantages of the hydrophobic membranes, several methods are available to make membrane surfaces more hydrophilic (Pereira Nunes and Peinemann, 2006).

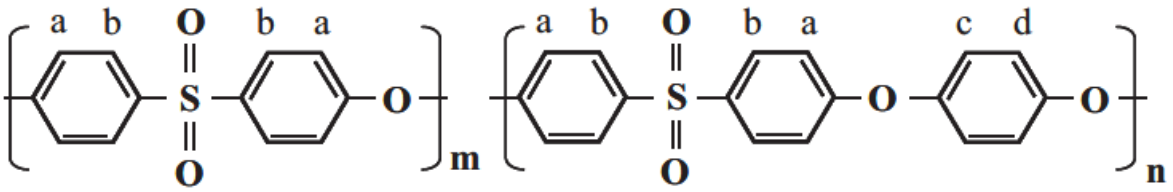

Figure 15 Chemical structure of polyethersulphone (Klaysom *et al.*, 2011)

One such method is sulphonation. Sulphonation is a successful method for the incorporation of other hydrophilic polymers which are soluble in water. However, hydrophilization of membranes by using large quantities of water-soluble polymers has the disadvantage that the hydrophilic nature of the membrane constantly decreases when they are used in aqueous media, since the water-soluble polymer is washed out. Therefore, the sulphonation degree should be controlled to limit the water solubility of the resulting polymer. Insolubility can also be achieved by crosslinking with additives such as polyols or polyphenols (Pereira Nunes and Peinemann, 2006). Sulphonation is an aromatic electrophilic substitution reaction where electro-donating substituents favour the reaction, whereas electro-withdrawing groups do not. Therefore, it is difficult to sulphonate PES because of the electron withdrawing effect of the sulphone linkages which deactivate the adjacent aromatic links for electrophilic substitution (Guan *et al.*, 2005).

Sulphonated polyethersulphone is a sulphonic acid functionalized poly(arylene) ionomer in which the aromatic rings of the polymer backbone are connected through alternate sulphone (-SO_2-) and ether (-O-) linkages as is shown in Figure 16. The sulphonic group is generally attached to the activated position ortho of the aromatic ether. This also makes the polymer ion-exchangeable (Pica, 2016).

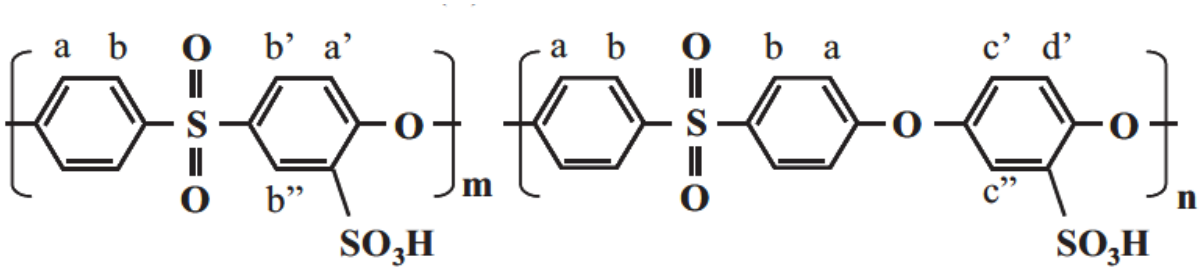

Figure 16 Chemical structure of sulphonated polyethersulphone (Klaysom *et al.*, 2011)

The sulphonate groups (SO_3^-) could be introduced using different methods, sulphonation can be done pre- or post-polymerization. Pre-sulphonation is done using modified monomers. When using the post-sulphonation route, suitable sulphonation agents such as chlorosulphonic acid, sulphur trioxide- triethyl phosphate complex, trimethylsilyl chlorosulphonate, acetyl sulphate or concentrated sulphuric acid can be used in sulphonation of the polymers (Klaysom *et al.*, 2011). The degree of sulphonation can be controlled by varying reaction time and temperature, and varying the sulphonating agent-to-polymer ratio. No more than one sulphonic group per repeat unit is generally substituted. Through a selective post-sulphonation reaction the backbone structure of PES is modified whereby locally and densely sulphonated PES is prepared on the pendant side phenyl groups along the main chains. SPES ionomers are soluble in widely used polar solvents such as dimethylformamide, dimethylacetamide, and N-4-methyl-2-pyrrolidone (NMP). SPES with high sulphonation degree is also soluble in (hot) water (Klaysom *et al.*, 2011; Pabby, A.K; Rizvi, S.S.H; Sastre Requena, 2015).

The microstructure of SPES membranes is affected by a microphase separation between hydrophobic and hydrophilic regions that occurs in the presence of water. The hydrophilic regions are responsible for water adsorption and the hydrophobic regions, made up by the polymer backbone, provide dimensional and mechanical stability. The sulphonation degree has an affect on the two phase separated microstructures and the water adsorption, which in turn influences proton conductivity and mechanical properties (Pica, 2016).

2.3.3 Summary of literature on membrane types, materials and synthesis

In this study, the synthesis-structure-property relationship of sulphonated polyethersulphone for use in water-selective membranes is reported. Sulphonate groups were introduced into PES polymer by means of a sulphonation reaction using chlorosulphonic acid. The optimal sulphonation degree is determined.

Informed by the literature review, the following can be concluded:

- Recovery of water vapour from flue gas using polymer-based composite hollow fibre membranes post WFGD can be a viable option, specifically when a power station is operated in areas with limited access to water. If at least 40 % of the water in the flue gas can be recovered, the power plant can shift from a nett water consumer into a nett water producer in a dry cooled power plant. Membrane technology for water vapour recovery has a high energy efficiency, and CO_2 can be captured simultaneously (Carpenter, 2012).
- The most effective configuration of membranes would be the hollow fibre configuration because hollow fibres can easily be developed into modules, have a high membrane area to module volume ratio which results in high productivity per volume unit and cost efficient production.
- PES could provide the appropriate support structure based on its thermal stability which is compatible with the ambient temperature range of flue gas.
- SPES is a suitable material for the composite layer due to its good permeation and selectivity properties. The ideal degree of sulphonation is determined.

2.4 Research questions

The research questions that need to be answered to accomplish the research aims, are as follows:

Table 6 Research questions

Main Research Question Can hollow fibre membranes be produced for potential use in water vapour recovery?
1) What is a suitable hollow fibre membrane support material, and can the HF support be produced at SAIAMC?
2) What is a suitable polymer for the selective layer with a promising permeability towards water vapour and a significantly high H_2O/N_2 selectivity?
3) How can the selective layer be formed onto the HF support?
4) What is a suitable solvent for selective polymer that does not dissolve polymeric supporting material?
5) Can the polymer for selective layer be synthesized by controlling reaction variables?
6) What is the optimum sulphonation degree of the selected polymer?
7) What are the chemical, physical and thermal properties of the membrane materials (both support and selective layer)?

These research questions can be further broken down into the following sub-questions.

With regards to synthesis:

- What are the appropriate process conditions for the synthesis of PES HF support?
- What are the optimal process conditions for the fabrication of SPES polymer?
- How can the functionalised SPES material be coated onto the polyethersulphone support hollow fibres?

And with regards to analysis:

- Can Fourier-Transform Infrared Spectroscopy be used to confirm the sulphonation of polyethersulphone?
- Can ^{1}H Nuclear Magnetic Resonance Spectroscopy be applied to determine the degree of sulphonation of sulphonated polyethersulphone composite material?
- Can the Ion Exchange Capacity be determined by titration?
- Can the Ion Exchange Capacity be used to calculate the degree of sulphonation of the sulphonated polyethersulphone selective material?
- What is the thermal stability of PES and SPES, at what temperature do these polymer materials decompose?
- What is the optimal degree of sulphonation for sulphonated polyethersulphone?

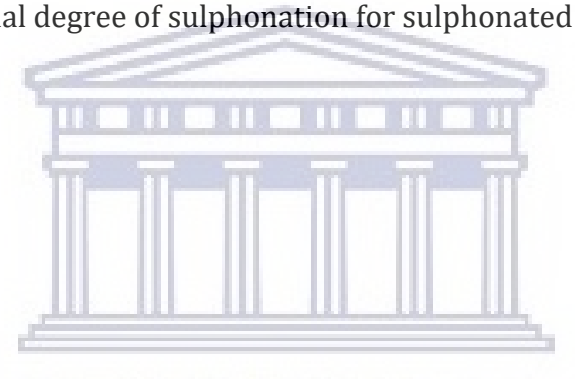

Chapter 3 Methodology for synthesis and analysis of polyethersulphone hollow fibres and sulphonated polyethersulphone

This chapter comprises of a description of the experimental methodology for the synthesis of the polyethersulphone support material: the spinning set-up and conditions are discussed as well as materials and chemicals used. The second part of this chapter encompasses of the methodology used for synthesis of the sulphonated polyethersulphone, whereby all synthesis conditions are discussed. The materials and chemicals used are listed. Furthermore, the physical and chemical characterisation methods for analysis of the support and the selective polymer are detailed. Finally, the procedure followed for adhering the thin layer of sulphonated polyethersulphone to the polyethersulphone hollow fibre support is described.

3.1 Synthesis of hollow fibre support

3.1.1 Equipment used in synthesis of PES hollow fibres

A hollow fibre spin line was used to produce hollow fibre membranes via the dry-wet immersion precipitation phase separation process. The fibres were spun by co-extrusion of a polymer solution and a bore solution into a coagulation bath containing water.

The dry-wet spinning process consists of three stages of diffusion-induced phase separation:

i. Solvent evaporation or vapour penetration at the outer surface of the extruded polymer solution
ii. Immersion precipitation through the inside: nonsolvent from the bore liquid diffuses into the polymer solution
iii. Immersion precipitation via the outer surface when the nascent fibres enters the coagulation bath.

The hollow fibre spin line consists of three separate movable frames, clamped together. The first frame holds the spin set-up, the second holds the coagulation bath and the third

frame holds the rinsing bath. A machinery platform was installed along the length of the set up to complete the unit.

The first frame is where the spin set-up is located; it holds the following components:

- Control unit
- Dope solution assembly (dispensing vessel)
- Spinneret
- Lift system
- Gear pumps
- Emergency power cut-off
- Thermostatic bath
- Mechanical ventilation which is located next to the spinneret.

The second frame holds the stainless steel coagulation bath which is filled with 295 L tap water. It is fitted with rollers, a window and can be heated to 100˚C using a Kurval heating bath (12 kW). The bath is connected to a drainage system and has an emergency power cut-off. The third frame consists of the rinsing bath which holds 188 L tap water and is connected to the drainage system. The bath is equipped with rollers to guide the fibre through the water. It has an inlet and outlet for optional heating or continuous rinsing of the water. The system is connected to a 380 V power socket. Figure 17 shows a schematic representation of a spin line, and Figure 18 shows an image of the spin line used.

The polymer solution is filtrated before use in the spin line. Therefore, the dope solution is passed through a fine Aluminium filter (custom made at ''Equipment & Prototype Centre'' of TU/e, pore size 5 mm). The vessels (1 L and 2 L) that hold the dope solution can be pressurized with nitrogen to increase the rate of filtration. The 2 L vessel can additionally be heated using a thermostatic bath. Both vessels have a pressure relief valve that is activated at 3 bar. After the vessel is filled with the filtered dope solution, it is transported to the spinning set up and installed onto the dope delivery assembly. The assembly can be heated to 75˚C using a thermostat bath. An internal coagulant (bore solution) facilitates the coagulation of the polymer from the inner wall of the hollow fibre

membrane. In general, the bore solution consists of water or a mixture of water and solvent (DMSO or NMP). When activating the flow, the bore solution is always turned on first, followed by the flow of the dope solution to avoid blockage of the spinneret. All gear pumps are primed with their respective fluids and the spinneret is installed. The bore solution is connected to the appropriate inlet on the spinneret. The double walled coagulation bath is equipped with a pressure relief valve set to 0.6 bar to prevent pressure build-up. Optionally, a chimney is installed between the coagulation bath and the spinneret to control the humidity around the hollow fibre. This is achieved by passing hot water along the inside of the chimney wall. The hot water is supplied by a thermostat bath.

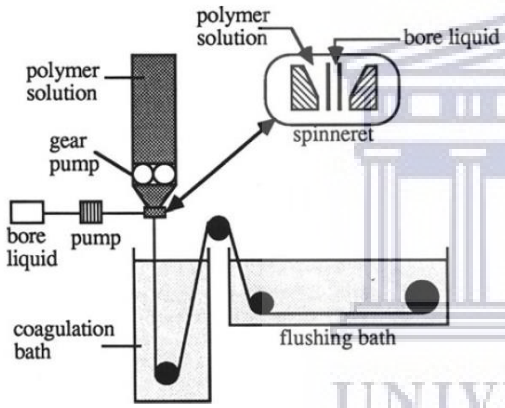

Figure 17 Schematic view of spin line (Mulder, 1992)

Figure 18 Image of the dry-wet spin line at TU/e

A number of parameters can be varied in order to obtain hollow fibres with desired properties. In this section only the physical parameters are listed:

- Temperature of the dope solution assembly, spinneret and coagulation bath
- Bore, shell and throughput speed
- Speed of the rollers (up to 30 meters/min)
- Air gap (distance between the spinneret and coagulation bath)
- Installation of a chimney to control the humidity and temperature between the spinneret and coagulation bath.

When the spinning is done, first the flow of the dope solution is switched off, followed by the flow of the bore solution. After the hollow fibres are collected in the collection

container the rollers are turned off. The coagulation and extraction baths are emptied in the sewage through a hose system by opening 2 valves. The storage container is emptied using a submersible pump. Finally the baths are rinsed with tap water using a water hose.

3.1.2 Chemicals used for synthesis of hollow fibres

The polyethersulphone hollow fibre support material was prepared via a phase-separation process using the immersion precipitation technique. Table 7 lists the chemicals used.

Table 7 Chemicals used for synthesis of PES hollow fibres

Chemical	Formula	Specification	Supplier
Polyethersulphone	$(C_{12}H_8O_3S)_n$	M_W 58,000 g mol^{-1}	Pentair X-Flow
N-4-methyl-2-pyrrolidone	C_5H_9NO	99 % extra pure	Acros Organics
Dimethyl sulphoxide D_6	$(CH_3)_2SO$	≥99.5 %	Acros Organics
Tetramethyl silane	Si $(CH_3)_4$	≥99.9 %	Merck
Water	H_2O	Ultrapure, 18.2 MΩ.cm	Veolia

3.1.3 Experimental procedure and parameters for synthesis of hollow fibres

A polymer solution of 20 wt% polyethersulphone was prepared by dissolving the polymer in a suitable solvent, in this case N-4-methyl-2-pyrrolidone was used. Mixing took place overnight at room temperature in a roller mixer to ensure a uniform dispersion (Figure 19). After dissolution of the polymer, the dope solution was filtrated by passing the solution through an Aluminium filter into the filtration vessel as shown in Figure 20. The PES/NMP mixture was transferred into a dispensing vessel (Figure 21), and left to ensure degassing/evaporation of present air bubbles overnight. Subsequently, hollow fibres were spun using the degassed PES.

Figure 19 Polymer being mixed on a roller mixer

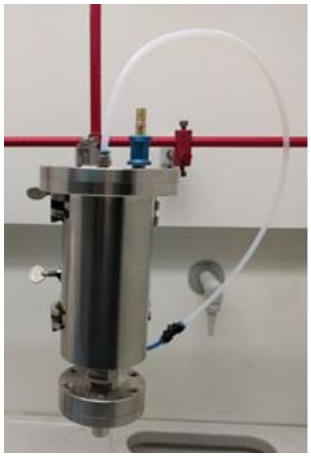

Figure 20 Filtration vessel

Figure 21 Holding vessel

The spinning suspension was extruded through a spinneret into the coagulation bath. The schematic overview and image of the spinneret is shown in Figure 22 and Figure 23 respectively. Ultrapure water was used as bore coagulant. This inner coagulant was supplied to the injection capillary of the spinneret through a pump at a flow of 0.30 ml/min. The flow of the polymer dope solution was activated by switching on the pump for the inner coagulant. While the dope solution was flowing out of the spinneret, a visual check was done to see whether the dope solution no longer contained any air bubbles, the solution was left to flow within the coagulation bath. If there were no longer any bubbles visible, the pump for the coagulation solution was switched on. After being co-extruded from the spinneret, the pre-nascent fibre was exposed to an air gap of 20 cm before reaching the first coagulation bath filled with tap water. The take-up roller continued to roll the fibres into the second coagulation bath which also contained tap water. The take-up speed of the two rollers was set in a way that it does not pull too hard on the fibres so that they were not impaired. After the second coagulation bath the as-spun fibres were collected by the second take-up roller and immersed in tap water for 24 hours to ensure that complete phase separation had occurred. The fibres were used immediately for characterisation. Alternatively they were dipped in a 50 wt% glycerol aqueous for 48 hours followed by drying at ambient temperature and storage for use at a later stage.

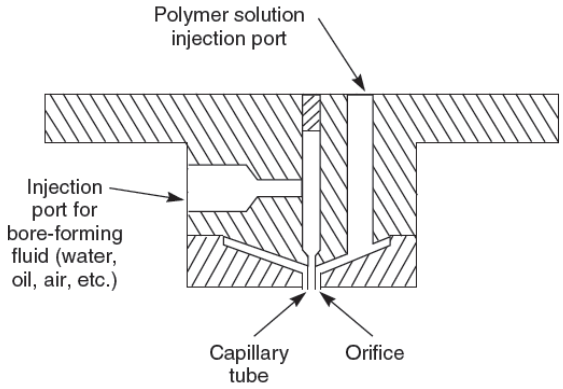

Figure 22 Twin-orifice spinneret (Baker, 2012)

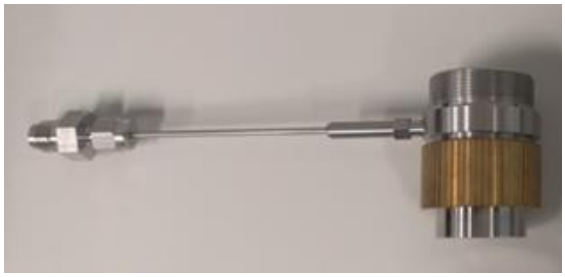

Figure 23 Image of a spinneret

The morphology of hollow fibres comprises of the inner and outer diameter of the hollow fibre (and thus the wall thickness), but also the pore size and fibre structure. An important parameter that determines the morphology of hollow fibres is the dope solution, it needs to exhibit sufficient chain entanglement in order to form the ideal outer skin layer (Hao, Zuo and Chung, 2014). To form a defect-free outer layer, the dope solution needs to have the right viscosity (generally >100 Poise). A lower polymer concentration reduces wall thickness and results in surface defects and lower selectivity. The optimal polymer concentration is at or above its critical concentration (Hao, Zuo and Chung, 2014). Additionally, the chemistry of the internal coagulant and its flow rate are of importance. The air gap, the temperature of the coagulant bath, the humidity of the surroundings, and the tearing rate (take-up rate) of the rollers also effects the morphology of the hollow fibre membranes. After initial testing with varying conditions, such as air gap, the flowrates for both dope solution as internal coagulant, the optimum conditions were determined in order to obtain good quality hollow fibres. Table 8 lists the spinning conditions for synthesis of PES hollow fibres.

Table 8 Utilized variables for HF spinning process

Variables	Composition or value
Dope composition (w/v)	20:80 w/v PES:NMP
Bore/inner coagulant fluid composition	Ultrapure water
External coagulant	Tap water
Spinning temperature (˚C)	23
Coagulant bath temperature (˚C)	17-19
Dope flowrate (mL/min)	0.30
Bore flowrate (mL/min)	0.30
Air gap (cm)	20
Room temperature (˚C)	22-23˚C
Relative Humidity (%)	60 %

3.2 Synthesis of sulphonated polyethersulphone

3.2.1 Chemicals used for synthesis of SPES

The sulphonation of polyethersulphone was performed by using sulphuric acid as the solvent and chlorosulphonic acid as a sulphonating agent. Table 9 shows an overview of all chemicals used for synthesis and analysis of sulphonated polyethersulphone.

Table 9 Chemicals used for SPES composite

Chemical name	Formula	Specifications	Supplier
Sulfuric acid	H_2SO_4	98 %	Merck
Chlorosulphonic acid	$ClSO_3H$	99 %	Sigma Aldrich
N-4-methyl-2-pyrrolidone	C_5H_9NO	99 % extra pure	Acros Organics
Sodium chloride	NaCl	≥99.0 %	AkzoNobel
Hydrochloric acid	HCl	37 %	Sigma Aldrich
Sodium hydroxide	NaOH	≥99.0 %	Merck
Oxalic acid dihydrate	$H_2C_2O_4*2H_2O$	>98 %	Sigma Aldrich
Silver nitrate	$AgNO_3$	99 %	Sigma Aldrich
Di methyl sulphoxide D_6	$(CH_3)_2SO$	≥99.5%	Acros Organics
Tetramethyl silane	$Si(CH_3)_4$	≥99.9 %	Merck
Acetone	CH_3COCH_3	≥99.5 %	Sigma Aldrich
Polyethersulphone	$(C_{12}H_8O_3S)_n$	M_W 58,000 g mol^{-1}	Pentair X-Flow
Sulphonated polyethersulphone (DS30%)	--	M_W 110,000 g mol^{-1}	Konishi Ltd
Phenolphthalein	$C_{20}H_{14}O_4$	<1 %	Sigma Aldrich
Methanol	CH_3OH	≥99.8 %	Alfa Aesar
Ethanol	C_2H_5OH	≥99.5 %	TechniSolv
Water	H_2O	Ultrapure, 18.2 MΩ.cm	Veolia
Glycerol	$C_3H_8O_3$	≥99 %	Merck

3.2.2 Procedures followed for synthesis of SPES

Firstly, PES pellets were dried in the oven overnight for 15 hours. A 100 ml glass 3-neck reactor, equipped with a mechanical top stirrer and a water bath, was charged with PES pellets, and sulphuric acid. The dissolution was carried out overnight (15 hrs at 350 rpm) to make sure all polymer material was fully dissolved and formed a homogeneous solution. The chlorosulphonic acid (CSA) was transferred into a cylindrical separatory funnel using a glass pipette. This was done as a safety measure, to minimize contact with the skin in case of spillage. Subsequently, the chlorosulphonic acid was added to the reactor containing the polymer solution; this was done by gradually and slowly dripping it by controlling the valve, while stirring the solution at 250 rpm. Fumes were collected through the outlet and passed through 2 gas wash bottles. The resulting reaction mixture is then stirred for varying times to improve sulphonation of the polymer. The sulphonation reaction was carried out in an ice bath to simultaneously prevent evaporation of solvents and avoid pressure build-up in the system. Figure 24a shows the reactor in which the sulphonations take place, and Figure 24b shows the overall sulphonation set-up.

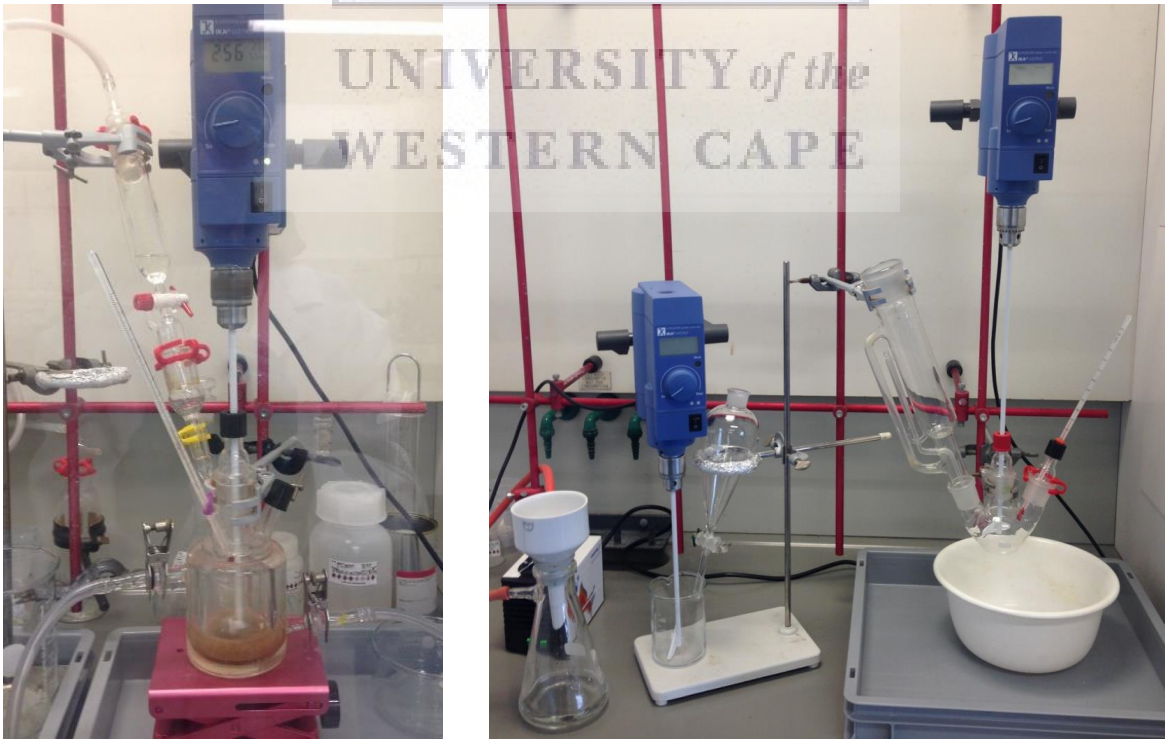

(a) *(b)*

Figure 24 (a) Sulphonation reactor *(b) Overall sulphonation set-up*

After set reaction time, SPES mixture was poured into a cone shaped funnel. Subsequently, the mixture was quenched/gradually precipitated into a beaker with ice-cold de-ionized water under rapid mechanical agitation as Figure 25 shows. The resulting liquid/solid mix was then poured into a pressure assisted Buchner funnel with a filter paper in it. A vacuum created in the flask under the Buchner funnel allows atmospheric pressure onto the liquid/solid mix to force the liquid through the filter paper. To create this vacuum a pump was utilized as shown in Figure 26. The side-arm flask was connected with a hose to the vacuum pump. Eventually the polymer was rinsed repeatedly with de-ionized water to neutralize the acidity. This was done until the pH of the filtrate was ~6-7 which was determined using pH indicator paper). After rinsing of the precipitate, the pump was turned off and the precipitate was recovered from the funnel. The collected SPES polymer was dried overnight under vacuum (100 mbar) at 100˚C. The filtrate water was disposed as chemical waste.

Figure 25 Precipitation set-up

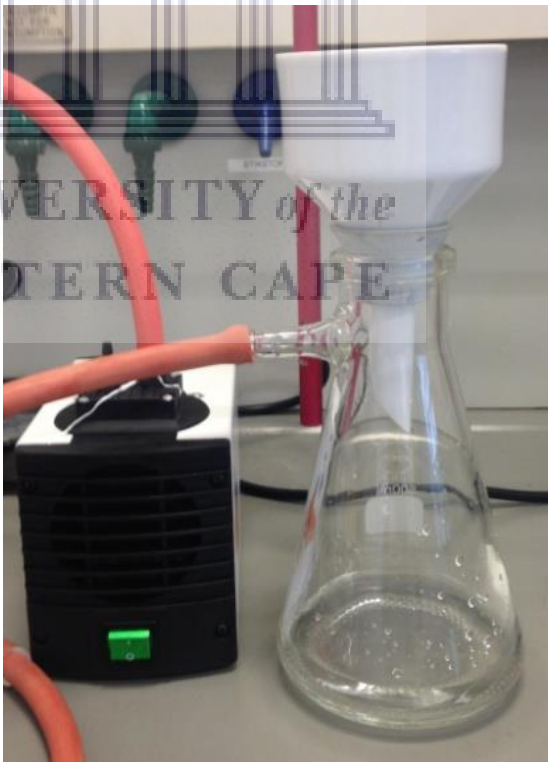

Figure 26 Filtration with Buchner funnel and vacuum

The initial concentration ratio of PES/CSA was maintained at 40/60 (w/v) in all experiments except for the first, where a concentration ratio of 20/80 PES/CSA (w/v) was used. Time and temperature of the sulphonation reaction were varied to achieve SPES with different degrees of sulphonation. Reaction times were varied between 4.5, 7, and 9 hours. A longer reaction time of 25-26 hours was also executed. The reaction temperatures used were 5°C, 10°C, 20°C and 25°C. The choice for these reaction parameters was based on reporting of (Lu *et al.*, 2005). The reported reaction time was the total time for reaction: from the moment the reactant (chlorosulphonic acid) was added to the polymer solution until the moment the solution was precipitated in water. Table 10 shows an overview of the sulphonation conditions.

The dried SPES material was a clumpy substance and therefore further processing was required. The SPES was crushed into a powder using a mortar and liquid nitrogen.

Table 10 Sulphonation conditions

Sample name	Time (hours)	Temperature (˚C)	Stirring rate (RPM)	PES/CSA ratio (w/v)
SPES-01	4.5	5	250	20/80
SPES-02	7	5	250	20/60
SPES-03	26	5	250	20/60
SPES-04	9	5	250	20/60
SPES-05	9	10	500	20/60
SPES-06	9	20	400	20/60
SPES-07	25	20	400	20/60
SPES-08	5	30	250	20/60
SPES-09	5	20	250	20/60
SPES-10	7	20	250	20/60
SPES-11	7	10	250	20/60
SPES-12	5	10	250	20/60
SPES-13	9	10	250	20/60
SPES-14	9	20	250	20/60
SPES-15	7	5	250	20/60
SPES-16	5	5	250	20/60

To compare the synthesized SPES membrane materials and commercial sulphonated polyethersulphone (SPES-K from Konishi) several characterisation methods were performed to investigate the polymeric materials.

3.2.3 Characterisation of PES, SPES, hollow fibres and composite membranes

In the process of optimizing the fabrication parameters, the intermediate PES hollow fibres were placed under an optical microscope to measure the dimensions (wall thickness, inner- and outer diameter) with ''Micro Capture'' software. When the optimal hollow fibre support was obtained, the membranes were further examined with scanning electron microscopy (JEOL-IT-100) as described in the following section.

3.2.4 Scanning Electro Microscopy – Morphology of PES and SPES

In order to understand the influence dip-coating had on the morphology of the SPES coated PES HF membranes, the cross-sections and surface of the prepared membranes were observed using scanning electron microscopy (JEOL-IT-100) operating at a voltage of 15 kV. In SEM, a finely focused electron beam with low energy is directed onto the sample material and the surface of the sample is scanned. As the beam reaches and enters the material, several interactions occur which lead to the emissions of photons and electrons from or near the sample surface. An image is formed with a detector that detects the received signals from the electron-sample interactions.

To obtain sharp cross-sectional surface fractures, the hollow fibres were immersed and fractured in liquid nitrogen to prepare samples of 1 cm that were attached to a SEM sample holder. Since polymers are non-conductive, the samples were coated with a very thin conductive layer. Without this coating layer, the samples would be charged and heated/melted, which would distort the SEM image. The sample was sputter coated in the ''JEOL JFC-2300HR'' to cover the sample with a few nanometres thick layer of gold. The surface and cross-sectional images of the fibres were obtained and the software was used to establish the wall thickness, inner- and outer diameter. From the obtained SEM images the thickness of the thin film was measured.

3.2.5 Thermogravimetric Analysis – Thermal stability of PES and SPES

Thermogravimetric Analysis is a thermal analysis method that measures the changes in the physical and chemical properties of a material as a function of increasing temperature with a constant heating rate. Thermal stabilities of PES, SPES-K and all synthesized SPES materials were investigated on a ''Perkin Elmer TGA 4000'' under nitrogen gas using a heating rate of 10˚C min^{-1} from room temperature to 600˚C. The obtained spectra show the mass change in percentages as a function of increasing temperature with a constant heating rate. From this, the decomposition temperature of the sulphone group and the polymer main chain can be deducted. With this data, an assessment can be made as to whether the hollow fibre membranes are resistant towards the process conditions in power plants.

3.2.6 Fourier Transform Infra-Red – Chemical composition of PES and SPES

Fourier Transform Infrared Spectroscopy is a technique to record the infrared absorbance spectrum of materials in order to study and identify the chemical functional groups in chemical substances. Infrared spectroscopy exploits the property that molecules absorb infrared light depending on their chemical composition. The functional groups of SPES-K and all synthesized SPES polymers were investigated using ''Varian 3100 FTIR Excalibur'' with a ''Golden gate ATR'' in the wavenumber range of 500-4,000 cm^{-1} (in transmittance mode).

3.2.7 ^{1}H Nuclear Magnetic Resonance – Chemical structure of PES and SPES

^{1}H NMR is a technique to accurately identify the molecular structure of a material by observing and measuring the interaction of nuclear spins when placed in a powerful magnetic field. This technique provides information about the composition of atomic groups within the molecule, adjacent atoms, molecular dynamics and quantitative information on the atomic ratios, and the proportions of different compounds in a mixture. In present study the polymer materials were scanned to detect the occurrence of a sulphone group and to quantify this SO_3H pendant on the aromatic rings. The ^{1}H NMR spectra were recorded on a ''Bruker 400 Ultrashield'' at a resonance frequency of 400.15 MHz at room temperature. The sulphonated PES samples (10 mg) of different sulphonation degrees were dissolved in deuterated dimethyl sulfoxide (DMSO-d_6) (60 mg) solvent using tetramethyl silane (TMS) as the internal standard. Dissolution was carried out for 20 minutes in a rotary mixer at 500 rpm at 50˚C.

The sulphonation degree of the SPES samples is quantitively determined by evaluating the signal intensity/peak area representing all the protons. Figure 27 shows the nomenclature of the characteristic protons in the aromatic ring of the sulphonated PES repeat unit.

The method is based on the comparison of the peak area of the H_E signal (AH_E), which represents one proton of the sulphonated phenyl ring, with the peak areas of all the other

aromatic hydrogen signals ($\Sigma AH_{A,A',B,B',C,D}$). The following equation shows the mathematical expression:

$$\frac{DS}{8-2DS} = \frac{AH_E}{\Sigma AH_{A,A',B,B',C,D}} \qquad 6$$

Where A_{HE} represents the area of the signal, and the sum term is the integrated peak area of the signals corresponding to all the other aromatic protons (Guan *et al.*, 2005).

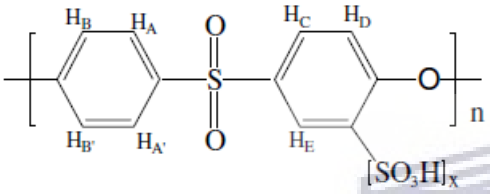

Figure 27 Chemical structure and atomic numbering of SPES, x=DS

The integrals of the signal regions were evaluated using Mestre Nova software. The calculation of the DS from ^{1}H NMR spectra requires the precise definition of signal integrals. Ideally the well assigned signals are baseline separated. However, often, the broadened ^{1}H NMR signals of polymers obstruct the accurate integration which results in an inaccurate degree of sulphonation (Komber *et al.*, 2012). The integration was carried out 5 times for each integral, and the average value was taken. The error margin was between 0.5-2.5 % This is an acceptable error margin for this study.

3.2.8 Analysis of Ion Exchange Capacity of SPES

The ion exchange capacity (IEC) provides information on the charge density in the membranes, which is an important factor related to the conductivity and transport properties in membranes (Klaysom *et al.*, 2011). It provides the amount of the acid groups present in the polymer that are responsible for proton conduction. The IEC of the sulphonated polyethersulphone membranes were measured using an acid-base titration method. The cation exchange membrane (SPES) is first brought into the H^+ form, after which the H^+ is replaced by Na^+. The released amount of H^+ was subsequently determined by titration with NaOH (Klaysom *et al.*, 2011).

First, the polymer solution (25 wt/vol%) was cast on a glass substrate using a casting blade (300 µm), and precipitated in a deionized water bath to form a flat sheet membrane via phase inversion. 1 g of wet polymer was weighed, and placed in a 250 ml Erlenmeyer. The cation exchange membrane was then soaked in 150 ml HCl (0.1 M). This was stirred overnight for 15 hours using a magnetic stirrer. This step was conducted to bring the membrane into the H^+ form. The following morning the HCl solution was filtered out from the flask. The membrane was washed with ultrapure water to remove excess HCl. The membrane was left in water for an hour, while rinsing with water several times. This was done to remove the HCl that was absorbed into the membrane. Thereafter, the polymer was washed until the pH of the solution became neutral. To check whether the last rinsing water was free of Cl^-, some drops of 0.1 M $AgNO_3$ were added; if Cl^- was still present this would have led to a precipitation of AgCl. The surface water was removed from the membrane with a tissue and the membrane was put into a 100ml flask. Subsequently, 50ml NaCl (2.0 M) was added and stirred for at least 1 hour to replace the H^+ by Na^+. The NaCl solution was replenished twice more to ensure complete exchange. The three NaCl solutions were then combined in a 250 ml flask. The combined solutions were titrated with standardized 0.100 M NaOH using a pH electrode. The titration was performed in the ''Compact Titrator G20'' with a ''DMi 140SC'' electrode (Mettler Toledo). The output of the titrator was the volume necessary to reach the equivalency point. The membrane was taken out of the solution and gently dried with tissue paper to measure the wet weight of the membrane. Afterwards, the membrane was dried in a vacuum oven at 50˚C until the weight remained constant, normally after 48 hours of drying. The dry weight of the membrane was then measured.

The ion exchange capacity in mmol/gram dry membrane was calculated using following equation:

$$Ion\ Exchange\ Capacity\ \left(\frac{mmol}{g\ (dry\ membrane)}\right) = \frac{volume\ added\ NaOH}{dry\ weight\ membrane}\left[\frac{ml}{g}\right] * NaOH\ concentration\ \left[\frac{mmol}{ml}\right] \quad 7$$

To obtain accurate and reliable titration results, the exact concentration of the volumetric solution must be determined. This can be achieved by performing a titre determination. The nominal concentration of a volumetric solution used as a titrant is known, however, the concentration could differ from the actual concentration because of a variety of influences e.g. degradation of titre solution. Therefore it is necessary to determine the actual concentration with a titrimetric standard in order to obtain correct titration results.

The titration was performed with oxalic acid dihydrate ($H_2C_2O_4$*$2H_2O$). Firstly, 0.22 g $H_2C_2O_4$*$2H_2O$ was dissolved in 50 ml Ultrapure water. A few drops of phenolphthalein indicator were added. This was followed by titration of the oxalic acid dihydrate with the NaOH solution until the colour turned light pink. The volume necessary to achieve this end point is *v* (ml). The NaOH titre is then calculated by following equation:

$$C\ \ NaOH = \frac{2\ m}{126.07\ v}\left[\frac{mol}{l}\right] \quad 8$$

Where C is the actual molar concentration of the volumetric solution (NaOH), *m* is the exact weight of oxalic acid dihydrate in gram, 126.07 g/mol is the molecular weight of oxalic acid dihydrate, and *v* is the volume necessary to reach the endpoint of the titration. With this method, the exact titre (NaOH) concentration was determined, which was then used for calculating the degree of sulphonation.

Finally, the sulphonation degree was calculated by the released H^+ in this acid-base titration.

$$DS = \frac{0.232\,[M(NaOH) \times V(NaOH)]}{W - 0.081\,[M(NaOH) \times V(NaOH)]} \times 100\% \qquad 9$$

Where M(NaOH) is the exact concentration of the NaOH solution (mol dm^{-3}), V (NaOH) is the NaOH solution used to neutralize the solution (dm^3), W is the sample weight (g), 232.258 g/mol is the molecular weight of the PES repeat unit, and 81.071 g/mol is the molecular weight of the SO_3H group (Guan *et al.*, 2005).

3.3 Coating PES with SPES thin layer

The SPES materials utilized for coating PES hollow fibres were prepared to have a concentration of 6 wt% in selected solvent. SPES was dissolved in NMP in a rotary mixer for 3 hours at 200 rpm at ambient temperature. This polymer solution was then transferred into a beaker containing a suitable solvent. The dip-coating was executed by immersing a PES hollow fibre gently into the solution, gently removing it and hanging it to dry. The SPES coated PES hollow fibre was allowed to cure for 48 hours at ambient temperature. After that, further characterisation was carried out.

The PES support is dip-coated with functional SPES by immersing the hollow fibres in a solution containing SPES polymer solution and solvent. In order to coat the PES support fibres with a thin film of SPES, a solvent should be chosen that dissolves the SPES but not PES. Table 11 shows possible solvents for PES and SPES with different degrees of sulphonation. The degree of sulphonation has a major impact on the solubility of SPES in different solvents. Literature shows that SPES with a DS >29 % is soluble in ethanol whereas PES is not soluble (Lu *et al.*, 2005). This means that the aim should be to synthesize SPES with a sulphonation degree >29 %.

Table 11 Solubilities of PES and SPES at various DS (Lu *et al.*, 2005)

Solvent	PES	DS14.01%	DS23.73%	DS29.47%	DS41.22%
N,N-Dimethylformamide	+	+	+	+	+
N,N-Dimethylacetamide	+	+	+	+	+
N-methyl-2-pyrrolidone	+	+	+	+	+
Dimethyl sulfoxide	+	+	+	+	+
Chloroform	+	△	−	−	−
Dichloromethane	+	△	−	−	−
1,2-Dichloroethane	△	−	−	−	−
Water	−	−	−	−	±
Methanol	−	−	−	−	+
Ethanol	−	−	△	+	+
Acetone	−	−	−	△	△
Tetrahydrofuran	−	−	−	−	△
Diethylether	−	−	−	−	−
Hexane	−	−	−	−	−

Solubility: (+) soluble at room temperature, (−) insoluble, (±) soluble at high temperature, (Δ) swollen.

3.3.1 Preparation of flat sheet membranes

Flat sheet (FS) membranes were cast from SPES. Four SPES samples were selected to prepare flat sheets from, namely SPES-K, SPES-03, SPES-05, and SPES-06. This was done to investigate the morphology, and to measure their water permeance. SPES was dissolved in NMP to obtain a 20 wt% polymer solution. Dissolving was performed by placing the samples on a rotary mixer for 15 hours at 200 rpm at room temperature. The phase inversion method was used to fabricate these flat sheet membranes. The polymer solution was cast on glass substrate with a casting knife and subsequently soaked in an ultrapure water bath to be peeled off the glass substrate. To control the FS membrane thickness, two different casting knifes were used to obtain a thickness of 150 and 300 µm respectively. The films are rinsed in tap water for at least 24 hours before analysis. The water permeance was measured in an ''Amicon cell'', detailed in the following paragraph.

3.3.2 Water permeance analysis of flat sheet membranes

After casting the flat sheet membranes as described in the previous section, their water permeance was measured. Four membranes were selected as described in the previous paragraph. It was reported that SPES with a degree of sulphonation >20 mol% was preferable (Guan *et al.*, 2006; Unnikrishnan *et al.*, 2010). Therefor the following SPES samples were chosen for investigation: SPES with a DS of 25, 30, 40, and 45 %. The measurements were conducted in an ''Amicon type stirred cell'' produced at the Equipment & Prototype Centre of TU/e. This is a simple and reliable method that allows for analysis of membranes or for the treatment of process streams. The filtration is driven by N_2 pressure while gentle magnetic stirring right above the membrane surface minimizes concentration polarization. The dead-end pressure cell containing the membrane is equipped with a pressure safety relieve valve. This allows for venting of air while the cell is pressurized. A porous support plate channels the permeated liquid to the outlet where the volume is measured with a top scale. Figure 29 shows the water permeance measurement set-up. The standard volume of the Amicon cell is 600 ml, but it can be expanded to 5 L or 10 L by connecting a dispensing vessel.

To determine the water permeation coefficient, firstly the pressure cell was filled with deionized water. A maximum of 5 bar pressure was applied by opening the nitrogen pressure regulator. The water is being pushed in to the stirred cell containing a flat sheet membrane with an effective area of 39 cm^2. The permeate was collected in a beaker and the mass accumulation over time was recorded by a precise balance (Ohaus PA2102C). The pure water flux over applied pressure was used to calculate the water permeation coefficient. Figure 28 shows how the membrane permeability coefficient is calculated.

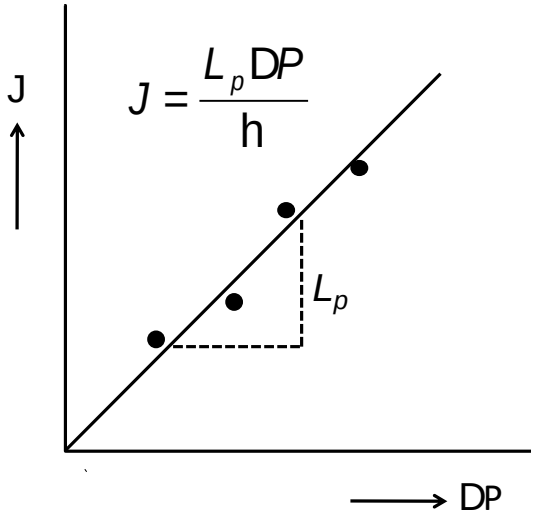

Figure 28 Typical pressure-flux curve to calculate the membrane permeability coefficient L_p (TU/e, 2017)

Figure 29 Image of the Amicon cell set-up including the dispensing vessel

The permeance measurements were performed at a pressure between 1 to 4 bar.

Chapter 4 Results and discussion

This chapter presents the findings of the PES hollow fibre fabrication process. It describes the observations after the execution of the sulphonation reactions. It also presents details of the physical and chemical characterisation of polyethersulphone, commercial sulphonated polyethersulphone and synthesized sulphonated polyethersulphone materials. Firstly, the surface and cross-sectional morphology of the membrane materials were examined as obtained by the use of Scanning Electron Microscopy, followed by characterisation of the thermal stability using Thermogravimetric Analysis. The chemical composition of the membrane materials is discussed based on using Fourier Transform Infrared and ^{1}H NMR Spectroscopy. This is followed by a discussion of the determination of degree of sulphonation using ^{1}H NMR spectra and Ion Exchange Capacity. Finally, the water permeance of SPES membrane is discussed. The samples discussed are denoted as follows: polymer material used for the selective layer of the membrane (SPES), followed by the sample number that is linked to synthesis parameters as summarized in Table 10, followed by the degree of sulphonation as measured with ^{1}H NMR. In some cases, the DS is rounded up with some percent: for example SPES-04-DS10 is measured to have a DS of 8 mol%, but for the sake of clearness it is noted as DS10. From the 16 samples summarized in Table 10, only selected samples are discussed in the following section. Reason for this is that some degrees of sulphonation weren't divergent enough to be discussed separately. Those samples were however investigated, and the results can be retrieved in Appendix 1.

4.1 PES hollow fibres

4.1.1 Structure and morphology

The dope- and bore solution flowrates and the air gap were varied to obtain PES hollow fibre support membranes with desired dimensions. Cross-sectional morphology of the spun PES hollow fibres was characterized using an optical microscope. The inner and outer diameter as well as the wall thickness were measured. Figure 30a and Figure 30b show the cross-sectional structures of the optimized PES hollow fibre support membrane.

The average outer and inner diameter were 1,200 µm and 850 µm respectively, leading to an average wall thickness of 350/2 = 175 µm. The minimal wall thickness measured was 170 µm, showing good dimensional consistency of the produced fibre. After initial analysis under the optical microscope, the PES hollow fibres were analysed further under a scanning electron microscope.

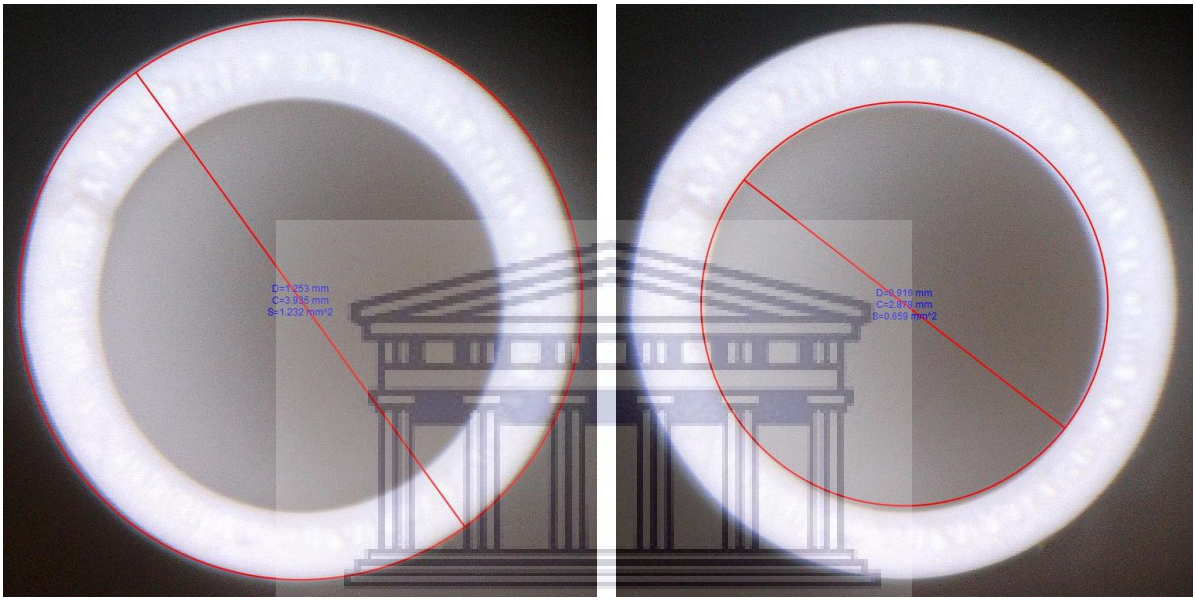

(a) *(b)*

Figure 30 Optical image of the cross-section of PES hollow fibre support membrane (a) outer diameter (b) inner diameter

The surface of the PES hollow fibre membrane is shown in Figure 31 with a magnification (mag.) of 900x, 1,5000x , 3,500x, and 10,000x. Figure 31 exhibits a porous structure of the external surface of the PES HF membrane. Figure 32 shows the SEM morphology of the hollow fibre membranes cross-sections at different magnifications. The support has a porous finger-like asymmetric structure induced by phase inversion. There appear to be two arrays of layer finger like structures: one array near the inner skin (lumen side) and one near the outer skin (shell side) of the membrane. This results in a low tortuosity and a high porosity. A similar membrane morphology was reported in literature (Ran, Fen; Li, Dan; Niu, 2019). The macro voids appear to be larger on the inner array.

Macro voids are avoided as they lead to weak spots in the membrane, and should be avoided or at least minimized in membranes for gas separation (Mulder, 1992). They are generally formed when coagulation takes place at a fast pace. Since the bore coagulant

water is a strong non-solvent to PES, coagulation takes place fast when the polymer solution is brought into contact with water. On the other hand slow coagulation results in a more sponge like structure.

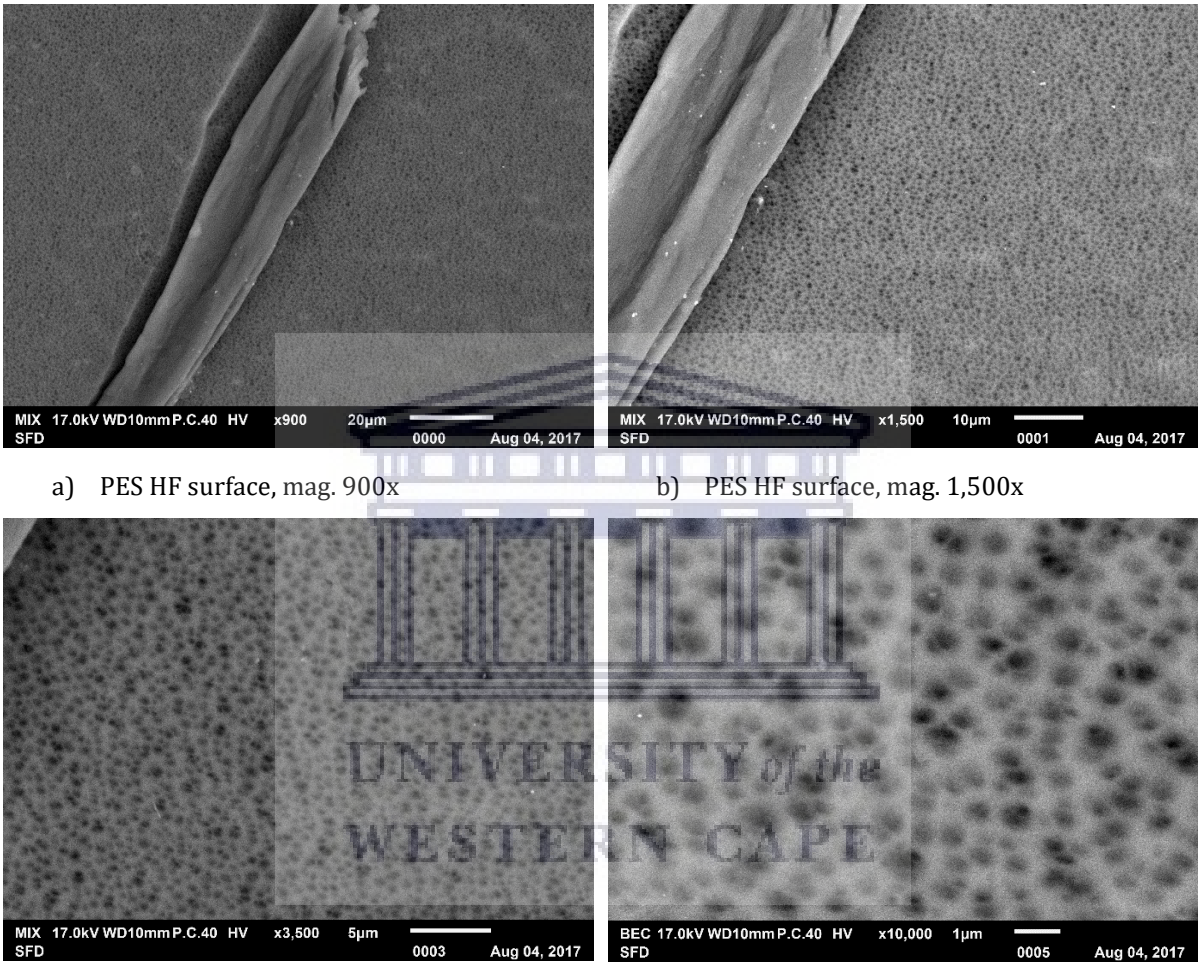

a) PES HF surface, mag. 900x b) PES HF surface, mag. 1,500x

c) PES HF surface, mag. 3,500x d) PES HF surface, mag. 10,000x

Figure 31 SEM images of external surface of PES hollow fibre support membrane

As reported by Peng et al. there are three key factors for the fabrication of macro void free hollow fibre membranes: a critical polymer concentration, critical take-up speed and critical air gap (Peng, Chung and Wang, 2008). These parameters function interdependently. The polymer dope should have sufficient chain entanglement which causes a high viscosity. For this purpose the concentration of the polymer solution should be adjusted and the viscosity experimentally determined as a function of the concentration. From the slope change, the critical dope concentration can be determined

(Shung, 1997). Additionally, a non-solvent could be added to the polymer solution, preferably one with a high molar mass (such as polyvinylpyrrolidone) as this will result in a high viscosity dope.

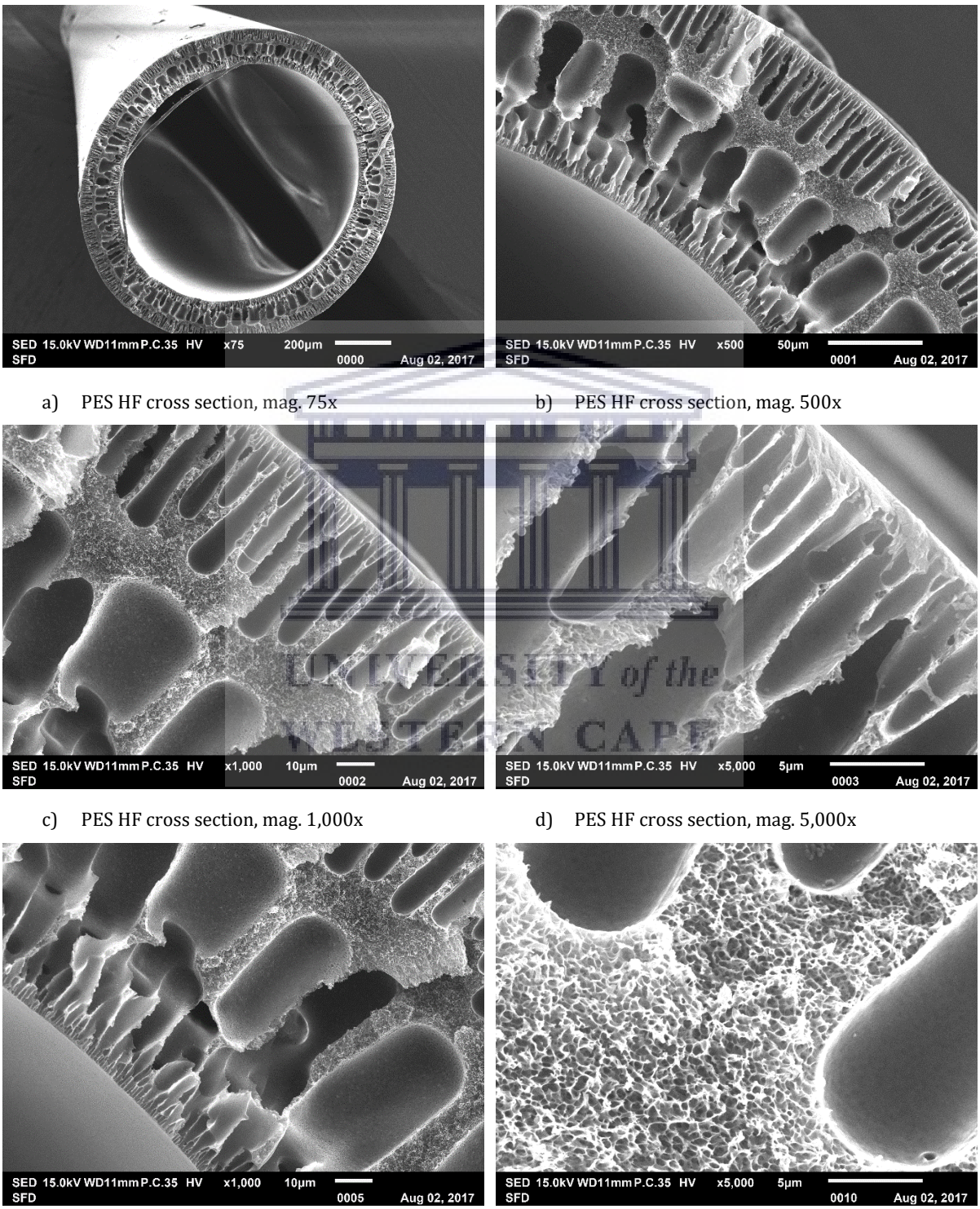

a) PES HF cross section, mag. 75x

b) PES HF cross section, mag. 500x

c) PES HF cross section, mag. 1,000x

d) PES HF cross section, mag. 5,000x

e) PES HF cross section, lumen side, mag. 1,000x

f) PES HF cross section, mag. 5,000x

Figure 32 SEM images of the cross-section of PES hollow fibre support

Since the main focus of this study was directed towards the selective layer, no additional spinning experiments were conducted with non-solvent additives. A promising and worthy of further investigation PES support polymer solution would consist of 20 % PES, 5 % SPES and 15 % PVP in NMP as was derived from preliminary experiments of the research group Membrane Materials and Processes at the University of Technology in Eindhoven.

4.2 Sulphonated polyethersulphone

4.2.1 Thermal stability – TGA

The thermal stabilities of the PES and SPES samples were studied by TGA. PES is a highly thermostable polymer; the 5 wt% loss is above a temperature of 500˚C, and there is only one weight loss step that is ascribed to the decomposition of the polymer main chain. For the SPES, three weight loss transitions in three different temperature ranges were observed as shown in Figure 33. The first step around 100˚C is related to the loss of the absorbed water. The second step between 300-450˚C is attributed to the thermal decomposition of the SO_3H groups. The third thermal degradation of SPES is at about 490-500˚C and is assigned to the degradation of the polymer main chain. From the thermal decomposition spectra it is observed that the weight loss of SPES membranes between 300-450˚C tends to increase with increased amount of SO_3H groups introduced into the polymer chain. As the asymmetry increases with sulphonation degree, this results in greater degradation of the samples between 300-450˚C. These results are comparable to the observations of (Guan *et al.*, 2005).

It is obvious that the sulphonated PES materials exhibited lower decomposition temperatures in regards to polyethersulphone. This can be explained by the asymmetry in the PES structure due to the introduction of the sulphone groups. This results in the polymer being less stable. The membranes need to be stable under the existing environmental condition of the flue gas stream, which is 50-70˚C. This is the case for all SPES with varying degrees of sulphonation. The samples displayed in Figure 33 are of SPES samples with degrees of sulphonation of 0, 4, 10, 15, 25, 30, 40, and 45 mol%.

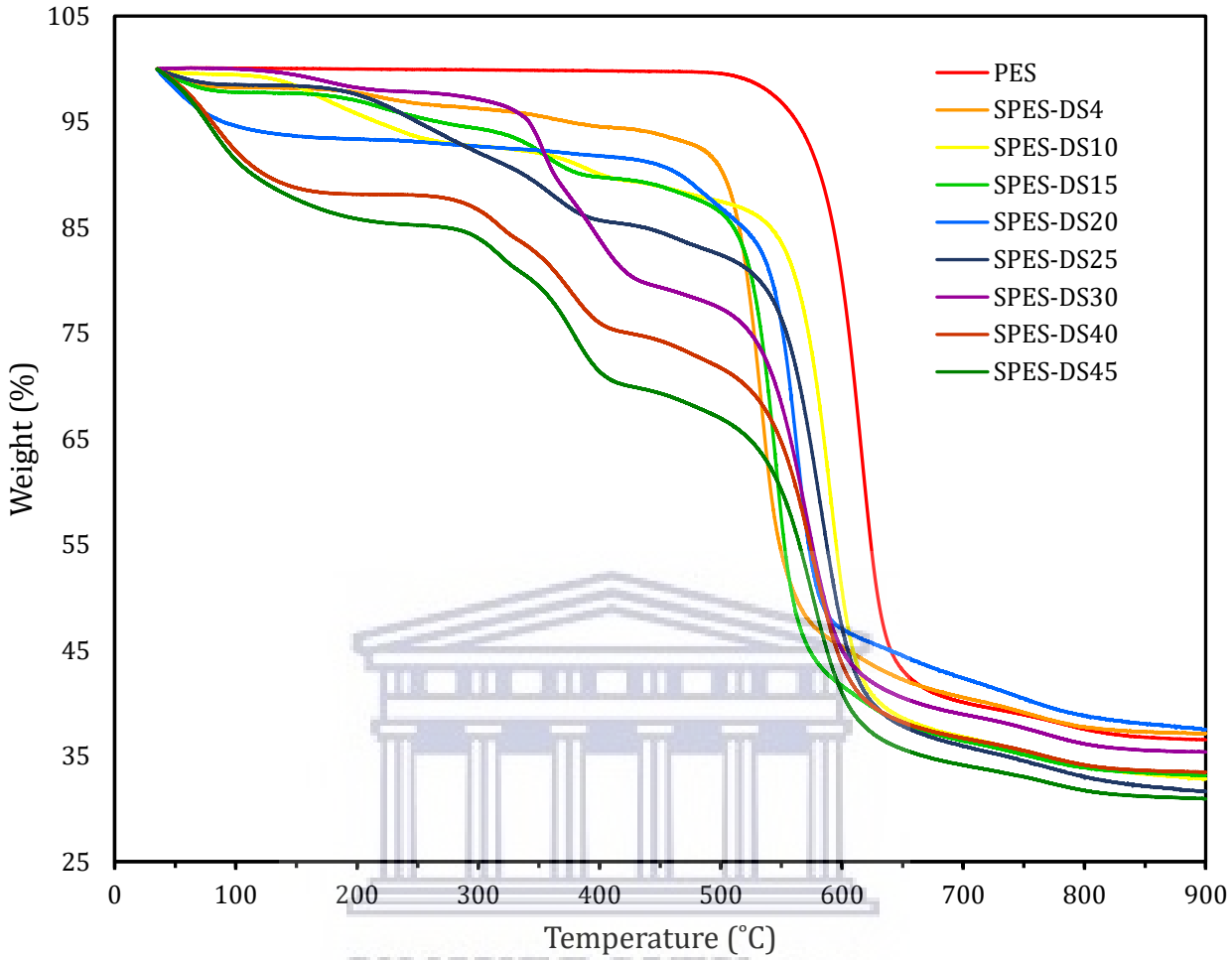

Figure 33 TGA thermograph for PES and SPES with different DS

4.2.2 Chemical composition – FTIR

The absorbance spectra recorded with Fourier Transform Infra-Red Spectroscopy was used to confirm the presence of the pendant group on the polymer chain. The absorbance peaks are linked to the chemical structure of the groups. Allocation of the absorbance peaks to the groups are shown in Table 12.

Table 12 Absorbance peak allocation (Klaysom *et al.*, 2011)

	Absorbance peak allocation
1580 cm^{-1} and 1490 cm^{-1}	Vibration of aromatic ring skeleton
1152 cm^{-1}	Aromatic sulphone group, symmetric stretch vibration
1245 cm^{-1}	Aryl oxide
1028 cm^{-1}	SO_3H symmetric stretching vibrations
1180 cm^{-1}	SO_3H asymmetric stretching vibrations
3420 cm^{-1}	Stretching of the hydroxyl group of sulphonic acid groups

Figure 34 shows the recorded spectra of the SPES samples. The absorbance peak at 1028 cm^{-1} which is allocated to symmetrical stretching of the sulphonate groups is visible in all SPES samples. It is observed that the characteristic absorption increased with increasing degree of sulphonation. The asymmetric stretching vibrations of the sulphonate group are believed to be around 1180 cm^{-1}, however they are not readily visible which might be due to the presence of the other overlapping absorbance spectra in that area. The aromatic sulphone stretching vibrations are visible around 1145 cm^{-1} in stead of 1152 cm^{-1}. The stretching of the hydroxyl group of sulphonic acid groups is perceived around 3420 cm^{-1} (Lu *et al.*, 2005). Furthermore, the vibration of the aromatic ring skeleton is visible around 1490 cm^{-1}.

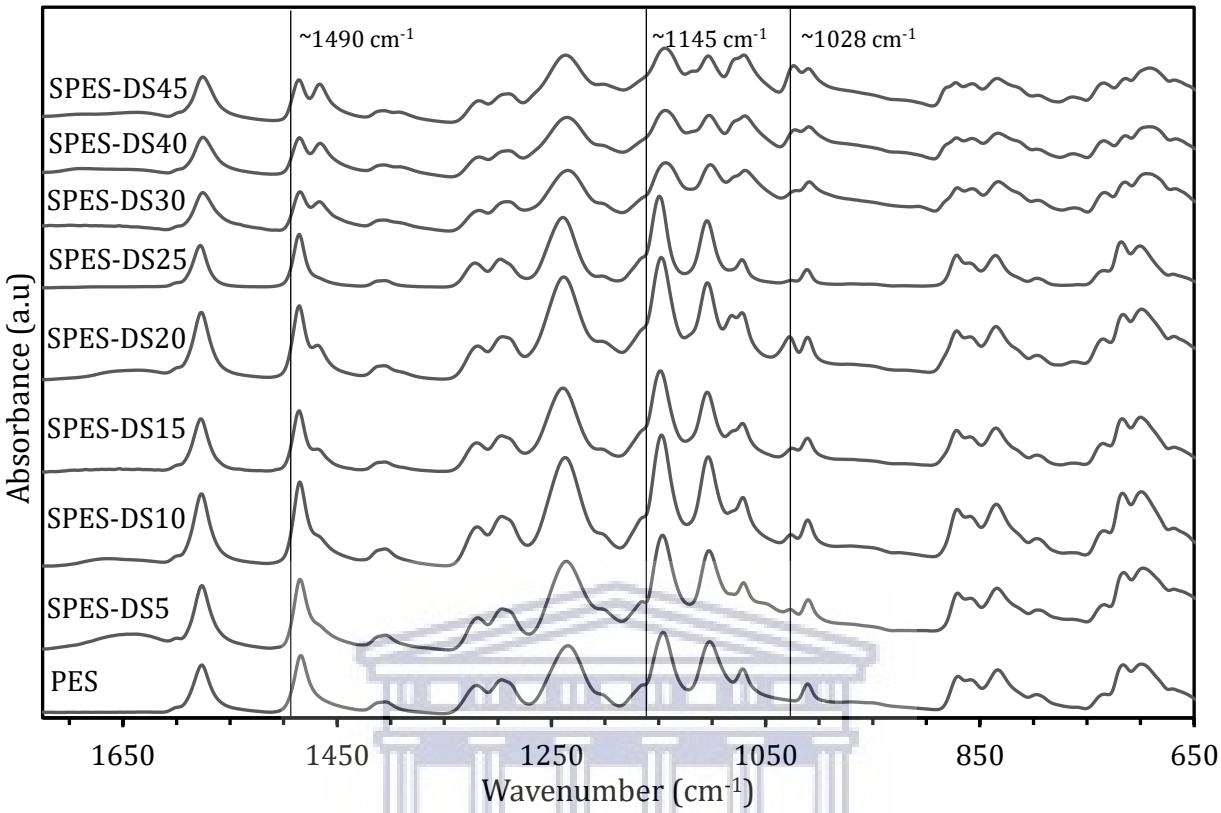

Figure 34 FTIR absorbance spectra of PES and SPES

According to (Deimede *et al.*, 2000), all absorption bands, either of sulphone or sulphonate groups are considered to be sensitive to interactions with their environment. To get a better understanding of these interactions, four spectral windows are pointed out, related to the peaks of the symmetric stretch vibration of sulphonate (1028 cm^{-1} Figure 35, the aromatic sulphone groups (1145 cm^{-1} Figure 36), the stretching of the hydroxyl group of sulphonic acid groups at (3450 cm^{-1} Figure 37), and the vibration of the aromatic ring skeleton (1490 cm^{-1} Figure 38).

The spectral window depicted in Figure 35 shows the symmetric stretch of the sulphonate group. A slight red shift from 1028 cm^{-1} to 1024 cm^{-1} of the sulphonate symmetric stretch takes place at samples with higher sulphonation degree. This is an indication that the sulphonate group most probably interacts with the main chain sulphone group. This is in good accordance to (Deimede *et al.*, 2000).

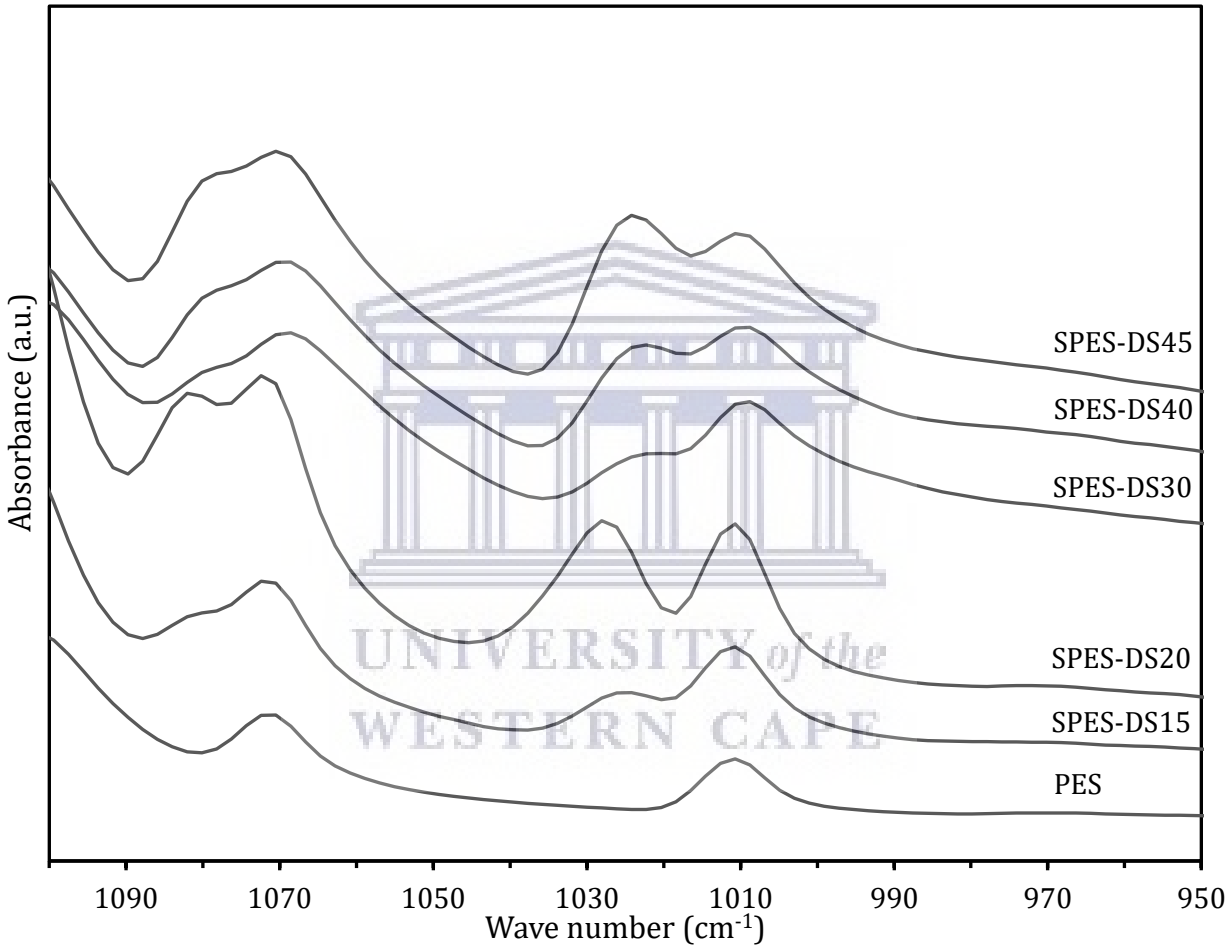

Figure 35 FTIR absorbance spectra of the sulphonate symmetric stretch vibration

As mentioned earlier, the assymetric stretching vibration of sulphonic acid groups are known to appear at 1180 cm^{-1}. However they could not readily be observed, which might be due to near overlapping absorbance. A similar observation had been reported by (Kim, Choi and Tak, 1999).

The symmetric stretch vibration of the aromatic sulphone group is recorded at 1145 cm^{-1}, and a slight red shift of the sulphonate symmetric stretch takes place at samples with higher sulphonation degree. The red shift is visible from 1145 cm^{-1} to 1143 cm^{-1}.

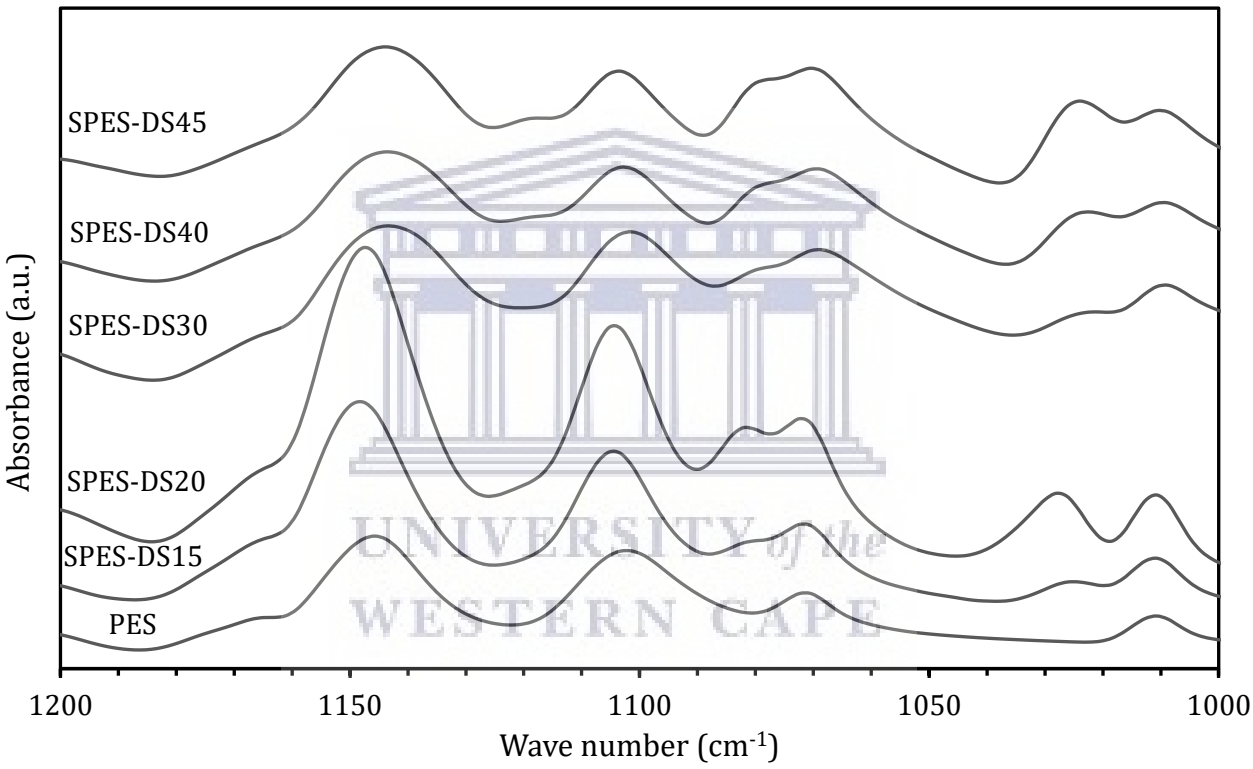

Figure 36 FTIR absorbance spectra of the aromatic sulphone group

The stretch band at 3400-3500 cm^{-1} shown in Figure 38 is characteristic of the hydrogenation bond. It indicates the higher affinity of SPES materials to water with increasing sulphonation degree. It is observed that SPES from Konishi has a less pronounced stretch band around 3500 cm^{-1}. From these observations it can be concluded that the sulphonic groups were introduced into the PES polymer chain. SPES-DS20 does not follow the trend which could be due to a measuring error, this sample should be disregarded in this analysis. These findings are congruent with (Klaysom *et al.*, 2011).

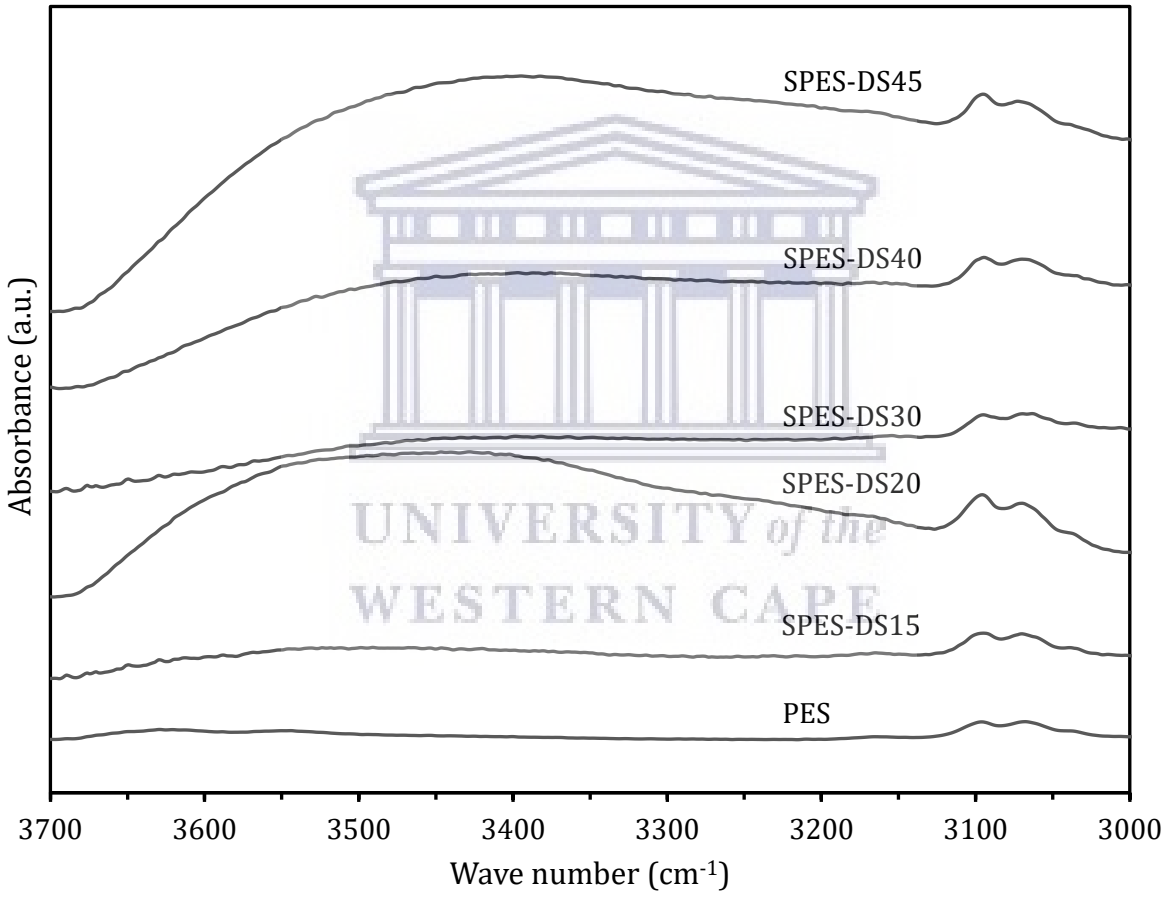

Figure 37 FTIR absorbance spectra of the hydroxyl group of sulphonic acid

The vibration of the aromatic ring skeleton is visible around 1490 cm^{-1}, it becomes less pronounced with increasing degree of sulphonation as depicted in Figure 38.

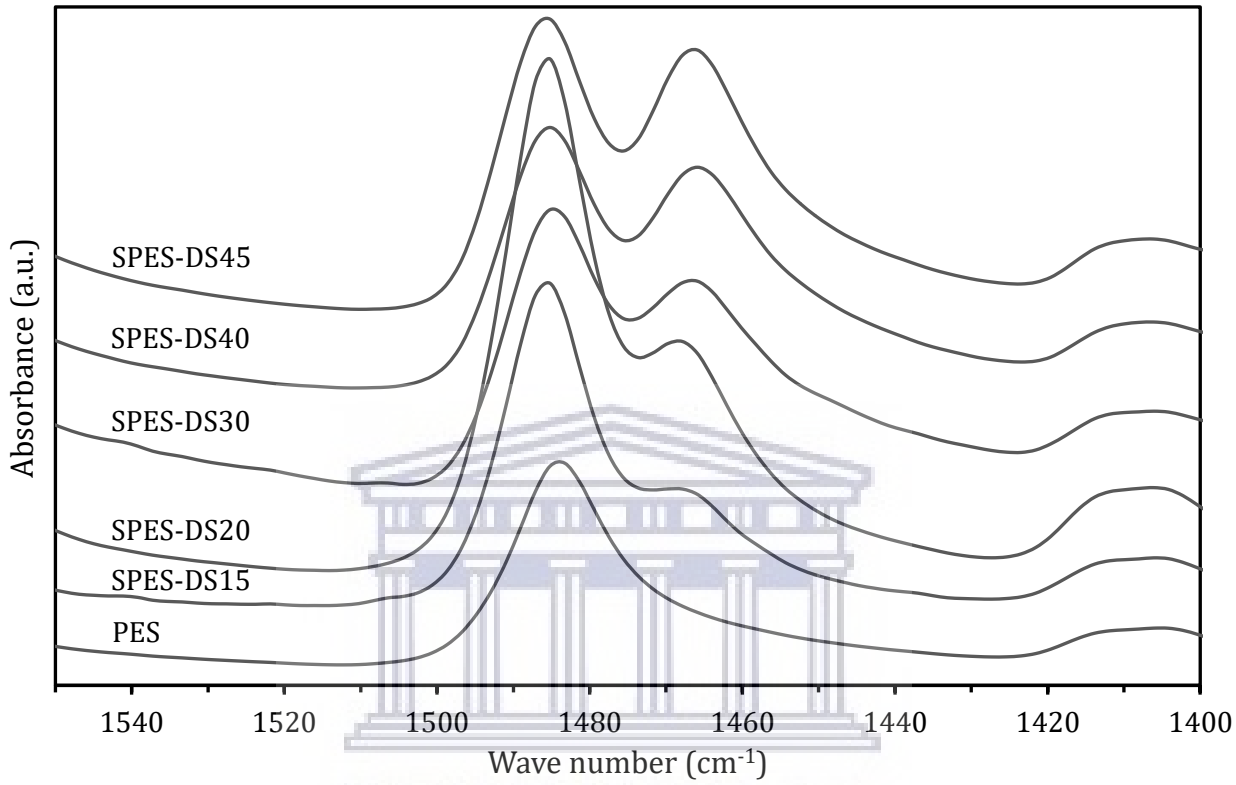

Figure 38 FTIR absorbance of the aromatic ring skeleton

4.2.3 Chemical structure – ^1H NMR

The sulphonation sites of the PES and SPES were determined by characterisation with ^1H NMR spectroscopy. All measurements were carried out in 5 mm o.d. NMR tubes at room temperature. Thirty two scans were recorded applying $\pi/2$ ^1H pulses and a delay time of 10 seconds. 15,000-20,000 scans were recorded to obtain a good signal-to-noise ratio also for low intensity signals. The integrals of the signal regions were evaluated with the fitting program of Mestre Nova software.

The peak of the internal standard is visible at 0 ppm. The DMSO-D_6 signal and the H_2SO_4 signals are observed at 2.5 ppm and 3.33 ppm respectively. The aromatic proton signal integrals are evaluated which allowed for confirmation of sulphonation and assignment of a degree of sulphonation by calculation.

Initially, an overview is given of all recorded ^{1}H NMR spectra of relevant SPES samples which are PES, and SPES samples with degrees of sulphonation of 10, 15, 20, 30, 40, and 45 mol%. Some samples (SPES-DS10 and SPES-DS25) are left out of this analysis because they are close to samples SPES-DS15 and SPES-DS20. Next, the most divergent samples are discussed and a clearer view of the signals of importance is provided.

The spectra in Figure 39 show the presence of a sulphonic acid group causing a significant down-field shift from 7.27 to 8.30 ppm of the hydrogen located in the σ-position at the aromatic ring (H_E), which is attributed to two electron-withdrawing groups of sulphone and sulphonate. Furthermore, it was observed that the intensity of this signal increased with increasing degree of sulphonation. These ^{1}H NMR spectra show the same characteristics as those reported by (Guan *et al.*, 2005).

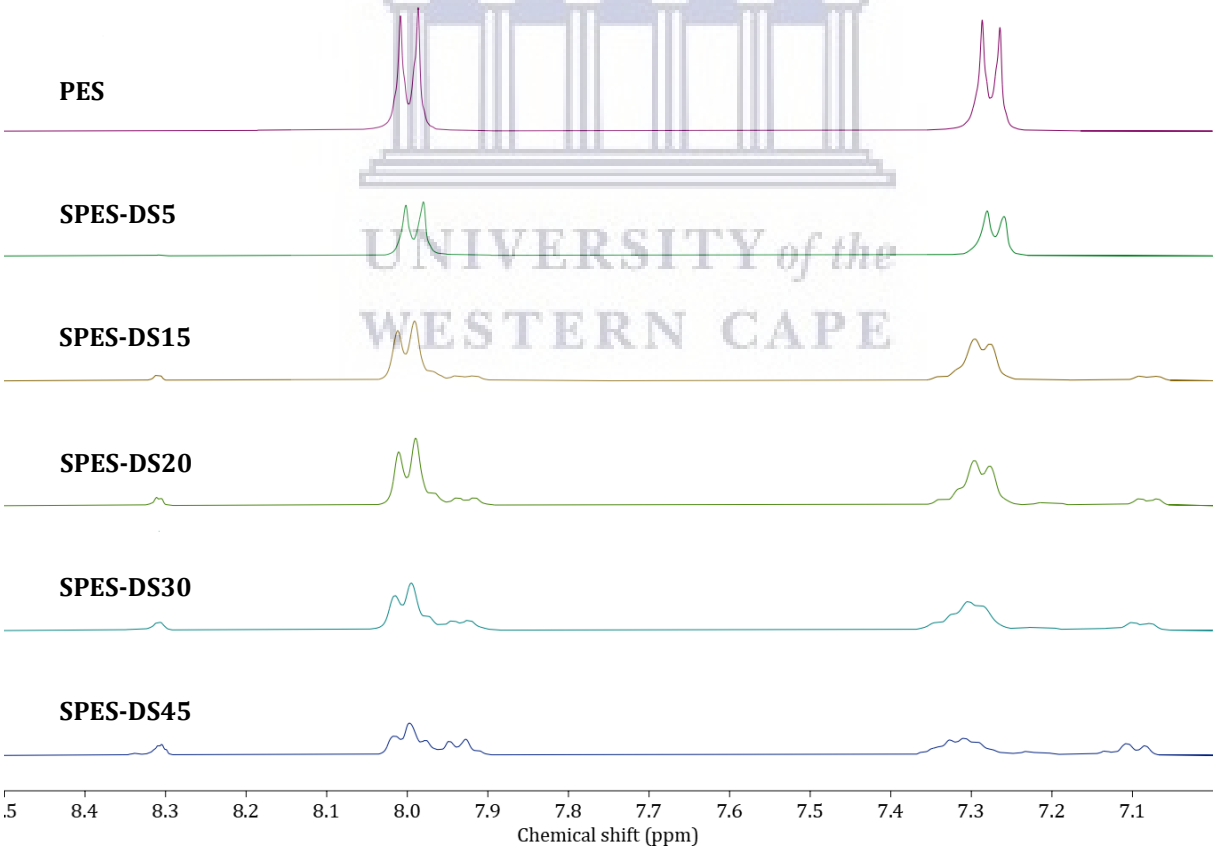

Figure 39 ^{1}H NMR spectra of PES and SPES materials

Figure 40 shows the aromatic proton signal more clearly for four samples with degrees of sulphonation of 5, 20, 30, and 45 mol%. It was clearly observed that the intensity of this signal for the aromatic proton signal at 8.3 ppm increased with increasing degree of sulphonation.

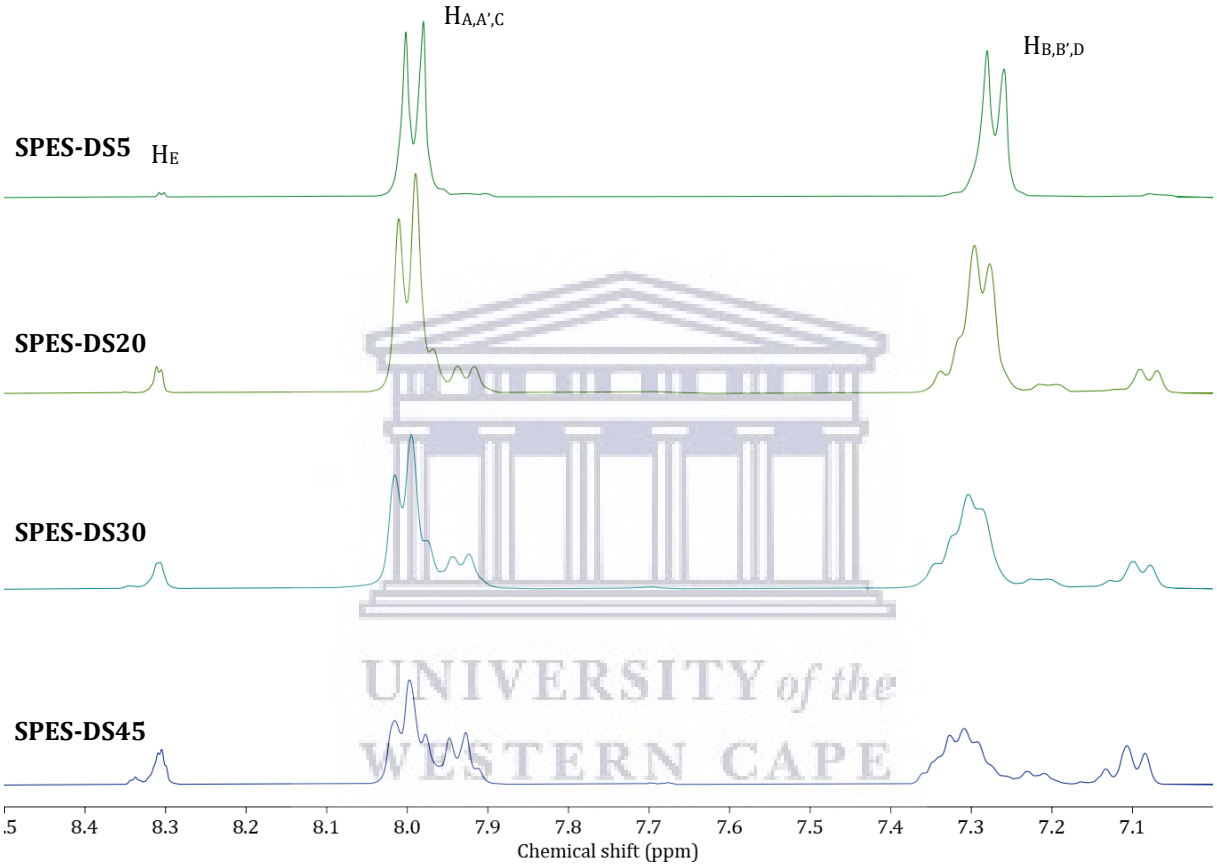

Figure 40 ^{1}H NMR spectra of PES and SPES materials

This trend of increasing intensity of the aromatic proton's signal at 8.3 ppm is once more emphasized in Figure 41, where only two samples in the higher DS range, namely a sulphonation degree of 30 an 45 mol% are compared with polyethersulphone.

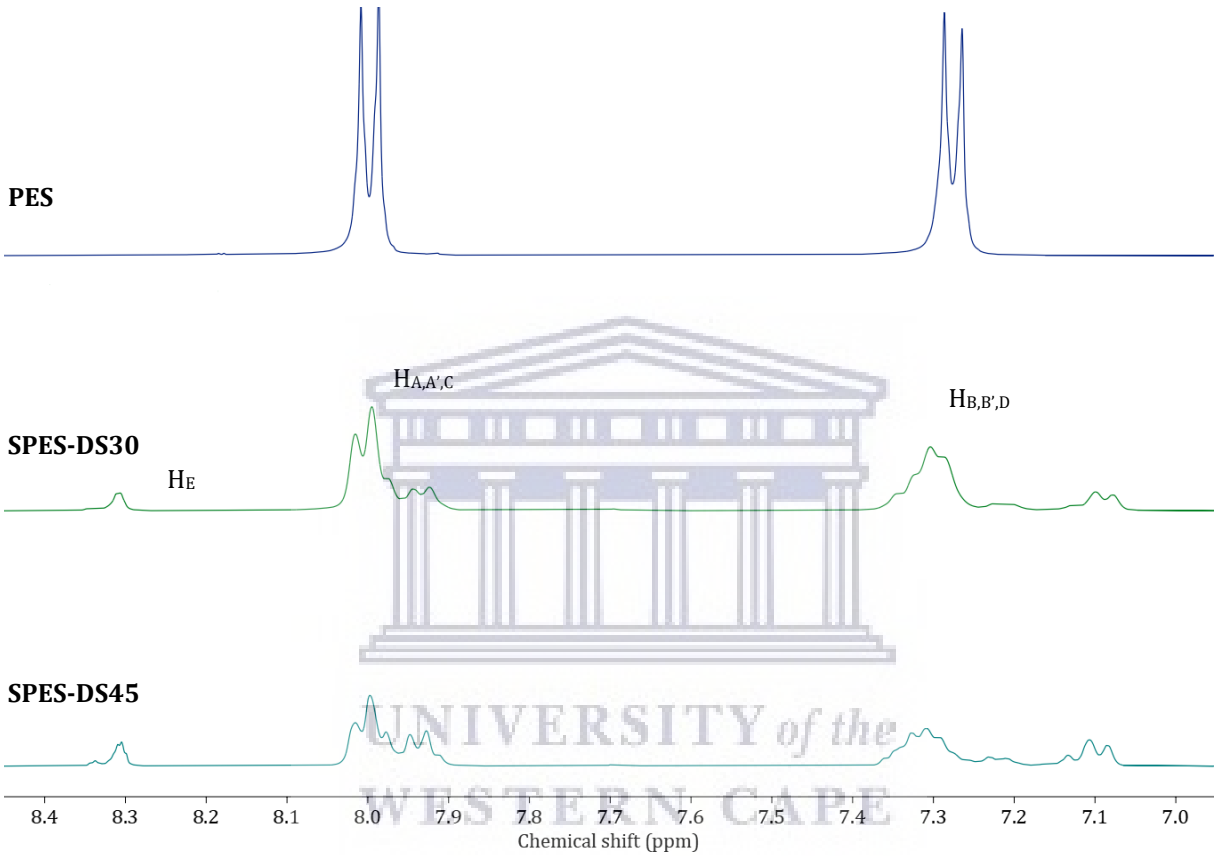

Figure 41 ^1H NMR spectra of PES and SPES materials

The calculation of the DS by ^1H NMR spectroscopy was carried out by comparison of the peak area of H_E with the peak areas of all the other aromatic hydrogen signals ($\Sigma AH_{A,A',B,B',C,D,E}$). The key integral H_E represents one proton of the sulphonated phenyl ring. The mathematical expression is described in Equation 6. Figure 42 shows the chemical structure with mentioned aromatic hydrogen signals and the proton of the sulphonated phenyl ring.

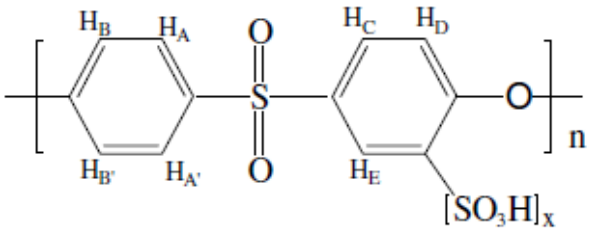

Figure 42 Chemical structure and atom numbering of SPES, x=DS (Guan *et al.*, 2005)

4.2.4 Functional groups – Ion Exchange Capacity

Ion exchange capacities of the sulphonated polyethersulphone membranes were measured using an acid-base titration method. For this purpose, flat sheet membranes were cast from SPES/NMP solution (20/80 w/v). The titrations were performed using the ''Compact Titrator G20'' with a ''DMi 140SC'' electrode (Mettler Toledo). It was observed that not all SPES membranes could be recovered for weighing. The membrane would disintegrate in the solution and some of the results are thus lacking. The reason for this phenomena is that the hydrophilic SPES films that were coagulated in a water bath, showed mechanical instability upon drying. Initially the films are soft because of the gel-like structure containing water, but upon drying, the water slowly evaporates from the membrane resulting in a brittle structure. Initially, a SPES concentration in NMP of 15 % was used to cast the films, but it was observed to be rather difficult to remove the films from the glass plate without breaking. After drying, the films became so brittle that they easily broke into small pieces. Therefore, a SPES solution of 20 % was prepared, and a stable film layer seemed to be obtained in a wet state. However, after drying it was clear that the films were too brittle still. These findings are similar to the ones reported in literature, where it was pointed out that a SPES concentration of at least 35 wt% is necessary to obtain a tough film (He, 2001).

The DS values of the samples that did not break up into pieces during the IEC measurements were determined and are listed in listed in Table 13. The DS values calculated from IEC are mostly in good agreement with the DS values obtained through ^{1}H NMR analysis for two out of three samples that were recoverable. For the sample within the higher DS bracket the deviation is higher. This could be due to loss of a piece

of the membrane in the rinsing step, since with higher hydrophilicity it is likely that it unnoticedly dissolved in water.

Table 13 Comparison of DS calculated with ^{1}H NMR and IEC

Sample name	DS by ^{1}H NMR (mol%)	DS by IEC (mol%)
SPES-01-DS2	1.67	--
SPES-02-DS3.5	3.49	--
SPES-09-DS4	4.04	--
SPES-10-DS4.5	4.59	--
SPES-04-DS8	8.07	7.78
SPES-07-DS15	14.42	--
SPES-08-DS20	18.83	--
SPES-03-DS25	22.00	19.95
SPES-05-DS40	40.35	30.07
SPES-06-DS45	44.82	--
SPES-SOL	--	--

The DS value calculated from the IEC analysis seems to be consistently lower than the DS values obtained by ^{1}H NMR analysis except for one sample (SPES-05-DS40), which is addressed earlier. As was observed by (Guan *et al.*, 2005), an insignificant difference between values obtained through IEC titration and ^{1}H NMR was expected.

The DS values calculated from IEC measurements would be higher if all polymer material was recovered. The discrepancy between the results obtained by the two methods could also be accounted for by flat sheet membranes being used for titration whereas for the ^{1}H NMR method the bulk polymer was used. If the polymer would have been used for titration, all sulphonic acid groups would be titrated, but by using flat sheet membranes, the ion exchange does not depend solely on the DS of the polymer but also on the sample size and porosity. In addition, the ions were only exchanged on the surface of the flat sheets which made the IEC obtained by titration lower that the ones obtained by the ^{1}H NMR method (Kim, Choi and Tak, 1999).

4.2.5 DS as a function of synthesis conditions

The sulphonation parameters were varied by temperature (5˚C, 10˚C, and 20˚C), by reaction time (5, 7, 9, and 25 hours), and by stirring rate (250, 400 and 500 rpm).

Table 14 presents the effect that reaction time, reaction temperature, and stirring rate have on the sulphonation degree of the membrane material. It can be seen that a wide range of DS was achieved, from roughly 2 to 45 mol%. The concentration ratio of PES/CSA was maintained at 20/60 (w/v) for all samples described.

Table 14 Correlation between reaction conditions and DS

Sample name	Reaction time (hours)	Reaction temperature (˚C)	Stirring rate (RPM)	DS by ^{1}H NMR (mol%)	DS by IEC (mol%)
SPES-01-DS2	4.5	5	250	1.67	--
SPES-02-DS3.5	7	5	250	3.49	--
SPES-09-DS4	7	10	250	4.04	--
SPES-10-DS4.5	5	10	250	4.59	--
SPES-04-DS8	9	5	250	8.07	7.78
SPES-07-DS15	5	20	250	14.42	--
SPES-08-DS20	7	20	250	18.83	--
SPES-03-DS25	26	5	250	22.00	19.95
SPES-05-DS40	9	10	500	40.35	30.07
SPES-06-DS45	9	20	400	44.82	--
SPES-SOL	25	20	400	--	--

The degree of sulphonation as a function of the reaction time is shown in Table 15 and Figure 43. During the sulphonation reactions, the reaction temperature was varied from 5˚C, 10˚C and 20˚C. Two reactions were allowed to proceed at different times of 5 hours (including one reaction at 4.5 hours) and 9 hours. SPES-05-DS40 is in good accordance with the findings of (Lu *et al.*, 2005). However, in their study a stirring rate of 800 rpm was used, and with a reaction temperature of 10˚C and a reaction time of 9 hours, a degree of sulphonation of 29.47 % (IEC) to 30.77 % (^{1}H NMR) was achieved, whereas in present study a DS of 30.07 % (IEC) to 40.35 % (^{1}H NMR) was achieved with a lower stirring rate. Overall, it can be concluded that the DS achieved in present study are comparable to (Lu *et al.*, 2005).

Table 15 Correlation between reaction time and DS

Sample name	Reaction time (hours)	Reaction temperature (˚C)	Stirring rate (RPM)	DS by ^{1}H NMR (mol%)	DS by IEC (mol%)
SPES-01-DS2	4.5	5	250	1.67	--
SPES-02-DS3.5	7	5	250	3.49	--
SPES-04-DS8	9	5	250	8.07	7.78
SPES-03-DS25	26	5	250	22.00	19.95

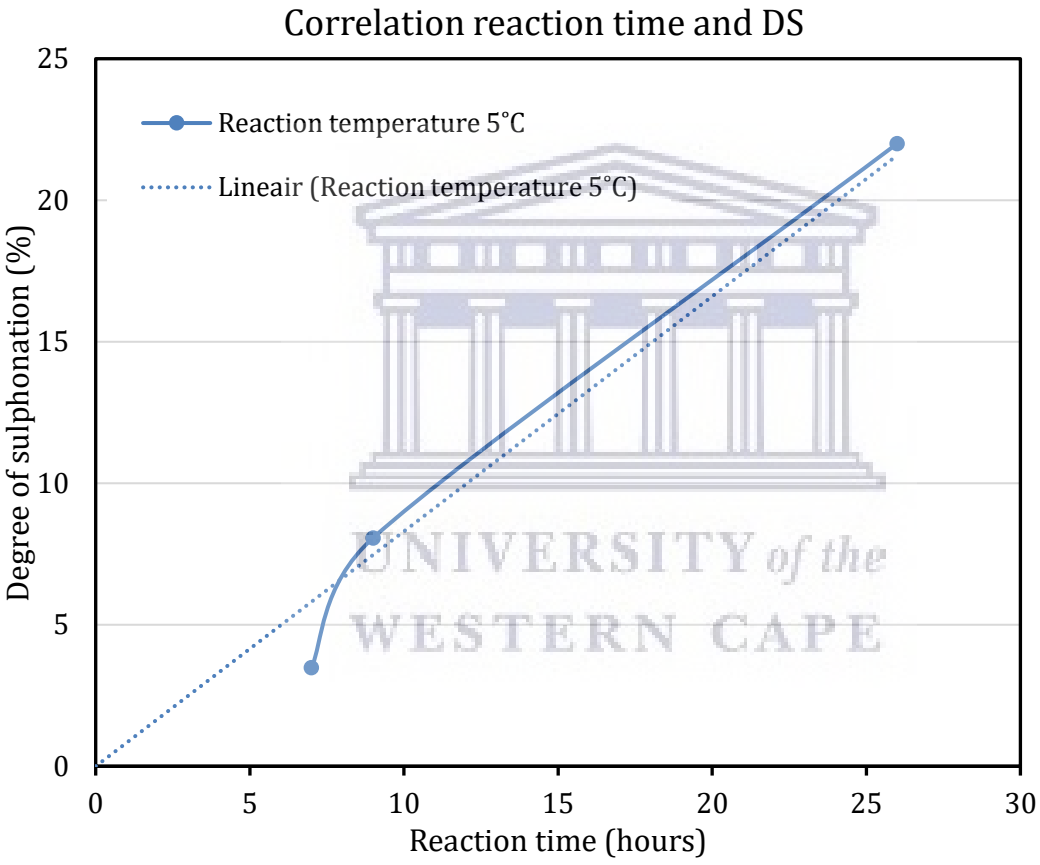

Figure 43 Degree of sulphonation as a function of reaction time

Figure 43 shows the correlation between the sulphonation time and the obtained sulphonation degree. Since there are just three data points it is difficult to draw any conclusions. It would have been interesting to see what the sulphonation degree would have been at 15 and 20 hours reaction times.

The correlation between reaction temperature and sulphonation degree is presented in Table 16 and Figure 44.

Table 16 Correlation between reaction temperature and DS

Sample name	Reaction time (hours)	Reaction temperature (˚C)	Stirring rate (RPM)	DS by ^{1}H NMR (mol%)
SPES-01-DS2	4.5	5	250	1.67
SPES-10-DS4.5	5	10	250	4.59
SPES-07-DS14	5	20	250	14.42
SPES-02-DS3.5	7	5	250	3.49
SPES-09-DS4	7	10	250	4.04
SPES-08-DS19	7	20	250	18.83

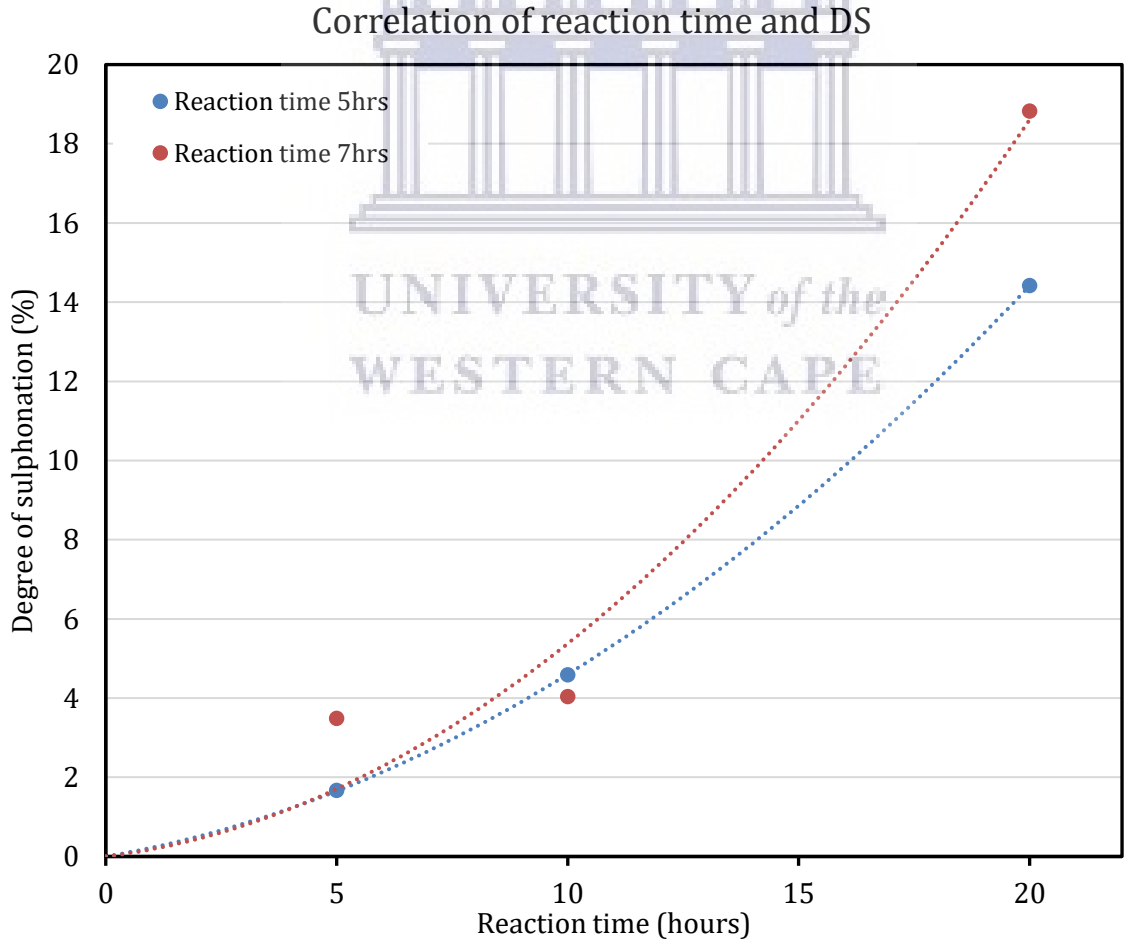

Figure 44 Degree of sulphonation as a function of reaction temperature

At 10˚C the sulphonation degree is higher at a reaction time of 5 hours compared to 7 hours. This could fall within the error of the ^{1}H NMR measurement. The calculation of the sulphonation degrees using IEC could not be executed at any of these samples due to the samples not being recoverable after titration. Unfortunately, time constraint made it impossible to cast flat sheets membranes once more to perform the titrations.

When analysing the sulphonation degree of various samples, it is clear that the stirring rate has a strong influence on the progression of the sulphonation. As seen in Table 17, the increase of the stirring rate from 250 rpm to 500 rpm shows a tenfold increase in DS. While the relative small difference between the reaction times between sample SPES-09-DS4 and SPES-05-DS40 is acknowledged, the remarkable increase of the DS value must have been induced by the increased stirring rate.

Table 17 Correlation between stirring rate and DS

Sample name	Reaction time (hours)	Reaction temperature (˚C)	Stirring rate (RPM)	DS by ^{1}H NMR (mol%)	DS by IEC (mol%)
SPES-09-DS4	7	10	250	4.04	--
SPES-05-DS40	9	10	500	40.35	30.07

Table 18 and Figure 45 show the DS as a function of reaction temperature and time, with fixed stirring rate of 250 rpm. It is seen that the DS gradually increases with increasing temperature.

Table 18 Degree of sulphonation as a function of time and temperature

Sample name	Reaction time (hrs)	Reaction Temperature (˚C)	DS by ^{1}H NMR (mol%)	Notation
SPES-01	4.5	5	1.67	SPES-DS2
SPES-02	7	5	3.49	SPES-DS3.5
SPES-04	9	5	8.07	SPES-DS10
SPES-03	26	5	22	SPES-DS25
SPES-10	5	10	4.59	SPES-DS5
SPES-09	7	10	4.04	SPES-DS4
SPES-05	9	10	40.35	SPES-DS40
SPES-07	5	20	14.42	SPES-DS15
SPES-08	7	20	18.83	SPES-DS20
SPES-06	9	20	44.82	SPES-DS45

It was observed that the polymer solubility in water increases with its sulphonation degree. The sulphonated PES could not be recovered by precipitation in water when the DS is too high: it would simply dissolve in water. The highest DS that was recovered was SPES with a DS of 44.82 mol%. Between the highest achieved DS and the non-recoverable SPES, (SPES-SOL, as it was soluble in water), there might be a DS which can be determined if the synthesis parameters are further finetuned.

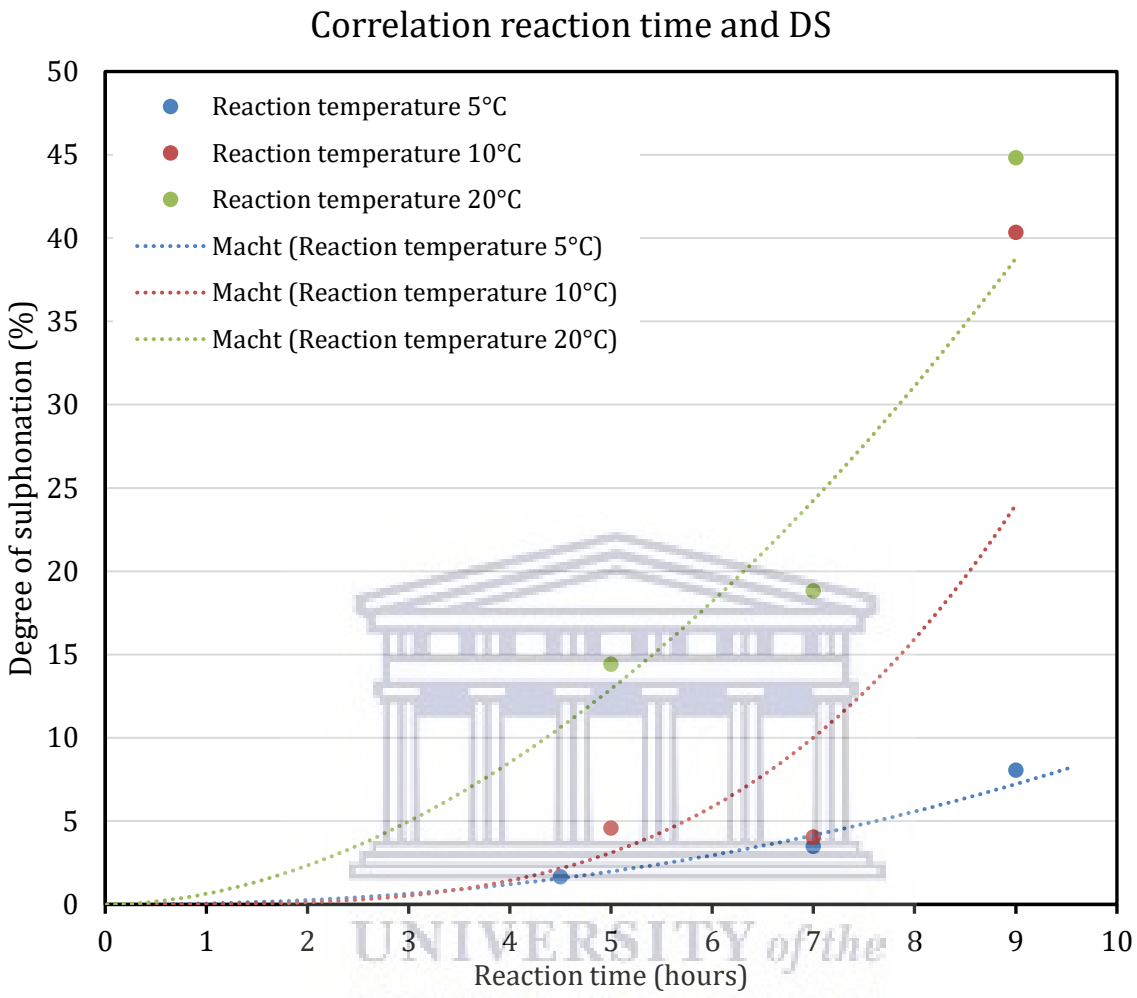

Figure 45 Degree of sulphonation as a function of reaction time and temperature

4.3 Coating PES with SPES thin layer

Solubilities of polyethersulphone and sulphonated polyethersulphone were tested. PES is soluble in selected polar aprotic solvents and in chlorinated solvents (Guan *et al.*, 2005). The solubility tests were conducted using methanol and ethanol as solvents for SPES with various DS. The results showed that for SPES to be soluble in methanol, the degree of sulphonation needed to be >30 %. When the DS is over 44 %, the SPES becomes soluble in water as well. This reflects the more ionic nature of the polymers at that DS. The solubility of SPES with higher DS in water is a result of the presence of the pendant sulphone groups which decrease the orientation of the polymer molecules. The SPES samples used for coating and their concentrations are tabulated in Table 19.

Table 19 Determined SPES/PES solubilities

Sample	Concentration	Soluble in solvent
SPES-K-DS30	6 wt% in NMP	Methanol
SPES-05-DS40	6 wt% in NMP	Methanol
SPES-06-DS45	6 wt% in NMP	Methanol
SPES-05-DS40	8 wt% in NMP	Methanol
SPES-06-DS45	8 wt% in NMP	Methanol

4.3.1 SPES coated PES hollow fibre membrane

After dip-coating of the PES hollow fibres with a SPES layer, a significant change in sub-layer and skin layer morphology is demonstrated as depicted in Figure 46. The morphology changed from porous to a more sponge like structure. It seems that the porosity has decreased substantially. The formation of a thin dense layer on the lumen side of the HF is observed (Figure 46b). However, Figure 46f exhibits a porous structure at the lumen side of the membrane. This means that dip-coating the PES membrane with SPES once has not lead to a homogeneous morphology throughout the membrane. So it was decided to dip-coat the PES HF samples once more with SPES. This was done by dipping the PES hollow fibres in the coating solution once, wait for one minute and dip once more.

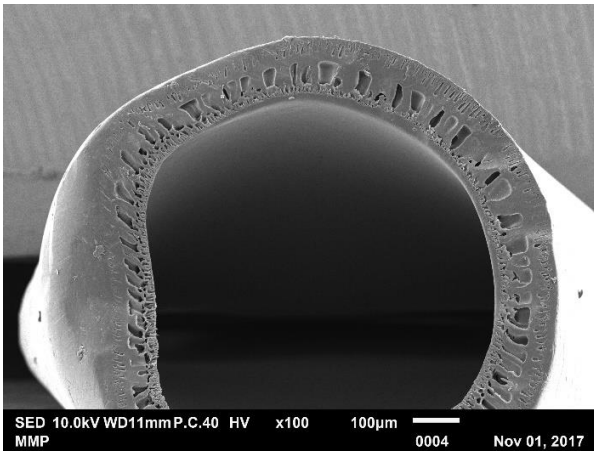

a) SPES coated PES HF, mag. 50x

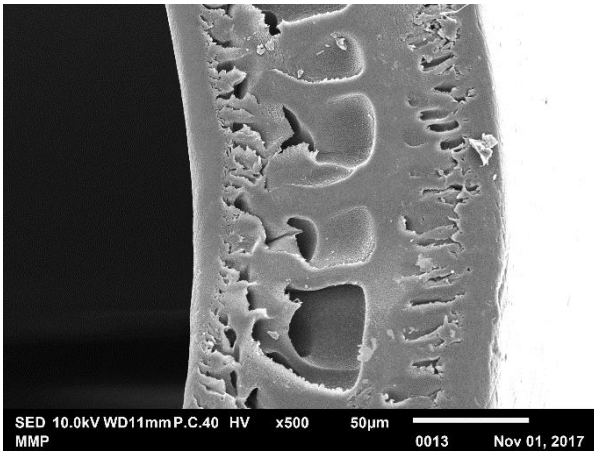

b) SPES coated PES HF, mag. 100x

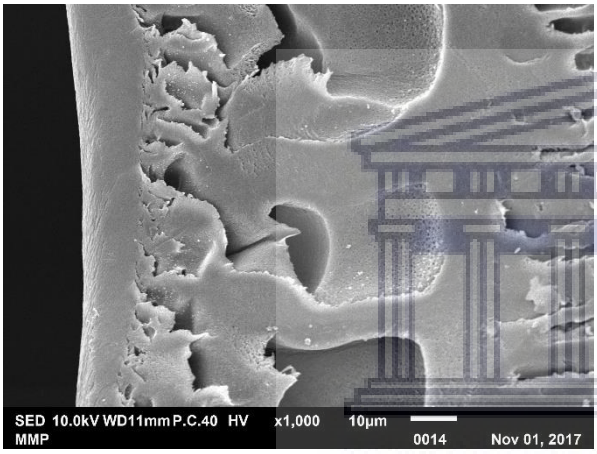

c) SPES coated PES HF, mag. 1,000x

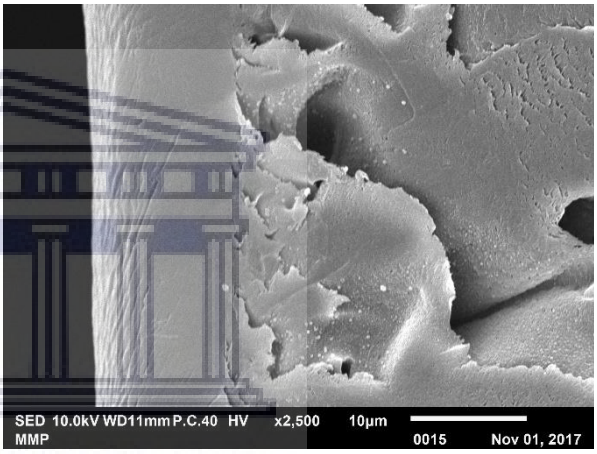

d) SPES coated PES HF, mag. 2,500x

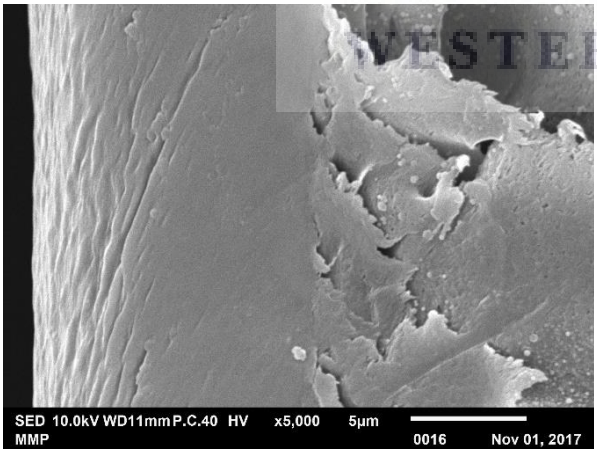

e) SPES coated PES HF, mag. 5,000x

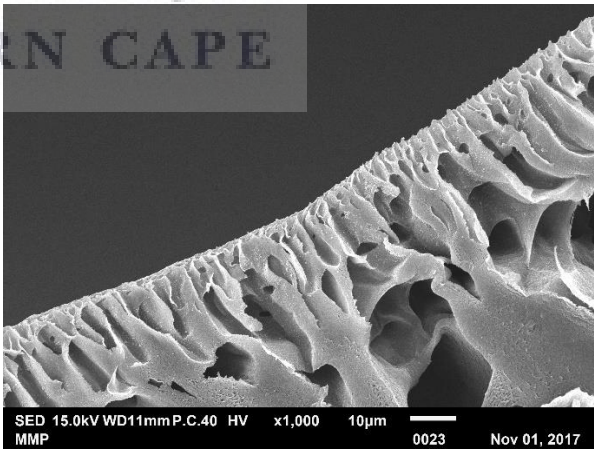

f) SPES coated PES HF, lumen side mag. 1,000x

Figure 46 SEM image of SPES coated PES HF membrane

The outer shell surface of SPES coated PES HF in Figure 47 exhibits an atypical structure. Since the water vapour selective HF membranes are supposed to be outside-in membranes, the selective layer is preferred on the outer shell of the membranes.

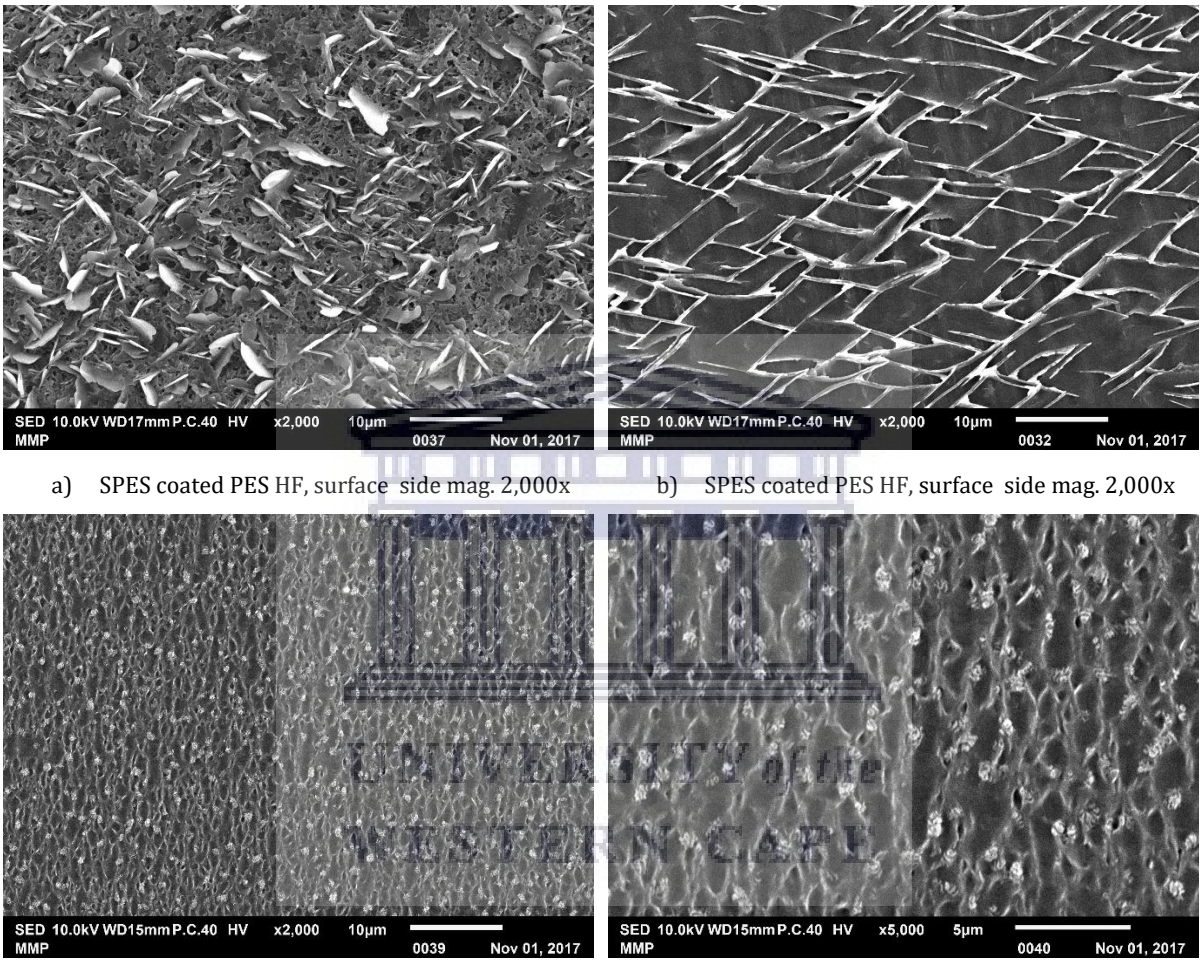

a) SPES coated PES HF, surface side mag. 2,000x

b) SPES coated PES HF, surface side mag. 2,000x

c) Surface view of SPES coated PES HF, mag. 2,000x

d) Surface view of SPES coated PES HF, mag. 5,000x

Figure 47 SEM image of SPES coated PES HF membrane

Figure 48 shows the morphology of the twice coated PES hollow fibre membrane at different magnifications. The cross sectional view demonstrates a significant change in skin layer morphology. A thin dense selective SPES layer has formed on the lumen side of the fibres. The two layers seem to attach to each other well, without any obvious lamination occurring. The minimum wall thickness is 150 μm with a minimum dense layer thickness of 10 μm. Figure 48e shows that there seems to be a start to the formation of a dense layer on the shell side of the hollow fibres.

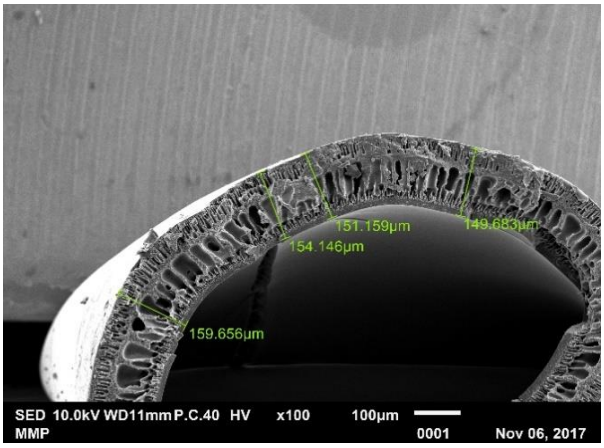

a) Cross section of SPES coated PES HF membrane, mag. 100x

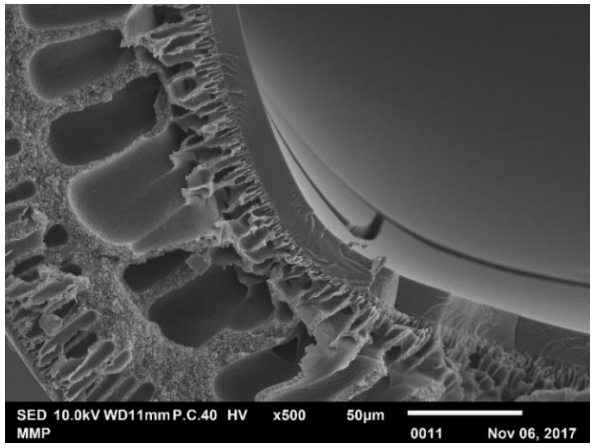

b) Dense film of SPES coated onto PES HF membrane, mag. 500x

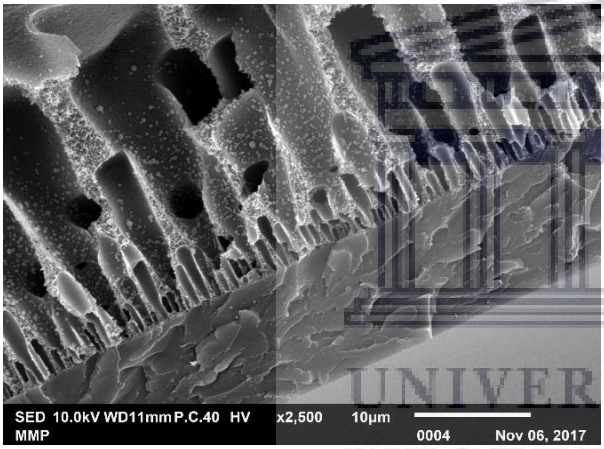

c) Dense film of SPES on the lumen side of the PES HF membrane, mag. 2,500x

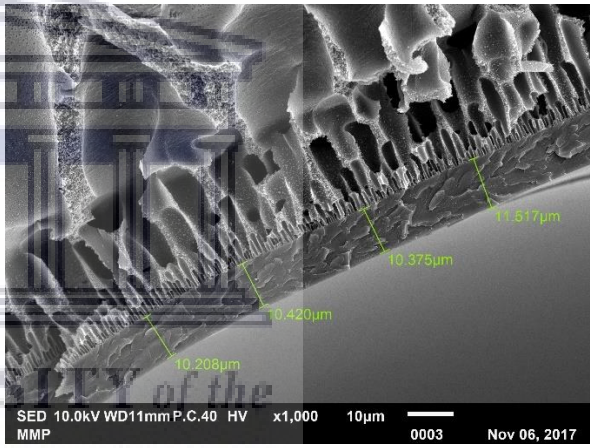

d) Thickness of the selective SPES layer on the PES HF membrane, mag. 1,000x

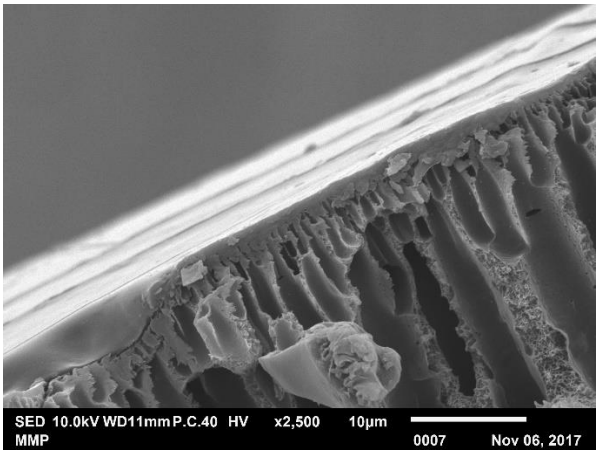

e) Shell side of the SPES coated PES HF membrane

Figure 48 SEM images of the cross-section of a SPES coated PES HF membrane

However, it is unexpected that the dense layer is formed on the inner surface of the hollow fibres. As for this application, outside-in membranes are required which means the selective layer is preferred on the outer shell of the membranes. It may have been possible that the capillary forces at play pulled in an excessive amount of coating solution that subsequently left the lumen side coated. The application of alternative coating methods, such as spraying the outer surface of the hollow fibre membranes with the coating solution homogeneously, may have to be applied, Finally, a curing step could have been added to the dip-coating procedure. Alternatively, HF PES membranes could have been dipped in the coating solution for an extended period and for repeated times, for example dipping the HF for 4-5 times, 2 min each time, to obtain a good SPES layer. It has been shown previously that adherence of the selective layer can be obtained on the outer skin of the HF support (Sijbesma *et al.*, 2008).

4.4 SPES flat sheet membrane

The flat sheet membranes were all cast from a 25 wt% SPES solution in NMP. After coagulation, it was quite difficult to remove the thin films from the glass substrate. This is due to SPES having high hydrophilicity and low coagulation rate in a water bath (Wang and Xu, 2015). With casting the SPES in a single layer it essentially became the support membrane. Once the SPES thin films were obtained from the substrate, they were soft because of the gel-like structure that contains water. The films fabricated with varying DS had various structure and colour. The membranes with low DS were opaque. With increasing DS, the thin films became more yellow. The evaporation of water from the membrane yielded a brittle polymer structure. According to literature sources on SPES with DS of 9 %, a higher polymer concentration (around 35 wt%) should be used to obtain more rigid membranes in a dry state (He *et al.*, 2002). SEM observations of the fabricated SPES thin films are summarized in Table 20.

It is evident that the DS, polymer concentration and coagulant bath all have a significant effect on the resulting morphology. This could be investigated more in the future. For reasons mentioned, it would have been interesting to co-cast layers of PES and SPES with a double casting knife, so that it could be verified how the SPES layer formed onto the PES support in flat sheet membranes.

Table 20 Overview of properties of SPES flat sheet membranes

Sample	Thickness	Precipitation liquid	Structure
FS-SPES-DS30-0.15	37 µm	Salt bath	Dense structure
FS-SPES-DS30-0.30	45 µm	Water	Spongy and dense structure
FS-SPES-DS25-0.50	101 µm	Salt bath	Porous with macro voids
FS-SPES-DS25-0.30	103 µm	Water	Porous, macro-voids, finger-like structure near top and dense top layer
FS-SPES-DS40-0.30	116 µm	Water	Porous with macro voids
FS-SPES-DS45-0.30	64 µm	Water	Porous with macro voids

It is observed that the thickness of the flat sheet membranes was significantly thinner than the cast membrane. Comparing the height of the casting knife and the thickness of the final membrane after coagulation, it became apparent that SPES membranes shrunk between 61 and 85 %. It is reported in literature that film shrinkage occurs during casting and/or during immersion in the coagulation bath. Stresses tend to build up during the immersion process in the cast polymer film as a consequence of combined wetting/de-wetting phenomena and polymer solidification. This induces the shrinkage of the formed membrane (Abdel-Hady, MM and Abdel-Hamed, 2012).

High shrinkage tendencies result in tension within the membrane, and it influences the structure of the membranes (Wang and Xu, 2015). However, since these flat sheets were only fabricated to give an idea of the water permeation, no further testing of mechanical properties were conducted.

(Yee, Zhang and Ladewig, 2013) reported that for mechanical stability and ease of handling, a membrane thickness of 30-50 µm is most preferred. Additionally, the membrane thickness seems to be mainly determined by the concentration of the casting solution, where higher weight percentages of the polymer in solvent result in thicker membranes. Ultimately, the formation of macro voids can be suppressed by using a polymer solution with higher viscosity because this facilitates a lower degree of water intrusion during phase inversion (Wang and Xu, 2015).

The surface and cross-sectional morphology of the flat sheet membranes were characterised using SEM. The flat sheet are observed to be porous with a sponge-like structure and obvious tear drop macro voids as is depicted in Figure 49.

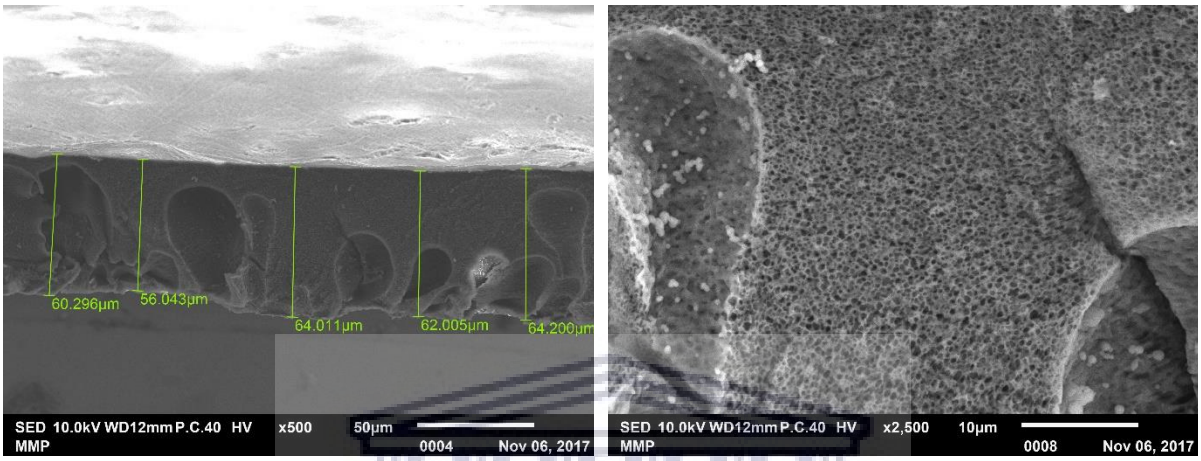

a) SPES-DS45-0.30, mag. 500x b) SPES-DS45-0.30, mag. 2,500x

Figure 49 SEM image of cross-section of flat sheet membrane made from 25 wt% SPES-DS45

Sponge-like structures appear in porous SPES membranes due to slightly delayed demixing. Macro voids occur almost in all SPES flats sheets, with the exception of SPES-K that was cast with a 150 µm casting knife. With increasing hydrophilicity, the chemical affinity between water and polymer is favourable. This results in the formation of large macro voids due to the swelling of coagulated polymer.

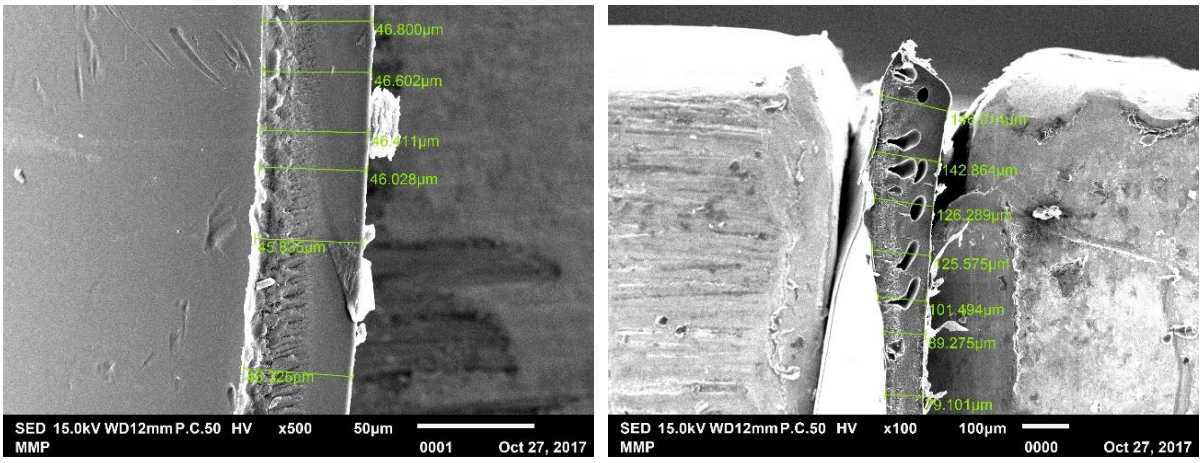

a) SPES-DS30-0.30, mag. 500 b) SPES-DS30-0.50, mag. 100x

Figure 50 SEM image of SPES flat sheet membrane made from 25 wt% SPES-DS30 using a 300µm and 500µm casting knife

Figure 50 shows the cross section of SPES with a DS of 30 mol%. It was observed that the thinner the casting knife, the denser the SPES flat sheet membranes became. This change in the morphologies can be attributed to the increased hydrophilicity of the polymer membrane as well as by the interactions between components in the casting solution and phase inversion kinetics. Additionally, coagulation in a salt bath seem to make the membranes less porous, as is seen in sample SPES-K-DS30-0.50, however it still had macro voids. The thickness seemed to have a more substantial effect on the morphology, as the dense layer was formed when using a casting knife with low thickness (150 µm) as is shown in Figure 51.

a) SPES-DS30-0.15, mag. 500x b) SPES-DS30-0.15, mag. 2,000x

Figure 51 SEM image of SPES flat sheet membrane made from 25 wt% SPES-DS30 using a 150µm casting knife

Generally, the thickness increases with DS, but since the DS differences are not too high in selected samples, this tendency is not clearly observable. Porosity usually also tends to increase with DS due to membrane swelling in phase inversion processes (Hoon *et al.*, 2013).

4.4.1 Water permeance measurements

Water permeance measurements were carried out for three flat sheet membranes prepared as described in section 3.3.2. These three samples were selected because it is reported that SPES samples with DS >20 % should be used for this purpose (Lu *et al.*, 2005). From the three samples used for water permeation measurements, only two

samples gave results. The SPES samples used for casting the flats sheet membranes were SPES-DS30, SPES-DS25, and SPES-DS40, with casting knife thickness of 300 µm as shown in Table 21.

Table 21 Flat sheet SPES membranes for water permeance measurements

Sample	Concentration	Casting knife	IEC (meq/g)
SPES-K-DS30	25 wt% in NMP	300 µm	0.30
SPES-K-DS30	25 wt% in NMP	150 µm	0.30
SPES-03-DS25	25 wt% in NMP	300 µm	0.19
SPES-05-DS40	25 wt% in NMP	300 µm	0.29

The water flux of SPES-DS25 is 5.63 L m^{-2} hr^{-1} bar^{-1}. For SPES-DS40 the flux is more or less doubled being 10.75 L m^{-2} hr^{-1} bar^{-1}, both depicted in Figure 52 and Figure 53. This means that with a degree of sulphonation that is twice as high, the water permeance also doubles. This is a result of the introduction of the sulphonic acid group which improves the water affinity of hydrophobic PES membranes, since polar functional groups can interact with water via hydrogen bonding. Other structural parameters that evidently affect the transport of water through the membranes are the porosity, tortuosity and thickness.

Clean water permeability is reported by (He, 2001) to be between 8.9 to 12.9 L m^{-2} hr^{-1} bar^{-1} for SPES membranes prepared by a coating solution of SPES/NMP/acetone of 25/37.5/37.5 wt%, and between 0.5 to 0.8 L m^{-2} hr^{-1} bar^{-1} for SPES/NMP/acetone of 30/35/35 wt%. This is due to the prior being more porous than the latter. The SPES had an IEC of 0.36 meq/g dry polymer.

(Sahebi *et al.*, 2016) reported water permeabilities of 2.1 to 2.9 L m^{-2} hr^{-1} bar^{-1} of SPES with 25 wt% and 50 wt% SPES in PES/NMP solution respectively. The degree of sulphonation of the SPES is unknown (Sahebi *et al.*, 2016). This makes it difficult to compare the findings, but it gives an idea of findings in similar works of research.

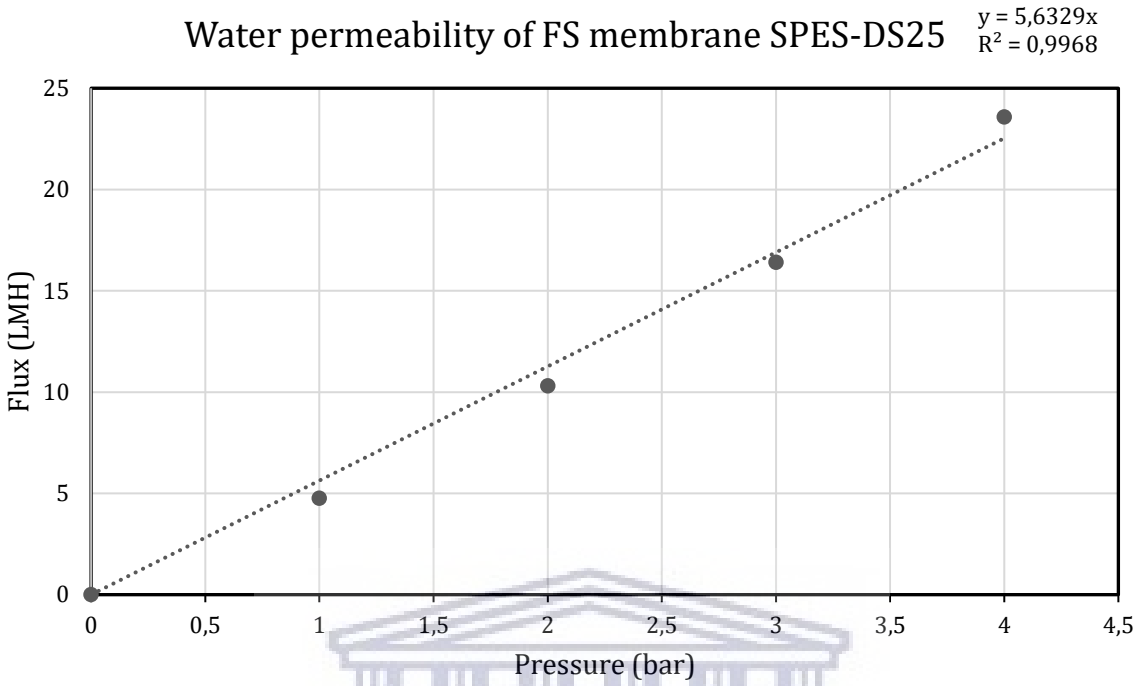

Figure 52 Water permeability of FS SPES-DS25

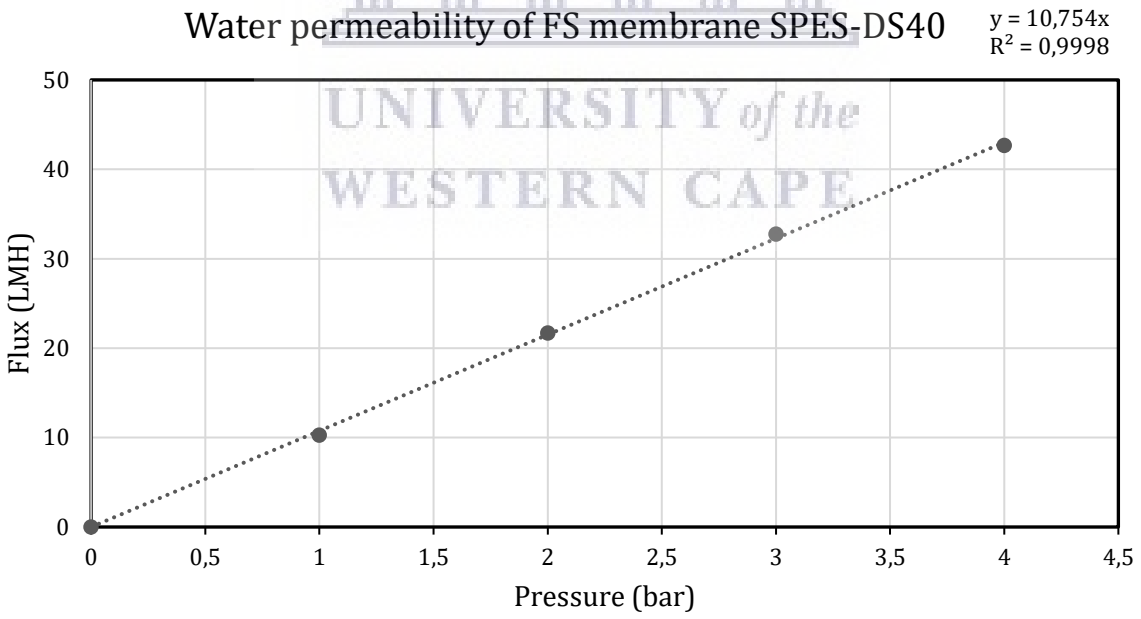

Figure 53 Water permeability of FS SPES-DS40

Chapter 5 Conclusions

This final chapter provides a conclusion to the findings obtained within the scope of present study. It presents an overview of the research aims and questions, methodology and results, followed by the discussion of its contribution to knowledge. It will reflect upon the limitations and anomalies, make recommendations, and lastly outline the scope for further research.

The research questions guided the experimental methodology used, resulting in the findings. Therefore, they are revisited in Table 22.

Table 22 Research questions addressed in the study

Main Research Question Can hollow fibre membranes be produced for potential use in water vapour recovery?
1) What is a suitable hollow fibre membrane support material, and can the HF support be produced at SAIAMC?
2) What is a suitable polymer for the selective layer with a promising permeability towards water vapour and a significantly high H_2O/N_2 selectivity?
3) How can the selective layer be formed onto the HF support?
4) What is a suitable solvent for selective polymer that does not dissolve polymeric supporting material?
5) Can the polymer for selective layer be synthesized by controlling reaction variables?
6) What is the optimum sulphonation degree of the selected polymer?
7) What are the chemical, physical and thermal properties of the membrane materials (both support and composite layer)?

The literature review led to a better understanding of the beneficial use of membranes for water vapour recovery purposes in wet flue gas desulphurization units of power plants. However, the literature review resulted in apparent gaps in the use of SPES for HF membranes. The methodology allowed for experimental insight to be gained in the fabrication of PES hollow fibres with optimum dimensions, the sulphonation reaction, and dip-coating of the HF support. Finally, the analytical methods used, served as a good starting point to characterise the morphology, chemical composition, and thermal properties in a structured manner. Water permeance measurements gave an idea of the quality of the membranes in comparison with those cited in the literature.

Interpretation of the research results

The results of this study demonstrate that membrane technology is rather complex and reliant on various interdependent factors. To understand this, the findings are revisited based on each sub-question and the findings are placed within the context of previous findings from literature. A summary of each question is presented in the following:

Question 1 and sub-questions

What is a suitable hollow fibre membrane support material? And can the HF support be produced at SAIAMC?

Polyethersulphone hollow fibres have been fabricated with favourable dimensions, namely HF with a minimum inner- and outer diameter were 850 µm and 1,200 µm respectively. The wall thickness obtained had a minimum of 170 µm. This was in good accordance with published studies. Polyethersulphone hollow fibres have been shown to have a good thermal stability.

However, in the future a non-solvent should be added to limit the amount of macro voids formed. Overall, these finding support one aim of the study, namely, to illustrate that good control over HF membrane properties is possible. The HF support membrane could very well be produced at SAIAMC, acquiring a spin line would be essential. Alternatively, commercial ultrafiltration PES HF could be purchased, whereupon an automized dip-coating system could be developed.

- What are the optimal process conditions for the fabrication of SPES polymer that is used in water recovery from flue gas application?

The formulation of dope solution was 20/80 w/v PES in NMP. This could be improved by adding a non-solvent. The air gap was 20 cm, with a dope and bore solution flowrate of 0.3 mL/min.

Question 2

What is a suitable polymer for the selective layer that is compatible with the HF support and has a promising permeability towards water vapour and a significantly high H_2O/N_2 selectivity?

SPES may not have the superior permeability and selectivity as SPEEK and PEBAX but this may be related to limited research efforts. The results available in literature did not disclose the sulphonation degree, which is an important parameter. SPES is very compatible with PES support. The SPES thin film obtained did not show any delamination or cracking. A better compatibility may allow for thinner membranes to be formed yielding a higher permeance despite the lower perceived permeability. The water vapour permeability and H_2O/N_2 selectivity were not measured in this study, and would require further research in future study.

Question 3

How can this suitable selective layer be formed onto the HF support?

The functional composite material SPES was dip-coated onto the polyethersulphone support hollow fibres? Dipping the PES HF twice in coating solution with methanol as solvent obtained a thin film of 10 μm. In the future, longer dipping times could be adhered to, and frequency of dipping could be increased to obtain optimal thickness of the selective layer. The selective layer was formed on the lumen side of the PES HF, this requires further investigation as a thin layer is preferably formed on the outer shell of the membrane.

Question 4

What is a suitable solvent for selective polymer that does not dissolve supporting material?

Methanol showed to be a suitable solvent for SPES with DS >30 %, this did not dissolve the PES hollow fibre support and a thin layer of SPES was applied on the lumen surface of the PES hollow fibres.

Question 5

Can the polymer for selective layer be synthesized by controlling reaction variables?

The sulphonation conditions were varied by temperature, by reaction time, and stirring rate. The samples obtained had a DS of roughly 2, 5, 10, 15, 20, 25, 40 and, 45 mol%. It was seen that the DS could be well controlled by adjusting the synthesis parameters.

Question 6

What is the optimum sulphonation degree of the selected polymer?

Negatively charged sulphonic acid groups were successfully introduced into the PES polymer via a sulphonation reaction. The charged groups introduced into the polymer chains not only improved the hydrophilicity of the PES polymers, but also made them ion-exchangeable. The DS can be easily controlled by varying the ratio of sulphonating agents and polymer materials, by adjusting the reaction time and temperature and the stirring rate in the reactor. SPES with a sulphonation degree of 40 mol% is the optimal membrane material, as it is suitable for dissolution in methanol and makes it possible for dip-coating the PES hollow fibres. The DS can be easily controlled by varying the ratio of sulphonating agents and polymer materials, by adjusting the reaction time and temperature and the stirring rate in the reactor.

Question 7

Does the synthesized membrane have good physical and thermal and properties?

- Can Fourier-Transform Infrared Spectroscopy be used to confirm the sulphonation of polyethersulphone?

The presence of the pendant sulphone group was confirmed by FTIR analysis, as the characteristic peaks of the SO_3H symmetric and asymmetric stretching vibrations were observed.

- What is the thermal stability of PES and SPES, at what temperature does it decomposes?

SPES decomposes at a temperature around 300-450˚C, whereas the PES polymer main chain decomposes around 490-500˚C. This makes the polymeric materials suitable for use in membranes for the purpose of water vapour recovery from a flue gas stream.

- Can ^1H Nuclear Magnetic Resonance Spectroscopy be applied to determine the degree of sulphonation of sulphonated polyethersulphone composite material?

From the ^1H NMR spectra the aromatic proton signal integrals were evaluated which allowed for confirmation of sulphonation and assignment of a degree of sulphonation by calculation.

- Can the Ion Exchange Capacity be determined by titration?/Can Ion Exchange Capacity be used to calculate the degree of sulphonation of the sulphonated polyethersulphone thin film material?

The brittleness of the flat sheet membrane made it difficult to recover the membrane after IEC titration. For most of the samples that were measured, the DS resembled the DS obtained with ^1H NMR. This brittleness of the flat sheet could be solved by casting thicker sheets of membranes, or using a higher SPES polymer concentration in casting solution.

Recommendations

There is still a lot of research to be done to get a better understanding of the applicability of SPES composite hollow fibre membranes for the purpose of water vapour recovery.

It is important to further investigate the formation of the dense layer on the inner skin of the hollow fibre membrane as the selective layer is preferred on the outer sell surface of hollow fibre membranes.

To examine the functionality of SPES/PES hollow fibre membranes, the water vapour permeability and H_2O/N_2 selectivity require further study. To this extend, SPES composite hollow fibre membrane modules could be fabricated to measure water vapour permeance properties and H_2O/N_2 selectivity in the humidified flue gas stream pilot set-up at SAIAMC.

Recent study by Noor et al. have investigated the dual spinning of PES and SPES by co-extrusion using a triple orifice spinneret to form the layers. This could be a more coherent and consistent method for fabricating SPES composite hollow fibre membranes (Noor *et al.*, 2018).

Alternatively, PES/SPES blends could be used whereby the SPES is applied onto the outer shell surface, as hydrophilic parts are mainly located on the membrane surface due to hydrophilic interactions with water. Therefore, sulphonic acids tend to move to the membrane surface.

Bibliography

Abdel-Hady, E., MM, E.-T. and Abdel-Hamed, M. (2012) 'Casting Membrane of Acrylamide/Polymethacrylic acid and Reinforced by PAC for Application in Fuel Cell Unit', *Journal of Membrane Science & Technology*, 02(01). doi: 10.4172/2155-9589.1000111.

African Development Bank Group (2018) *Environmental and Social Impact Assessment Summary for Medupi Flue Gas Desulphurisation Retrofit Project*, *African Development Bank Group*.

B.G. van Campenhout (2017) *Polymer membranes for the separation of CO , CO 2 and O 2*, *Eindhoven University of Technology*.

Babcock&Wilcox (2015) *Steam, Its Generation and Use*. Edited by G. L. Tomei. Charlotte, North Carolina, USA: Babcock & Wilcox Comapny. doi: 10.1017/CBO9781107415324.004.

Bagheri, F. (2018) 'Performance investigation of atmospheric water harvesting systems', *Water Resources and Industry*. Elsevier B.V., 20(May), pp. 23–28. doi: 10.1016/j.wri.2018.08.001.

Baker, R. W. (2006) *Membranes for Vapor/Gas Separation*, *Membrane Technology and Research Inc*. Menlo Park California. doi: 10.1017/CBO9781107415324.004.

Baker, R. W. (2012) *Membrane Technology and Applications*. doi: 10.1002/3527608788.

Bergmair, D. D. (2015) *Design of a system for humidity harvesting using water vapor selective membranes*. Technische Universiteit Eindhoven.

Bernardo, P. and Clarizia, G. (2013) '30 Years of Membrane Technology for Gas Separation', *Chemical Engineering Transactions*, 32, pp. 1999–2004. doi: 10.3303/CET1332334.

Bernardo, P., Drioli, E. and Golemme, G. (2009) 'Membrane gas separation: A review/state of the art', *Industrial and Engineering Chemistry Research*, 48(10), pp. 4638–4663. doi: 10.1021/ie8019032.

Bitter, J. G. A. (1991) *Transport Mechanisms in Membrane Separation Processes*. Edited by D. Luss. Enschede: Springer Science and Business Media.

Black & Veatch (1996) *Power Plant Engineering*. Edited by K. Drbal, Larry;Westra and P. Boston. Kluwer Academic Publishers.

Black & Veatch (no date) 'Medupi Power Station 6x800 MW (Gross) Units Wet Flue Gas Desulphurization (FGD) Retrofit Project Design Manual', pp. 1–129.

Bolto, B., Hoang, M. and Xie, Z. (2012) 'A review of water recovery by vapour permeation through membranes', *Water Research*. Elsevier Ltd, 46(2), pp. 259–266. doi: 10.1016/j.watres.2011.10.052.

Bram, M. *et al.* (2011) 'Testing of nanostructured gas separation membranes in the flue

gas of a post-combustion power plant', *International Journal of Greenhouse Gas Control*. Elsevier Ltd, 5(1), pp. 37–48. doi: 10.1016/j.ijggc.2010.08.003.

Bronkhorst, S. *et al.* (2017) 'Water –Market Intelligence Report', *GreenCape*. Available at: https://www.greencape.co.za/assets/Uploads/GreenCape-Water-MIR-2017-electronic-FINAL-v1.pdf.

Carney, Barbera;Shuster, E. (2014) 'Reducing Energy ' s Water Footprint : Driving a Sustainable Energy Future in achieving the least cost path to a sustainable low', *Cornerstone, The Official Journal of the World Coal Energy*, 2(1).

Carpenter, A. M. (2012) *Low water FGD technologies*, *IEA Clean Coal Center*.

Carpenter, A. M. (2017) *Water conservation in coal-fired power plants*.

Chang, Daniel; van Wijk, Leon; Bagus, M. (2018) *Medupi Flue Gas Desulphurization Technology Selection Study Report*, *Eskom Holdings*.

Chourou, F. *et al.* (2017) 'A new efficient model for multicomponent membrane separation and application to the Argon Power Cycle', in *Fall Technical Meeting of the Western States Section of the Combustion Institute*.

Copen, J. H., Sullivan, T. B. and Folkedahl, B. C. (2005) 'PRINCIPLES OF FLUE GAS WATER RECOVERY SYSTEM John H . Copen Terrence B . Sullivan', in *POWER-GEN International 2005*. Siemens.

Deimede, V. *et al.* (2000) 'Miscibility behavior of polybenzimidazole/sulfonated polysulfone blends for use in fuel cell applications', *Macromolecules*, 33(20), pp. 7609–7617. doi: 10.1021/ma000165s.

Delgado, A. and Herzog, H. J. (2012) 'A simple model to help understand water use at power plants', *Working Paper*, (March), pp. 1–21. Available at: http://sequestration.mit.edu/pdf/2012_AD_HJH_WorkingPaper-WaterUse_at_PowerPlants.pdf.

Delgado Martin, A. (2012) 'Water Footprint of Electric Power Generation : Modeling its use and analyzing options for a water-scarce future', *International Congress on Advances in Nuclear Power Plants*, 44(2006), p. 117. doi: 10.1021/es802162x.

Doran, P. M. (2013) *Bio Process Engineering Principles*. Academic Press.

Eskom (2018) *Water reuse and recycle practices at Eskom Power Plants*.

Eskom Holdings (2020) *Reduction in Water Consumption*, *Eskom Holdings*. Available at: http://www.eskom.co.za/OurCompany/SustainableDevelopment/Pages/Reduction_In_Water_Consumption.aspx.

Eskom Investment Support Project (2010).

Fang, L. F. *et al.* (2018) 'Evaluating the Antifouling Properties of Poly(ether sulfone)/Sulfonated Poly(ether sulfone) Blend Membranes in a Full-Size Membrane Module', *Industrial and Engineering Chemistry Research*, 57(12), pp. 4430–4441. doi: 10.1021/acs.iecr.8b00114.

Freeman, B. D. (1999) 'Basis of permeability/selectivity tradeoff relations in polymeric gas separation membranes', *Macromolecules*, 32(2), pp. 375–380. doi: 10.1021/ma9814548.

Freeman, B. D. and Pinnau, I. (2004) 'Gas and Liquid Separations Using Membranes: An Overview', in *Advanced Materials for Membrane Separations*. Washington DC: American Chemical Society. doi: 10.1021/bk-2004-0876.ch001.

Gohil, JM;Choudhury, R. (2019) *Nanoscale material in water purification*. Edited by D. Thomas, S; Pasquini, D; Leu, SY; Gopakamur. Elsevier Inc. Available at: https://www.sciencedirect.com/topics/engineering/symmetric-membrane%0Dv.

Guan, R. *et al.* (2005) 'Polyethersulfone sulfonated by chlorosulfonic acid and its membrane characteristics', *European Polymer Journal*, 41(7), pp. 1554–1560. doi: 10.1016/j.eurpolymj.2005.01.018.

Guan, R. *et al.* (2006) 'Effect of casting solvent on the morphology and performance of sulfonated polyethersulfone membranes', *Journal of Membrane Science*, 277(1–2), pp. 148–156. doi: 10.1016/j.memsci.2005.10.025.

Hao, L., Zuo, J. and Chung, T.-S. (2014) 'Formation of Defect-Free Polyetherimide/PIM1 Hollow Fiber Membranes for Gas separation', *American Institute of Chemical Engineers*, 60(11), pp. 3848–3858. doi: 10.1002/aic14565.

Harmison, M. (no date) 'Membrane Technology', in. Available at: https://slideplayer.com/slide/3411499/.

He, T. (2001) *Composite hollow fiber membranes for ion separation and removal*. Available at: http://doc.utwente.nl/36289/1/t000002f.pdf.

He, T. *et al.* (2002) 'Preparation of composite hollow fiber membranes: Co-extrusion of hydrophilic coatings onto porous hydrophobic support structures', *Journal of Membrane Science*, 207(2), pp. 143–156. doi: 10.1016/S0376-7388(02)00118-7.

Hoon, Y. *et al.* (2013) 'Polyamide thin- fi lm composite membranes based on carboxylated polysulfone microporous support membranes for forward osmosis'. Elsevier, 445, pp. 220–227. doi: 10.1016/j.memsci.2013.06.003.

Kim, I. C., Choi, J. G. and Tak, T. M. (1999) 'Sulfonated polyethersulfone by heterogeneous method and its membrane performances', *Journal of Applied Polymer Science*, 74(8), pp. 2046–2055. doi: 10.1002/(SICI)1097-4628(19991121)74:8<2046::AID-APP20>3.0.CO;2-3.

Klaysom, C. *et al.* (2011) 'Preparation and characterization of sulfonated polyethersulfone for cation-exchange membranes', *Journal of Membrane Science*. Elsevier B.V., 368(1–2), pp. 48–53. doi: 10.1016/j.memsci.2010.11.006.

Komber, H. *et al.* (2012) 'Degree of sulfonation and microstructure of post-sulfonated polyethersulfone studied by NMR spectroscopy', *Polymer*. Elsevier Ltd, 53(8), pp. 1624–1631. doi: 10.1016/j.polymer.2012.02.020.

Kools, W. F. C. (1998) 'Membrane formation by phase inversion in multicomponent

polymer systems; mechanisms and morphologies', *University of Twente*. doi: 10.1016/S0009-2509(97)00384-9.

Lu, D. *et al.* (2005) 'Sulfonation of Polyethersulfone by Chlorosulfonic Acid', 28, pp. 21–28. doi: 10.1007/s00289-005-0361-x.

Macknick, J. *et al.* (2012) 'Operational water consumption and withdrawal factors for electricity generating technologies: A review of existing literature', *Environmental Research Letters*, 7(4). doi: 10.1088/1748-9326/7/4/045802.

Maier, G. (1998) 'Gas Separation with Polymer Membranes', *Angewandte Chemie International Edition*, 37(21), pp. 2960–2974. doi: 10.1002/(sici)1521-3773(19981116)37:21<2960::aid-anie2960>3.0.co;2-5.

Mannan, H. A. *et al.* (2013) 'Recent Applications of Polymer Blends in Gas Separation Membranes', (11), pp. 1838–1846. doi: 10.1002/ceat.201300342.

Metz, S. J. (2003) *WATER VAPOR AND GAS TRANSPORT THROUGH POLYMERIC MEMBRANES*. Universiteit Twente.

Metz, S. J. *et al.* (2005) 'Transport of water vapor and inert gas mixtures through highly selective and highly permeable polymer membranes', 251, pp. 29–41. doi: 10.1016/j.memsci.2004.08.036.

Minnesota Water Works Operational Manual (2009). Available at: https://www.mrwa.com/mnwaterworksmnl.html.

de Miranda, D. M. V. *et al.* (2019) 'A bibliometric survey of Paraffin/Olefin separation using membranes', *Membranes*, 9(12). doi: 10.3390/membranes9120157.

Mulder, M. (1992) *Basic Principles of Membrane Technology*. Twente: Springer-Science & Business Media. doi: 10.1017/CBO9781107415324.004.

Noor, N. *et al.* (2018) 'Hollow fiber membranes of blends of polyethersulfone and sulfonated polymers', *Membranes*, 8(3), pp. 1–16. doi: 10.3390/membranes8030054.

Pabby, A.K; Rizvi, S.S.H; Sastre Requena, A. . (2015) *Handbook of Membrane Separations*. CRC Press.

Peng, N., Chung, T. S. and Wang, K. Y. (2008) 'Macrovoid evolution and critical factors to form macrovoid-free hollow fiber membranes', *Journal of Membrane Science*, 318(1–2), pp. 363–372. doi: 10.1016/j.memsci.2008.02.063.

Pereira Nunes, S. and Peinemann, K. . (2006) *Membrane Technology in the Chemical Industry*, *Wiley -VCH*. Edited by K. . Pereira Nunes, S, Peinemann. Wiley-VCH.

Pica, M. (2016) 'Sulfonated PES (SPES)', *Encyclopedia of Membranes*. Springer, Berlin, Heidelberg. doi: DOI https://doi-org.ezproxy.uwc.ac.za/10.1007/978-3-662-44324-8.

Pinnau, I. (2000) 'Membrane Separations Membrane Preparation', *Encyclpopedia of Separation Science*. Elsevier Science Ltd. Available at: https://www.sciencedirect.com/topics/materials-science/composite-membrane.

Potreck, J. (2009) *Membranes for flue gas treatment*. Twente Universiteit.

Poullikkas, A. (2015) 'Review of Design, Operating, and Financial Considerations in Flue Gas Desulfurization Systems', *Energy Technology & Policy*, 2(1), pp. 92–103. doi: 10.1080/23317000.2015.1064794.

Rackley, S. A. (2007) *Carbon Capture and Storage*. Elsevier. Available at: https://www.sciencedirect.com/topics/engineering/symmetric-membrane.

Ran, Fen; Li, Dan; Niu, X. (2019) 'Chapter 8 Polyethersulfone fiber', in Grumezescu, Valentina; Grumezescu, A. M. (ed.) *Materials for Biomedical Engineering - Biopolymer Fibers*. Elsevier Inc, pp. 245–288.

Sahebi, S. *et al.* (2016) 'Effect of sulphonated polyethersulfone substrate for thin film composite forward osmosis membrane', *Desalination*. Elsevier B.V., 389, pp. 129–136. doi: 10.1016/j.desal.2015.11.028.

Sarunac, N. (2010) *Power 101: Flue Gas Heat Recovery in Power Plants, Part III*.

Sarunac, N. (2020) *POWER, Power Magazine*. Available at: https://www.powermag.com/ (Accessed: 25 April 2020).

Shung, T. (1997) 'Formation of ultrathin high-performance polyethersulfone hollow-fiber membranes', 133, pp. 161–175.

Sijbesma, H. *et al.* (2008) 'Flue gas dehydration using polymer membranes', *Journal of Membrane Science*, 313(1–2), pp. 263–276. doi: 10.1016/j.memsci.2008.01.024.

Singh, R. P. and Berchtold, K. A. (2017) 'Water Treatment and Water-Vapor Recovery Using Advanced Thermally Robust Membranes for Power Production', in. Pittsburg: Los Alamos National Laboratory.

Sridhar, S., Bee, S. and Bhargava, S. K. (2014) 'Membrane-based Gas Separation: Principle, Applications and Future Potential', *chemical engineering digest*. Available at: https://pdfs.semanticscholar.org/3829/9fb900722280197fedbccbbd5d8682b405ac.pdf.

Srivastava, R. K. and Jozewicz, W. (2001) 'Flue gas desulfurization: The state of the art', *Journal of the Air and Waste Management Association*, 51(12), pp. 1676–1688. doi: 10.1080/10473289.2001.10464387.

Stephen, C. L. (2017) 'Reduction of wet flue gas desulphurisation water consumption through heat recovery Supervisor ':, (May).

TU/e (2017) 'Amicon Stirred Cell Manual'.

UNECE (2012) *Parties to UNECE Air Pollution Convention approve new emission reduction commitments for main air pollutants by 2020, 4 May 2012*. Available at: www.unece.org.

Unnikrishnan, L. *et al.* (2010) 'Polyethersulfone membranes: The effect of sulfonation on the properties', *Polymer - Plastics Technology and Engineering*, 49(14), pp. 1419–1427. doi: 10.1080/03602559.2010.496399.

Wang, Y. and Xu, T. (2015) 'Anchoring hydrophilic polymer in substrate : An easy approach for improving the performance of TFC FO membrane', *Journal of Membrane*

Science. Elsevier, 476, pp. 330–339. doi: 10.1016/j.memsci.2014.11.025.

Yampolskii, Y. (2012) 'Polymeric gas separation membranes', *Macromolecules*, 45(8), pp. 3298–3311. doi: 10.1021/ma300213b.

Yee, R. S. L., Zhang, K. and Ladewig, B. P. (2013) 'The effects of sulfonated poly(ether ether ketone) ion exchange preparation conditions on membrane properties', *Membranes*, 3(3), pp. 182–195. doi: 10.3390/membranes3030182.

Zhani, K; Zarzoum, K;BenBacha, H; Koschikowski, J; Pfeifle, D. (2015) 'Autonomous solar powered membrane distillation systems : state of the art', *Desalination and Water Treatment*, (November). doi: 10.1080/19443994.2015.1117821.

Appendix I: Results of remaining samples

Figure 54 shows the TGA spectra of all samples as discussed in Table 13.

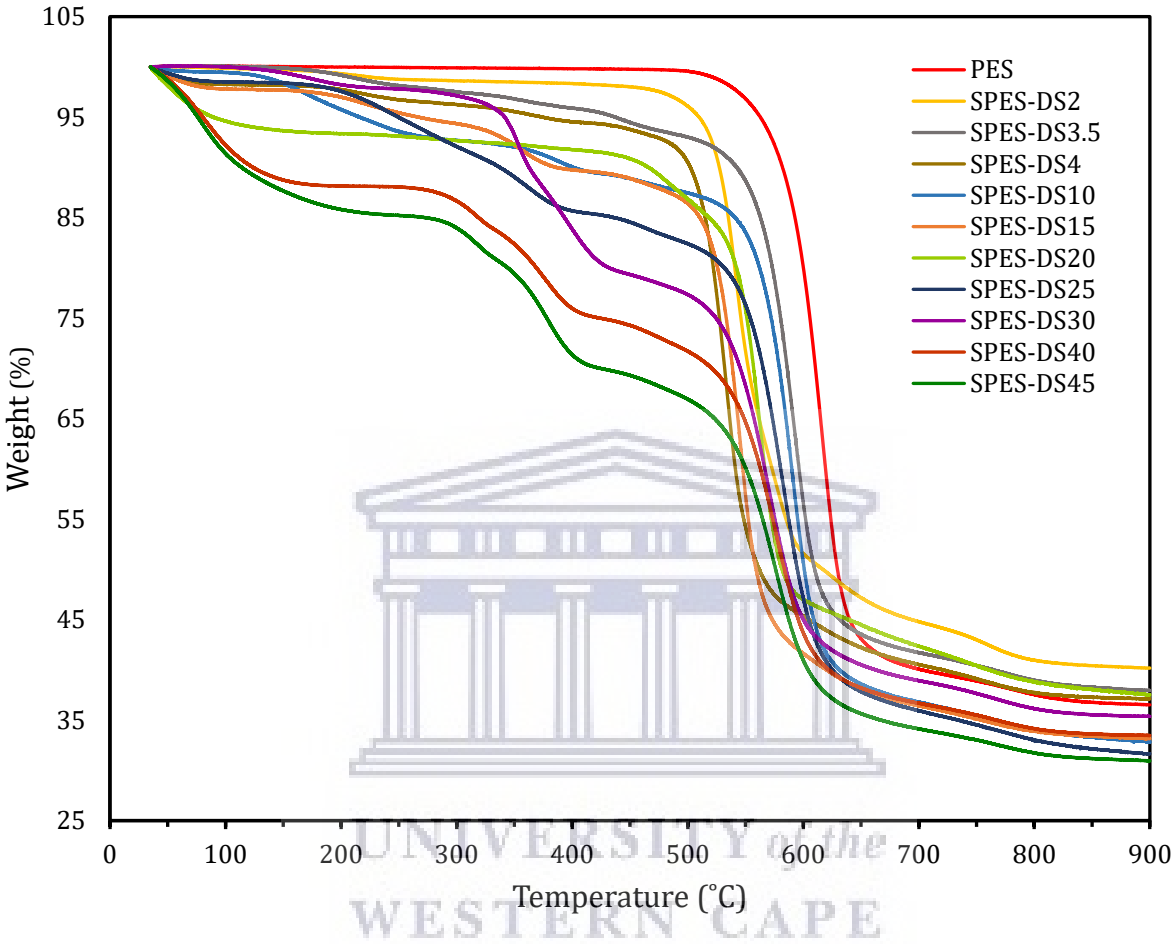

Figure 54 TGA thermographs of all samples

Figure 55 shows the absorbance spectra measure with FTIR for all samples as discussed in Table 13.

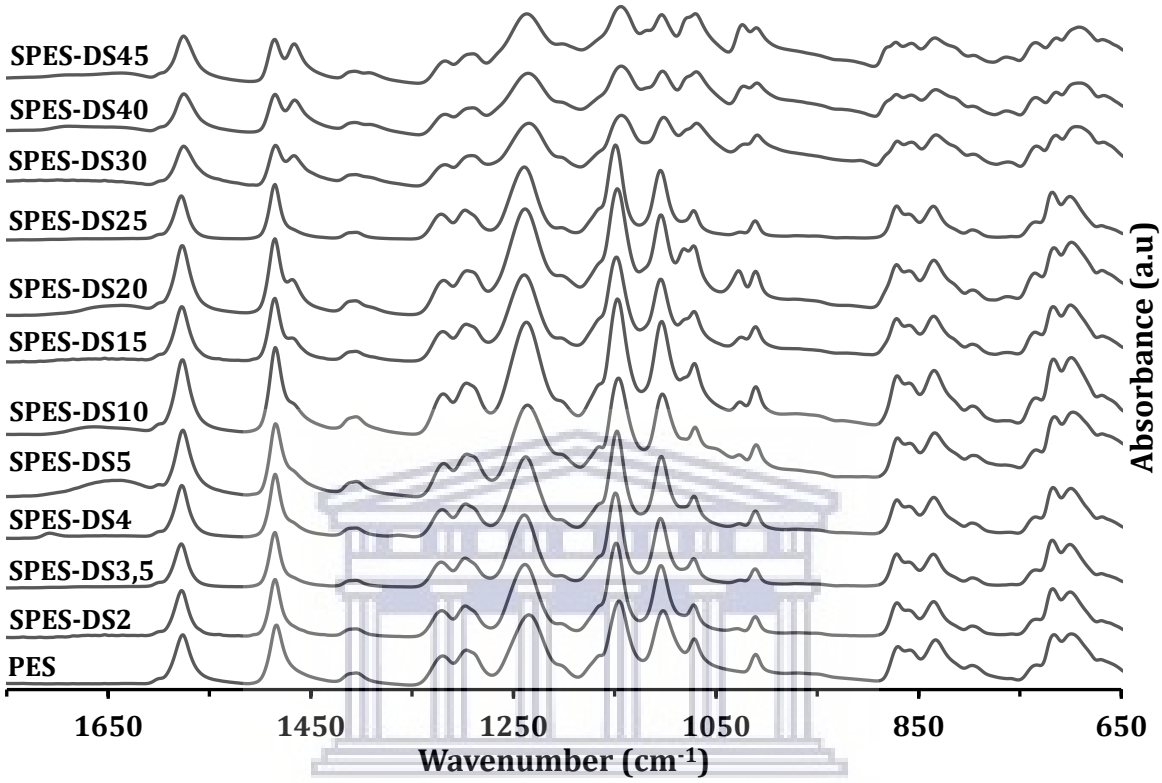

Figure 55 FTIR absorbance spectra for all samples

Appendix II: Synthesis of polyethersulphone hollow fibres by phase inversion

Phase inversion is a process whereby a polymer is transformed in a controlled manner from a liquid into a solid state in a previously homogeneous polymer solution. The process of solidification often begins with the transition of one liquid state into two liquid states (liquid-liquid demixing). During demixing, one of the liquid phases (the higher polymer concentration phase) will solidify so that a solid matrix is formed, and the polymer-poor phase will give rise to the pores. The membrane morphology can be controlled, which means that porous as well as nonporous membranes can be prepared, by controlling the initial stage of the phase transition. A wide range of different techniques fall within the concept of phase inversion, such as precipitation by solvent evaporation, precipitation from the vapour phase, precipitation by controlled evaporation, thermal precipitation, and immersion precipitation (Mulder, 1992; Pereira Nunes and Peinemann, 2006). For preparation of the hollow fibre support membranes in present study, the immersion precipitation technique is used.

Immersion precipitation is achieved by diffusion of nonsolvent from a coagulation bath into the polymer film and diffusion of the solvent from the polymer into the nonsolvent bath (Kools, 1998). When preparing flat sheet membranes, the polymer solution (casting solution) containing a polymer dissolved in a solvent is cast on a suitable support and then immersed in a coagulation bath containing a nonsolvent. When preparing hollow fibre membranes, the polymer solution containing polymer and solvent (dope solution) passes through a spinneret and is immersed in a coagulation bath containing a nonsolvent. Figure 56 shows a schematic view of the immersion precipitation technique using dry-wet spinning. The membrane structure that is obtained is a result of a combination of mass transfer and phase separation (Mulder, 1992).

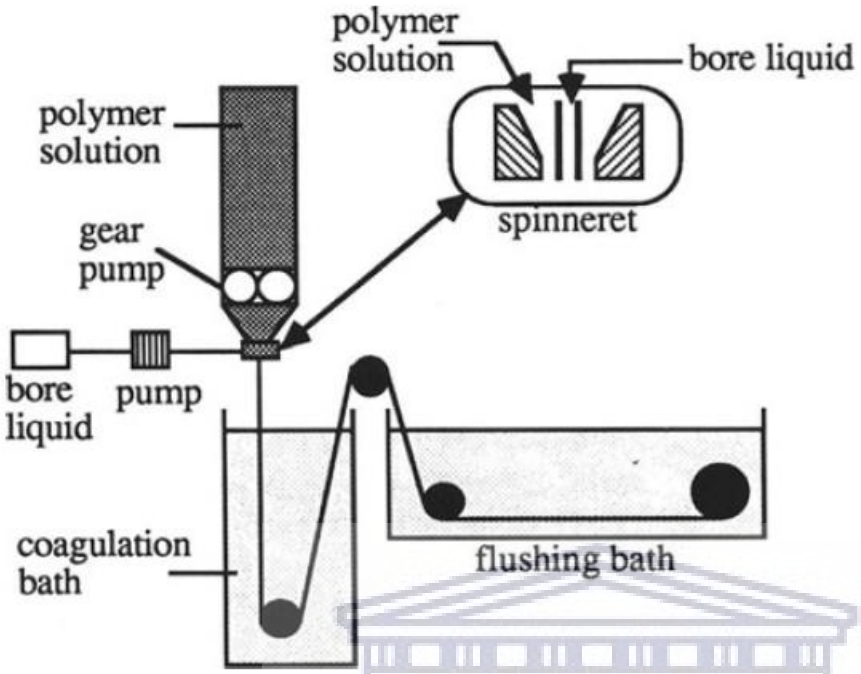

Figure 56 Schematic overview of the dry-wet spinning process (Mulder, 1992)

All phase inversion processes are based on the same thermodynamic principles as described below. Phase inversion is a versatile technique that allows for different morphologies to be obtained (Mulder, 1992).

Using immersion precipitation, membranes can be prepared in two configurations; flat membranes or tubular membranes. Tubular membranes can be classified in three types:

- hollow fibre membranes with a diameter of < 0.5 mm
- capillary membranes with a diameter of 0.5-5 mm
- tubular membranes with a diameter of >5 mm

The dimensions of the tubular membranes are so large that they have to be supported whereas the hollow fibres and capillaries are self-supporting (Mulder, 1992).

The preparation of hollow fibres and capillaries is possible using three methods;

- wet spinning (or dry-wet spinning) (immersion in a nonsolvent bath)
- melt spinning (extrusion of melted polymer)
- dry spinning (exposing to a nonsolvent atmosphere)

The initiation of the membrane formation process is crucial and determines to a large extent the final separation properties. The dimensions of the spinneret are very important in dry-wet spinning because it determines the fibre dimensions. This is not the case for melt spinning and dry-spinning, because the fibre dimensions are mainly determined by the ratio of the extrusion rate and the tearing rate with those methods (Mulder, 1992).

The preparation of flat sheet membranes and hollow fibres are quite different. The dope solution has a higher polymer concentration in spinning and is more viscous than casting solutions (used for flat sheet membranes). Reason for this is that hollow fibres must be able to perform the separation and withstand the applied pressure of the process without collapsing (being self-supporting). The mechanical demands placed on the microporous hollow fibre membranes are more demanding than for their flat sheet equivalent. Therefore, a finer, stronger, and higher density microporous structure is required. The thickness of the skin layer of hollow fibres is greater than flat sheet membranes because of the more concentrated polymer solution used. This has lower fluxes as a result. However this is compensated for by the low cost of producing a large membrane area of hollow fibres. Furthermore, when preparing hollow fibre membranes demixing takes place from the bore side and from the shell, whereas with flat sheet membranes demixing occurs only from one side (Mulder, 1992; Baker, 2012).

With dry-wet spinning a viscous polymer solution containing polymer, solvent and sometimes additives is pumped through the spinneret. The viscosity of the polymer solution must be high (generally >100 Poise). The bore injection fluid is pumped through the inner tube of the spinneret. After a short residence time in the air (air gap) or a controlled atmosphere (the term dry originated from this step), the fibre is immersed in a nonsolvent bath where coagulation occurs. After this, the fibre is collected with a godet.

The main spinning parameters are the extrusion rate of the polymer solution, the bore fluid rate, the tearing rate, the residence time in the air gap, and the dimensions of the spinneret. These parameters interfere with the membrane forming parameters, such as the composition of the coagulation bath, and its temperature. The dimensions of the hollow fibres are more or less fixed after immersion in the coagulation bath (Mulder, 1992; Baker, 2012).

The pore structure is generated by phase separation. After immersion in a nonsolvent bath, the solvent-nonsolvent exchange brings the initially thermodynamically stable system into a condition for which the minimum Gibb's free energy is attained by separating into two coexisting phases (Pereira Nunes and Peinemann, 2006).

There is no consensus in literature on the predominant mechanisms of phase inversion leading to pore formation and the thermodynamic involved. Figure 57 shows a simplified diagram of phase separation during membrane formation. The mechanism of phase separation depends on the crossing point into the unstable region. If the solvent-nonsolvent exchange brings the system first into a metastable condition (path A) the nucleation and growth mechanism (NG) is favoured. A dispersed phase consisting of droplets of a polymer-poor solution is formed in a concentrated matrix. If there is no additional nonsolvent added and the temperature doesn't change in the system, the composition inside the nuclei would, in the early stages, be practically the same as expected at the equilibrium, and would, practically not change with time. Only the size of the droplets increases with time. If the demixing path crosses the critical point, going directly into the stable region (Path B), spinodal composition (SD) predominates (Pereira Nunes and Peinemann, 2006).

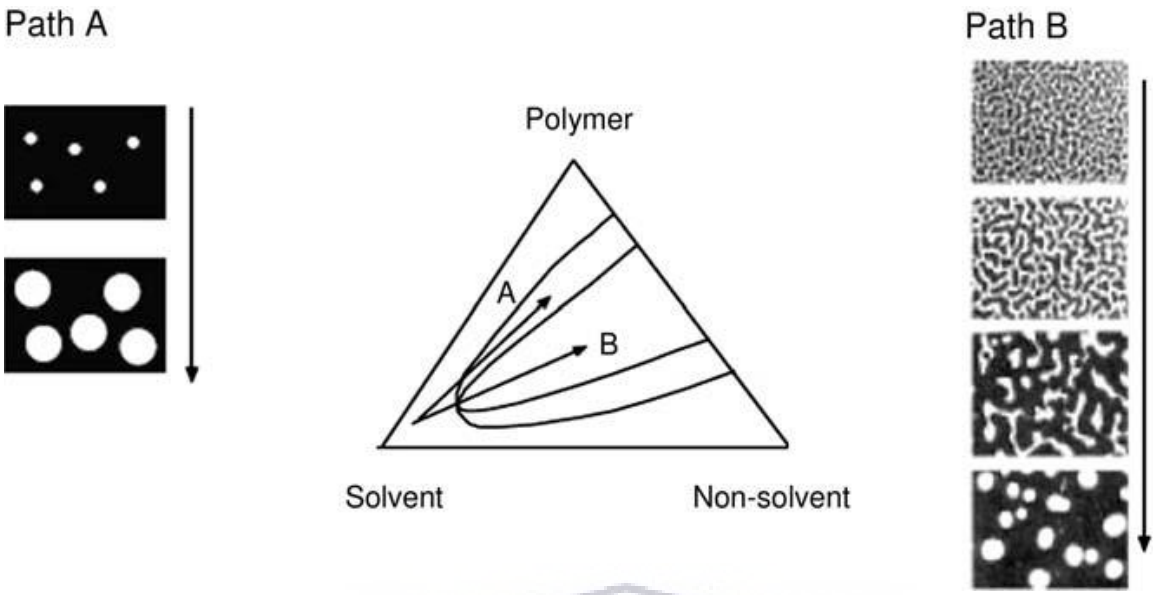

Figure 57 Mechanism of phase separation during membrane formation (Pereira Nunes and Peinemann, 2006)

A concentration fluctuation appears in the initially homogeneous system and progresses with increasing amplitude, which leads to a separation into two continuous phases. Here again, the polymer-poor phase will form the pores. The initial steps of phase separation, either by the nucleation and growth mechanism or the spinodal composition can be well described according to theories of phase separation. However at later stages, both NG and SD usually progress to a phase coalescence and it becomes difficult to predict the final structure. Besides the starting mechanism of phase separation, the point where the developing structure is fixed is as important (Pereira Nunes and Peinemann, 2006).

Simultaneously to demixing, as the concentration of the system decreases, by solvent-nonsolvent exchange, the mobility of the system decreases. There are different possible reasons for this; the polymer-solvent (or nonsolvent) interaction might be physically unfavourable, leading to stronger polymer-polymer contacts, there might be vitrification of the polymer concentrated phase, as the solvent concentration decreases, and in some cases partial crystallization may occur. If the system gels and solidifies directly after the first steps of phase separation (for instance at t_2), the membrane will have a fine pore structure which keeps the original characteristics given by the initial demixing mechanism. If NG demixing stops during the initial stages, the nuclei would grow and touch each other, forming interconnected pores. The SD demixing would favour the

formation of an interconnected pore structure from the beginning. An asymmetric structure is usually formed across the membrane since the solvent-nonsolvent exchange may lead to different starting conditions for phase separation at layers far from the surface. Besides the NG and SD demixing, other factors influence the morphology. The whole membrane structure usually can be classified as sponge-like or finger-like. Finger-like cavities are formed in many cases, as the nonsolvent enters the polymer solution. This macro void structure may contribute to a lack of mechanical stability to be used at high pressures. A combination of factors is responsible for the formation of macro voids. For practical purposes, the predominance of a sponge-like or a macro void structure can be induced in different ways. Basically the sponge-like structure is favoured by:

1. Increasing the polymer concentration of the casting solution
2. Increasing the viscosity of the casting solution by adding a crosslinking agent
3. Changing the solvent
4. Adding solvent to the nonsolvent bath

The growth of a polymer-poor phase by SD or NG is an isotropic process, which takes place as soon as the solvent-nonsolvent contents supply the thermodynamic condition for demixing. To understand the macro void formation, the coupling of the (NG or SD) demixing process with the rapidly moving front of nonsolvent must be considered. If the nonsolvent diffusion ratio into the polymer phase being formed exceeds the rate of outward solvent diffusion, the macro void formation is favoured. The diffusivity of water is usually expected to be one-to-two orders of magnitude higher than the diffusivity of bulkier organic solvent. The main driving force for the nonsolvent (usually water) influx is the locally generated osmotic pressure. This could be, hypothetically, approximately 100 bar with a difference of only 5 mol% nonsolvent concentration between the initial nucleus and the approaching front. As water moves into a polymer-poor nucleus, its wall is deformed expanding in the form of a tear. If the walls are fragile the nucleus may rupture giving rise to micro voids with unskinned walls. If the walls are stronger as in the case of nuclei growing in a matrix with higher polymer concentration, the deformation can be restrained or even totally inhibited, giving rise to a macro void-free structure (Pereira Nunes and Peinemann, 2006).

Appendix III: Risk Inventory and Evaluation of Sulphonation of Polyethersulphone

1 Identification			
Name of equipment or project	Sulphonation of polyethersulphone (PES)		
Project number (if relevant)			
Equipment builder	Pelin Oymaci Akin Aishah El Boukili	Position of builder	PhD. student (STO 0.50) MSc. student (STO 1.29)
Responsible researcher	Pelin Oymaci Akin Aishah El Boukili		
Facility manager			
Section	SMP	Section leader	Kitty Nijmeijer
Building + room no.	Helix STO 0.63	Date	11-07-2017
Users	Pelin Oymaci Akin Aishah El Boukili		
Any persons who are not shown above may only use the equipment with the agreement of, and after instruction by, the equipment builder as named above.			

2 Description of the equipment and / or work

State here: purpose, duration, schedule, working method(s), actions to be carried out etc. If possible add a photo or drawing.

Purpose:
The purpose of this experiment is to sulphonate the polymer polyethersulphone (PES).
In the following section, the sulphonation is explained as well as the specific hazards and precautions. Reaction will be carried out at temperatures between 0°C and 20°C at atmospheric pressure.

Reaction:
Sulphonation is an aromatic electrophilic aromatic substitution reaction, the electro-donating substituents favour the reaction whereas electron-withdrawing groups do not. A sulphonic acid group, SO_3H is introduced into the structure of a molecule or ion in place of a hydrogen atom. PES is notoriously difficult to be sulphonated due to the electron withdrawing effect of the sulphone linkages which deactivate the adjacent aromatic rings for electrophilic substitution.

Below the synthesis of Sulphonated Polyethersulphone is depicted:

H-O-S-Cl + CH_3

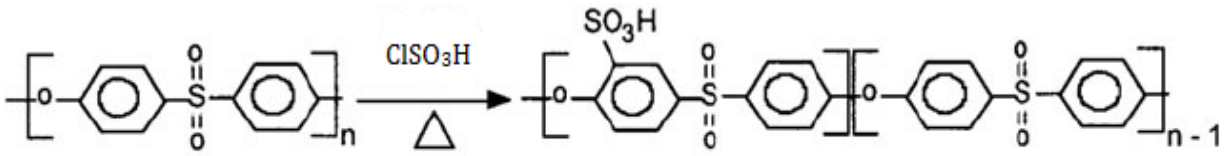

Synthesis of Sufonated Polyethersulfone

As the reaction moves to completion, HCl gas is released. This liberated HCl gas is absorbed into water to make a dilute HCl solution, therefore two gas wash bottles are used.

Chemicals
Chemicals required for this synthesis are shown in the table below:

Name	Formula	CAS nr	Risk Class	MW (g/mol)	Mp (°C)	Bp (°C)
Polyethersulphone (s)	$(C_{12}H_8O_3S)n$	25667-42-9	2	varies	NA	NA
Sulphuric acid (l)	H_2SO_4	7664-93-9	3	98.07	3-10	315-338
Chlorosulphonic acid (l)	$ClHO_3S$	7790-94-5	2	116.52	-80	151-152

Method:
PES is sulphonated by dissolving in concentrated sulphuric acid (98%) in a three neck reaction flask, and will be performed in a fume hood. Volumes of sulphuric acid used will vary between 25-100 ml. Used PES will be between 5g-25 g, and the volume of chlorosulphonic acid will be varied between 10-60 ml After dissolution of the polymer the sulphonating reagent (chlorosulphonic acid) is dropwise added to the dissolved PES solution at 10°C in an ice bath and left to react for 2 hours. The vessel is fitted with two gas wash bottles to remove the HCl gas evolved in the reaction. This liberated HCl gas is absorbed into water to make a dilute HCl solution. The resulting mixture is then precipitated into ice-cold deionised water under agitation. The resulting precipitate is recovered by filtration, and the filtrate is washed with deionised water until the pH value is at least 7. If transport of the chemicals is needed outside of the fume hood, it will be carried out using designated carrying material (e.g. transport bucket).

See Appendix 2 for the Standard Operating Protocol; a detailed description of the experiment.

The main safety concern is the use of sulfuric acid, which is classified to be a category 3 chemical. The amount of sulphuric acid used will not exceed 25 ml. It will be used in liquid form, . PES and chlorosulphonic acid have a risk classification of 2.

Both sulfuric acid and chlorosulphonic acid cause severe skin burns and eye damage (H314). In addition, sulphuric acid may be corrosive to metals (H290). Chlorosulphonic acid may cause respiratory irritation (H335). Furthermore it reacts violently with water (EUH014). Chlorosulphonic acid reacts with atmospheric moisture to form hydrogen chloride and sulphuric acid, and may contain sulphuric trioxide.

See detailed description of hazards further in this document.

Hazards and precautions

To prevent and minimize risk one should:

-Not breath dust/fume/gas/mist/vapours/spray

-Work in a well-ventilated area (fume hood),

-Wear protective gloves, a lab coat and safety goggles

For risk class 3 experiments, an exposure score is calculated using the NIOSH method.

The exposure score is determined by:
- The chance of the substance being emitted as a result of the substance's properties (E).
- The chance of the substances being emitted as a result of handling and/or the design of a set-up (H).
- The physical distance to the source and the presence of a number of sources in the same room (R).
- Technical and/or organizational measures which have been taken to reduce the chance of emission (C).
- The duration of exposure (T).
- The handling frequency/exposure frequency (F)

Calculating the exposure score;
$E.H.(R_{NF}+R_{FF}).C.T.F$ = Exposure Score

See below for the calculated risks of exposure:

Exposure	E	H	R_{NF}	R_{FF}	C	T	F	Score
Sulphuric acid	0.03	1	0.03	0.3	0.3	6	3/7	0.000208 Extremely low
Chlorosulphonic acid	0.1	1	. 0.03	0.3	0.3	6	3/7	0.000649 Extremely low

Duration and schedule
The experiments will be carried out for 6 months, 2-5 times a week. Parameters will be varied throughout within values mentioned above. The experimental set-up will be used during working hours.

The amounts of chemical used will be;
5-25 g PES
25-100 ml sulfuric acid
10-60 ml chlorosulphonic acid

3 Equipment to be used in the (fixed) installation

State here: equipment used, (simplified) process chart, relevant circuits, technical safety measures, piping, cables, the measurement and control method used, emergency stop facilities, chemicals used, layout of the equipment in the working area etc. Which critical components are custom made and which are purchased as standard components? If possible add a plan of the working area.

Mechanical stirrer will be used for dissolution of the polymer and also during the reaction. Temperature of the mixture will be monitored with a thermometer. A cylindrical separatory funnel will be used to add the chlorosulphonic acid dropwise to the polymer solution. The reaction will be performed in an ice water bath. All solutions and solids will be transferred in a bucket. The whole set-up will be carried out in a fume hood. Vacuum oven will be used to dry the polymers.

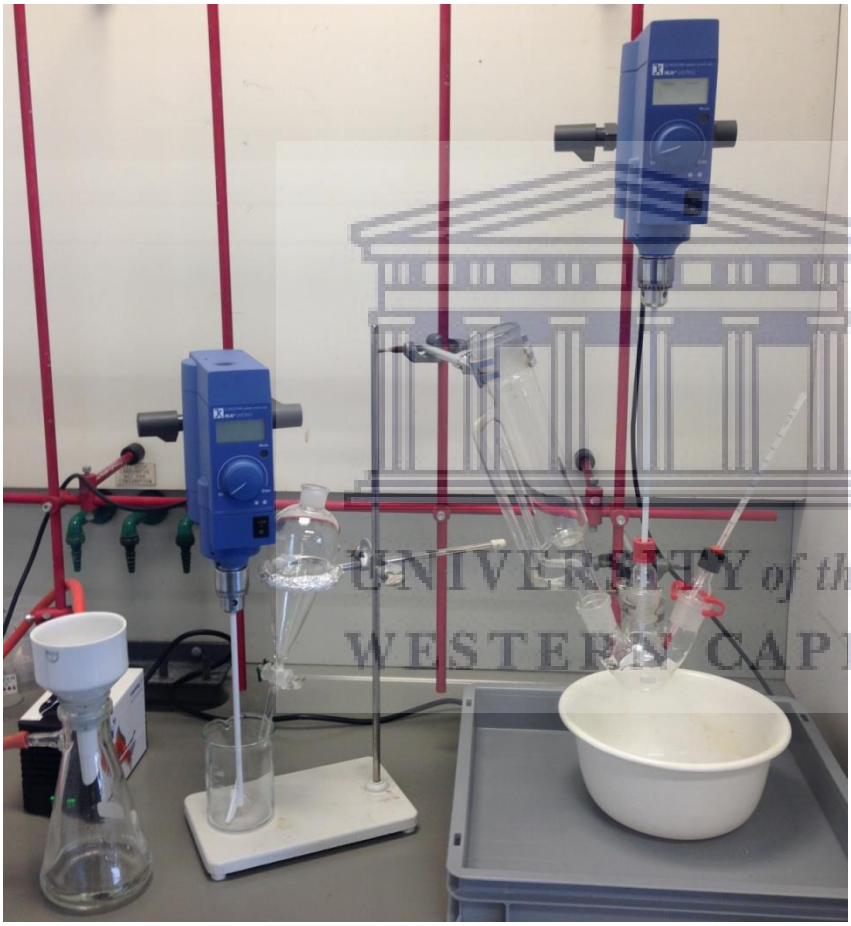

Figure 1 Sulphonation set-up

4 Identification of hazards and safety measures				
Are hazards expected to arise in carrying out the planned work?	**Yes**	**No**	**Explanation of the hazard** *(give a short description here of the hazard, specifying the nature of the hazard, conditions, actions taken etc.)*	**Measures to control hazards while carrying out the work** *(give a short description here and / or reference to a report or memo of the safety description)*
Fire and explosion hazard (R10, R11, R12, R15, R17, R18 and [fine] particulates) H220-H228, H242, H250, H251, H252, H260, H261, EUH018.		V		
High or low temperatures (surfaces, substances, working area)		V		
High pressure / equipment under pressure		V		
Hazardous substances (general)	V		Used solvent (sulphuric acid) and reactant (chlorosulphonic acid) are hazardous chemicals.	Working in a fume hood limits contact with these substances to a minimum. Furthermore personal protection gear (gloves, lab coat and safety goggles) is used to avoid contact. Any leftovers in the glassware will be neutralized with water.
Carcinogenic substances (R40, R45 or R49) H351, H350 or H350i		V		
Substances toxic to reproduction (R46, R60, R61, R62, R63 or R64) H340, H360f/d, H361f/d, H362		V		
Allergenic substances (R42, R43 of R42/R43) H334, H317		V		
Gases and gas bottles		V		
Bacteria, parasites and fungi or related (waste) products		V		
Genetically Modified Organisms (GMOs)		V		
Non-ionizing radiation (ELF, UV, IR or laser)		V		
Ionizing radiation (X-ray, radioactive substances)		V		
Electricity (high voltage or electrocution hazard)		V		
Harmful noise & vibrations [> 80 dB(A)]		V		
Long-term static loads or extreme positions		V		

Repetitive movements		V		
Trapping, cutting, crushing		V		
Other mechanical hazards	V		Mechanical stirrer can cause physical risk to people; entanglement to stirrer.	Long hair must be worn up, jewellery (bracelets) must be taken off during the experiments, no loose clothing will be worn.
Controls	V			
Risk of falling (≥ 2.5 m height)		V		
Human error	V		Spilling, dropping materials and unawareness can cause risks	Good laboratory practice is maintained, people using the equipment will be given an additional training before they start working. Personal protection gear is used at all times. Glassware and other equipment (e.g. mechanical stirrer motor) will be clamped during the experiment to avoid accidents.
Cleanliness and tidiness	V		Cleanliness and tidiness is maintained at all times.	Cleanliness is maintained by weekly lab duty, half yearly cleaning and weekly check-up
Slipping danger		V		

5 Hazards arising in special situations				
Are hazards likely to arise as a result of external and / or special situations	Yes	No	**Explanation of the hazard** *(give a short description here of the hazard, specifying the nature of the hazard, conditions, actions taken etc.)*	**Measures to control hazards while carrying out the work** *(give a short description here and / or reference to a report or memo of the safety description)*
Electrical fault		x		
Fault in water supply or drainage		x		
Fault in gas or compressed air supply		x		
Fault in ventilation or air extraction system	x		Release of hazardous fumes is possible.	The reaction will be take place in a closed system. HCl gas that evolved in the reaction will be absorbed into water to form diluted HCl by using two gas wash bottles. Furthermore, the reaction will take place in a fume hood, so the ventilation in the fume hood would be enough to prevent release. If ventilation in fume hood stops or becomes too low, an audio alarm gives warning. In that case, the lab will be evacuated.
Fault in control systems		x		
Blockage or isolation of equipment		x		
Leakage or breakage in equipment or samples	x		Hazardous chemicals can spill or leak from broken or cracked glassware.	Fume hood will be used throughout the experiment. Evaporation will occur inside the fume hood. In addition, glass container will be immersed in iced water bath during reaction. In case of any leakage or breakage in glassware, mixture will be neutralized. If spill occurs on surface, acid will be neutralized first and then proper absorbents like clay or vermiculite will be used. In addition, a dripping tray will be used throughout the experiment which limits the leaking of the chemicals. Personal protection equipment will be used and there will be no direct contact with the spill.

Changes in reaction or test conditions		x		
Presence of unauthorized persons	x		Unauthorized persons can be present in the lab and interact with the setup.	Unauthorized persons are not allowed to enter the lab.
Storage / transport of resulting substances / samples	x		Hazardous chemical bottles can drop and brake. Spilling or fuming in inappropriate storage conditions.	A bucket will be used to transfer chemicals, this will avoid drop. Chemicals will be stored in DUPA according to storage conditions stated by supplier.
Filling of equipment	x		Spill of hazardous chemicals is possible.	Filling of the equipment will be carried out in fume hood. In order to prevent spilling during filling the glassware, a pump system will be used for sulfuric acid. Chlorosulphonic acid will be used in small amounts and glass pipette will be used to transfer it. In case of spilling, the acids will be neutralized first with an alkali material such as sodium bicarbonate or limestone. After neutralization, solid absorbent like vermiculite or clay will be used to remove the leak. In addition, the filling will be performed on a dripping tray, which limits the leak of the chemicals in case of any spill. During the procedure, personal protection equipment will be used and there will be no direct contact with the spill.
Starting-up and/or building of equipment		x		
Ending of the work and/or dismantling of the equipment	x		Contact with hazardous chemicals	At the end of the experiment, the final product will be obtained. The residuals of the mixture will be first neutralized before cleaning. Personal protection equipment will be used and there will be no direct contact with the chemicals. Gloves for strong acids, safety goggles and lab coat will be used for personal protection.
Cleaning and/or maintenance of the equipment	x		Contact with hazardous chemicals	After reaction, residual of the mixture will be first neutralized. In addition, personal protection equipment will be used and there will be no direct

				contact with the chemicals. Gloves for strong acids, safety goggles and lab coat will be used for personal protection.
Long-term concentration		X		
Long working hours / overtime		X		
Combination with work by third parties		X		
Closed area (tank, underfloor area etc.)		X		
Storage / disposal of (by-) products	x		Contact with hazardous chemicals	The chemicals will be stored in DUPA with corresponding labels and pictograms. Products will be disposed in Category I. Personal protection equipment will be used and there will be no direct contact with the chemicals. Gloves for strong acids, eye goggles and lab coat will be used for personal protection.
Waste disposal	x		Contact with hazardous chemicals	Waste disposal will be according to TU/e waste procedure. Chemicals will be disposed in Category I. Personal protection equipment will be used and there will be no direct contact with the chemicals. Gloves for strong acids, eye goggles and lab coat will be used for personal protection.
Other (please state)…		x		

6 Risk groups and risk aspects

State which groups of persons may possibly come into contact with the equipment/machine, what risks arise and how the risks can be reduced.

	Yes	No	Explanation
Young people aged < 18		V	
Other language speakers	V		PhD and master students will use the setup. Training and work instructions will be given in English, to be sure that the procedure and the risks of working with the substances is understood.
Maintenance/repair personnel		V	
Visitors		V	Unauthorized people are prohibited to enter laboratory.
Cleaning staff		V	
Interns/temporary staff		V	
Persons working alone		V	
Pregnant women		V	
Women of child-bearing age	V		No additional risks.
Persons with special needs		V	
Security staff / BHV (emergency help) department	V		In case of an emergency, the security staff can come into contact with the chemicals used in the experiment, standard safety procedures apply.
Other (please state)…			

7 'Arbo' (Occupational Health and Safety) and Environment, working areas and procedures

	Yes	No	n.a.	Explanation
Aspects relating to working areas				
Air extraction/ventilation adequate	X			
Fire alarm adequate	X			
Lighting adequate	X			
Emergency lighting installed	X			
Emergency exits in order	X			
Specific emergency help facilities available	X			In case of contact (eye) with the acid, Diphoterine solution will be used as an emergency rinsing solution. This solution is located on the central hallway of the Helix building.
Storage of hazardous substances according to PGS-15	X			
Marking of the working area and equipment meets requirements (pictograms etc.)	X			
Protection against unauthorized persons adequate	X			
Instructions and procedures				
Information/instruction provided to involved persons	X			Date: 5 July 2017 Sjoukje Lubach will give an instruction

Working instructions with safety instructions available at workplace	X			
Instructions available for working alone		X		Working alone is not allowed in the lab.
Technical file complete and manual available			X	
Personal protection equipment is of good quality	X			
Wearing of safety glasses / hearing protection / safety clothing / safety shoes mandatory (delete non-applicable items)	X			
Reporting to BHV (emergency help) department required		X		
Switching-off smoke detectors necessary		X		
(Periodical) approval and maintenance laid down		X		
…				
…				

Hazards and Risks of chemicals used

Type	Compound	Compound formula	CAs nr.	Category	Limit values (mg/m^3)	MW (g/mol)	Vapour Pressure	Risks
Solid	PES	$(C_{12}H_8O_3S)n$	25667-42-9	2	NA	Varies	-	H302: Harmful if swallowed H315: Causes skin irritation H319: Causes serious eye irritation H335: May cause respiratory irritation
Liquid	Sulfuric acid	H_2SO_4	7664-93-9	3	0.05	98.07	0.00001 kPa at 20°C	H290: May be corrosive to metals H314:Skin corrosion/Irritation
Liquid	Chlorosulphonic acid	$ClHO_3S$	7790-94-5	2	1	116.52	0.13 kPa at 25°C	H314:Causes severe skin burns and eye damage H335: May cause respiratory irritation
Gas	Hydrogen chloride	HCl	-	-	-	-	-	H280: Gas under pressure H331: Acute toxicity if inhaled H314: Skin corrosion/irritation H335: Respiratory irritation EUH044: Risk of explosion if used under confinement
Gas	Sulphuric trioxide	SO_3	-	-	-	-	-	H290: Metal corrosion H330: Acute toxicity (inhalation) H314: Skin corrosion/irritation EUH014: Serious eye damage

Standard Operating Protocol

Summary

A polymer (PES) is first dried in an oven. The polymer (5-25 g) is then dissolved in an appropriate water soluble solvent (20-100 ml solution). Stirring is done using a mechanical stirrer to make sure that all polymer material is fully dissolved and form an homogeneous solution. Then the chlorosulphonic acid (40-60 ml) is added to the polymer while stirring the solution. The resulting reaction mixture is then stirred for some additional hours to improve the sulphonation of the polymer. The mixture is then gradually precipitated into ice-cold water. Precipitate is recovered using a Buchner funnel. The filtrate is diluted until the pH is at least 7.

Experimental

Personal protection

During experimentation, wear gloves, a lab coat and safety goggles. The type of gloves used require special attention. When handling the oven, heat resistance gloves should be used, when handling chemicals nitrile gloves should be used.

Solution preparation

Chemicals

- Polyethersulphone, PES (5-25 g)
- Sulphuric acid (98 %, 25-100 ml)
- Chlorosulphonic acid, CSA (10-60 ml)

Preparing PES solution

Polymer is dissolved in sulphuric acid, this is done at room temperature. Dissolving is performed in a three neck vessel equipped with mechanical stirrer.

Sulphonation of PES

Chemicals

- Sulphonated Polyethersulphone, PES (5-25 g)
- Chlorosulphonic acid, CSA (10-60 ml)

Preparing sulphonated PES

The chlorosulphonic acid is transferred into a cylindrical separatory funnel by pumping it into the funnel using a glass pipette. This is done to minimize contact; no pouring is needed. The chlorosulphonic acid is added to the PES solution while stirring the solution. The sulphonation reaction is carried out in an ice bath to simultaneously prevent evaporation of solvents and avoid pressure build-up in the system. The setup will be placed inside the fume hood. The resulting reaction mixture is stirred for some additional hours. The mixture is then gradually precipitated into a beaker with ice-cold water under agitation. This is done using a cone shaped separatory funnel.

The resulting precipitate is recovered by passing it through a Buchner funnel, connected to a side-arm flask, vacuumed by a pump. The filtrate is washed with deionized water until the pH is at least 7, and disposed as chemical waste.

Procedure

Weighing and experiments must be performed in the fume hood!

Polymer solution

Materials

- Three neck reaction vessel
- Mechanical stirrer
- Pumping device
- Thermometer

Procedure

- Weigh exact amounts of polymer PES (5-20 g)
- Place it in a vacuum oven for 10 hours at 130°C, this can be done overnight
- Take it out of the oven using heat resistant gloves
- Clamp the three neck reaction vessel onto a standard, use clamp clips (Fig. 1)
- Clamp the mechanical stirrer motor onto a standard above the reaction vessel, use clamp clips (Fig. 1)
- Connect the mechanical stirrer to the lab stirrer motor (Fig. 1)
- Place a thermometer into the opening of the three neck reaction vessel (Fig. 1)

- Measure exact amount of sulphuric acid (25-200 ml) into the three neck reaction vessel using the pumping device connected onto the bottle
- Transfer weighed an dried PES into the three neck reaction vessel
- Start stirring
- Let PES dissolve in sulphuric acid for two hours in your presence

Figure 2 Polymer solution preparation

Sulphonation

Materials

- Dipping tray
- Ice bath
- Glass pipette
- Cone shaped separatory funnel
- Cylindrical separatory funnel
- Beaker for precipitation
- Buchner funnel
- Erlenmeyer
- Vacuum pump

Procedure

- Place an ice bath with dripping tray under the three neck reaction vessel (Fig. 1)
- Connect the cylindrical separatory funnel onto one the remaining opening of the three neck reaction vessel (Fig. 1)

- Connect two gas wash bottles filled with water onto the opening of the cylindrical separatory funnel (Fig. 5, 6)
- Transfer the chlorosulphonic acid into a dripping funnel using a glass pipette (10-60 ml) (Fig. 2)
- Leave the mechanical stirrer on throughout
- Gradually add the chlorosulphonic acid to the PES solution
- Stir the reaction mixture for some additional hours
- Disconnect the cylindrical separatory funnel and clamp onto a standard, place a beaker under it.
- Dilute the remaining chlorosulphonic acid in the funnel with large volumes of water and set aside
- Clamp another stirrer motor to a standard for precipitation of the polymer solution (Fig. 3)
- Prepare a beaker with ice cold water and place it under the stirrer (Fig. 3)
- Pour the mixture from the three neck reaction vessel gradually into the beaker with ice cold water for precipitation to form (Fig. 3)
- Turn on the stirrer
- After set time of precipitation, turn off the stirrer
- Pour the mixture into a Buchner funnel (Fig. 4)
- Turn on the vacuum pump
- Recover the precipitation
- Wash the filtrate with deionized water until pH is 7
- Dispose the waste in category 1

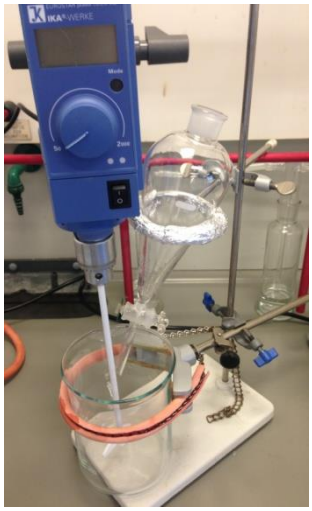

Figure 3 Precipitation

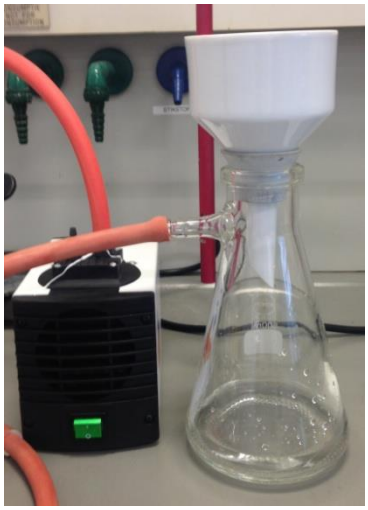

Figure 4 Filtration of polymer

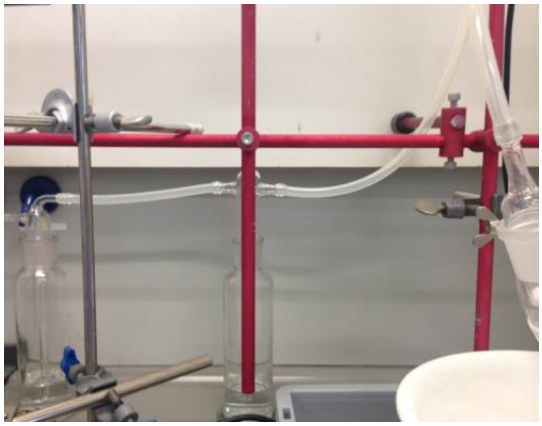

Figure 5 Gas wash bottles connected to vessel

Figure 6 Gas wash bottles

8 Remarks by facility manager / 'Arbo' (Occupational Health and Safety) and Environmental coordinator / AMSO

9 Signed for agreement					
In the opinion of the undersigned, the risk management measures are appropriate to the risks					
Equipment builder		Section leader		'Arbo' (occupational health and safety) and environmental coordinator	
Name		Name		Name	
Date		Date		Date	
Initials		Initials		Initials	
The section leader is responsible for the implementation of the agreements as laid down in this Risk Inventory & Evaluation form / Risk assessment					
Copies: Equipment builder Facility manager Section leader (E.g. group leader / head of capacity group) 'Arbo' (Occupational Health and Safety) and Environmental officer group 'Arbo' (Occupational Health and Safety) and Environmental coordinator faculty					

Appendix III: Standard operating procedure for dip-coating PES hollow fibre membranes with SPES

Safety Procedure for Methanol handling

PPE is worn at all times, and all proceedings are conducted in the fume hood!

Prepare polycarbonate cylinder

This cylinder will be used to dip polyethersulphone hollow fibres (PES-HF) in

- Cut of a piece with a length of 40 cm of polycarbonate tube
- Apply epoxy resin to one side of the tube, and leave to dry overnight

Dissolving SPES

Dissolve 5 wt% of SPES at room temperature in methanol (99,9 %)

- Weigh 2.5 g SPES and bring over in a plastic 1 L bottle
- Weigh 500 g methanol in a beaker on a balance
- Bring over the content of the beaker into a plastic 1 L bottle
- Place the bottle on a magnetic stirrer
- Stir the SPES/methanol until the SPES is fully dissolved

Prepare PES-HF

Make PES-HF ready for use in dip-coating (to minimize pore collapse)

- Take PES-HF out of water
- Dip PES-HF in a 50 wt% glycerol aqueous solution for 48 hours
- Take out PES-HF
- Dry in air at room temperature, place on a piece of paper

Hollow fibre dip-coating

Prepare composite hollow fibre membranes with SPES top layers

- Use Polyethersulphone hollow fibre membrane as support material
- Bring over the SPES solution into the prepared narrow polycarbonate cylinder with length 40 cm
- Dip-coat PES hollow fibres in the SPES/methanol solution using tweezers in the fume hood
- Apply three coatings to each hollow fibre make the layer defect free
- Each time 5 hollow fibres will be dip-coated (separately)